Identification and functional analysis of intestinal stem cell genes in homeostasis and cancer

Francisco Martín Barriga De Vicente

Doctoral Thesis UPF - 2013

Director

Eduard Batlle Gómez, PhD

Tutor

Antonio García de Herreros Madueño, PhD

Institute for Research in Biomedicine, Barcelona

Colorectal Cancer Laboratory

INSTITUTE FOR RESEARCH IN BIOMEDICINE

IRB BARCELONA

Experimental and Life Science Department

upf. Universitat Pompeu Fabra Barcelona

Results

Chapter 1: "The Intestinal Stem Cell Signature Identifies Colorectal Cancer Stem Cells and predicts disease relapse"

Hypotheses and Objectives of Chapter 1

Hypothesis:

It has been hypothesized that human CRCs are organized as a stem cell hierarchy, yet no evidence has been put forward towards the relationship of these colon cancer stem cells with normal intestinal stem cells. We hypothesize that the ISC program is present in colon cancer stem cells and that there is a clear parallel between normal colon and colon cancer. The expression of the ISC program in tumor cells may be involved in the regeneration of the disease upon therapeutic treatment.

Objectives:

-Identification of the full transcriptional program of the normal intestinal epithelium.

-Analysis of intestinal expression signatures in colon tumors.

-Purification of ISC-like cells from colon tumors and characterization of their tumor initiation ability.

Merlos-Suárez, A, **Barriga, FM**, Jung, P, Iglesias, M, Céspedes, MV, Rosell, D, Sevillano, M, Hernando-Momblona, X, da Silva-Diz, V, Muñoz, P, Clevers, H, Sancho, E, Mangues, R, Batlle, E. "The Intestinal Stem Cell Signature Identifies Colorectal Cancer Stem Cells and Predicts Disease Relapse". Cell Stem Cell (2011), 8, pp. 511-524.

Merlos-Suárez A, Barriga FM, Jung P, Iglesias M, Céspedes MV, Rossell D et al. The intestinal stem cell signature identifies colorectal cancer stem cells and predicts disease relapse. Cell Stem Cell. 2011 May 6; 8(5): 511-24. DOI: 10.1016/j.stem.2011.02.020

Chapter 2: Identification and functional characterization of Mex3a as a novel ISC gene.

Hypotheses and Objectives of Chapter 2

Hypothesis: The ISC gene expression program encodes several functions required to sustain self-renewal and multipotency during normal homeostasis and stress conditions. We hypothesize that Mex3a, a novel ISC-specific gene, promotes stemness through the regulation of the transcription factor Cdx2 and other potential targets.

Objectives:

-Validation of Mex3a as an ISC-specific gene and generation of a conditional knockout mouse model that would allow us to analyze Mex3a function *in vivo*.

-Phenotypic characterization of Mex3a WT and KO intestines.

-Generation and characterization of a Mex3a reporter allele *in vivo*.

-*In vitro* analysis of the function of Mex3a in primary ISC cultures and colon cancer cells.

2.1 Analysis of ISC signatures for candidate gene selection

As discussed in the previous chapter we have been able to identify the transcriptional landscape of the intestine, yet it is still unclear which functions are encoded within the ISC signature and which of these are relevant for the maintenance of the stem cell phenotype. Just by having a quick glance at the 54 genes of the EphB2 derived ISC signature (see Chapter 1), there seems to be an over-representation of Wnt targets (e.g. Lgr5, Ascl2, EphB3 and Ptpro among others) defined by their regulation at the transcriptional level and by the binding of TCF4 (TCF7L2) to their promoters/enhancer regions (Merlos-Suarez et al., 2011). Given the central role of Wnt signaling in intestinal homeostasis and cancer, it seems fitting that several targets and components of this pathway are enriched in ISCs.

Yet there are several other genes without any described relation to known pathways and that may point to new functions encoded in ISCs besides the regulation of any of the known signaling pathways involved in stem cell biology. We thus decided to analyze novel genes present in the ISC signature as a way to begin to dissect which are the relevant functions encoded within this program.

As a first criterion, we compared all available intestinal stem cell expression profiles and chose those genes whose expression was consistent among all of them. The rationale behind this filter was that any central function should be shared by several ISC types and be independent of the method used to purify ISCs. We compared three signatures: the EphB2 ISC signature from mouse small intestine (Merlos-Suarez et al., 2011), the Lgr5 signature from small intestine obtained in our lab, but based in the already published data (van der Flier et al., 2009) and the human EphB2 colon SC signature (Jung et al., 2011). **Figure 16** shows the Venn diagram of compared lists.

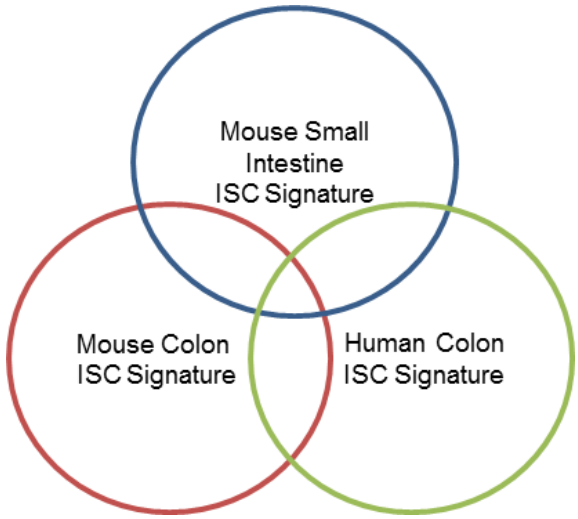

Figure 16: ISC signatures compared to generate the selection of genes to analyze.

Table 1 shows the list of most consistent ISC genes obtained from the comparison of the abovementioned signatures.

Of the list of 8 most consistent ISC genes, I decided to pursue the characterization of Mex3a. This was due to the striking loss of adult stem cells described for *mex-3* mutants in C. elegans (Introduction section 2.6). This phenotype was dependent on *pal-1*, the nematode homologue of Cdx2, and we hypothesized that the Mex3a / Cdx2 axis could be conserved in mammals.

Gene	Described in ISCs?	Protein (function)
Apcdd1	No	Receptor (Negative regulator of Wnt signaling) (Shimomura et al., 2010)
Ascl2	Yes	Transcription factor (ISC self-renewal) (van der Flier et al., 2009)
EphB3	Yes	Receptor (Intestinal architecture) (Batlle et al., 2002a)
Lgr5	Yes	Receptor (Positive regulator of Wnt signaling) (de Lau et al., 2011)
Mex3a	No	RNA binding protein (mRNA regulation?) (Buchet-Poyau et al., 2007)
Phgdh	No	Enzyme (Serine biosynthesis) (Klomp et al., 2000)
Slco3a1	No	Transporter (Prostaglandin metabolism) (Wang and Dubois, 2006)
Smoc2	Yes	Secreted protein (Antagonist of BMP?) (Munoz et al., 2012)

Table 1: List of most consistent ISC genes.

2.2 Validating Mex3a expression in ISCs

As a first approach, we validated the results obtained from the different mouse ISC signatures by RT-qPCR. **Figure 17** shows that Mex3a is enriched in ISCs obtained independently from EphB2 and Lgr5 sorting.

As mentioned in the introduction, the mex-3 family is composed of four genes: Mex3a, Mex3b, Mex3c and Mex3d (**Figure 11**). The expression levels of the Mex-3 family in ISCs were, in decreasing order as follows: Mex3c, Mex3a, Mex3d and Mex3b (data not shown). Mex3a was highly enriched in the $EphB2^{Hi}$ population, whereas the other Mex3 genes showed different expression patterns (**Figure 17C**). Furthermore, we found that Mex3a was enriched over 60 fold in $Lgr5^{+ve}$ cells when compared to Paneth cells (data not shown) implying that ISC enrichment of Mex3a in ISC was not due to co-purification of Paneth Cells. Overall, our RT-qPCR data confirms the observations from diverse microarray experiments and shows that Mex3a is a novel ISC-enriched gene.

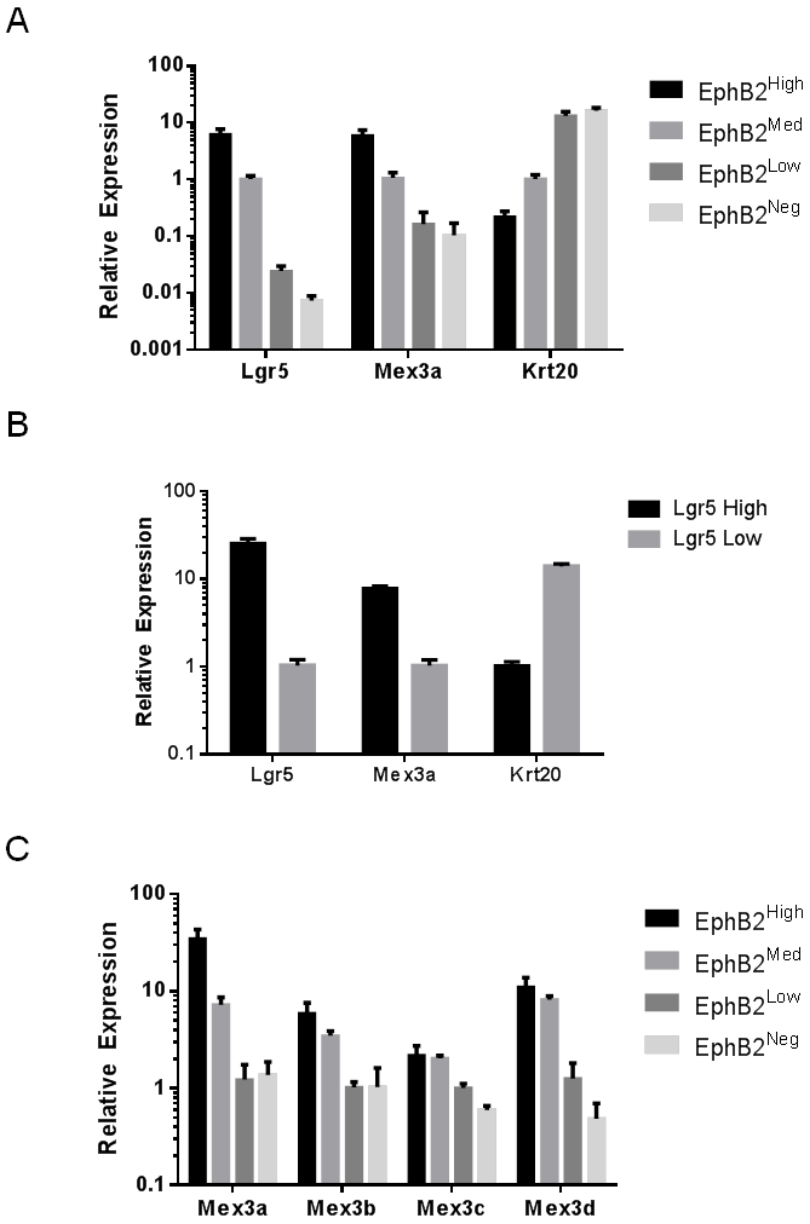

Figure 17: Mex3a is enriched in ISCs. A. Expression of Mex3a compared to Lgr5 and Krt20 in EphB2 populations from mouse small intestine. B. Expression of Mex3a compared to Lgr5 and Krt20 in Lgr5 populations from small intestine. C. Expression of Mex3a, Mex3b, Mex3c and Mex3d in EphB2 populations. Note that Mex3a is the only ISC specific of all Mex genes.

2.3 Function of Mex3a in the intestine: characterization of the cKO allele

2.3.1 Generation of a conditional Mex3a knock-out allele

To study the function of Mex3a in the intestine, we generated a new mouse model that would allow the complete or tissue specific ablation of Mex3a. To this end, we inserted loxP sites flanking the second exon of the mouse Mex3a locus, which encodes 70% of the protein. Of note, we noticed that there is a consensus translation start site at the beginning of exon 2, which theoretically could drive the expression of a large portion of the gene. This excluded the deletion of exon 1 as an effective approach. Another consideration to note is that Mex3a has only 2 exons, so the 3´ loxP site had to be placed within the 3´UTR of the gene. To avoid affecting important regulatory regions, we decided to place this loxP site in a region that showed very low conservation when compared to the human genome, using this as a criterion to avoid potentially relevant sites.

The initial targeting yielded 8/96 clones positive by long-range PCR (LR-PCR). Of these clones, 3 where positive by Southern Blot (**Figure 18B**). 2 of these clones were re-expanded and transfected with an FlpO-bearing plasmid to remove the Neo cassette. Of this treatment, 9/96 clones had excised the Neo cassette assessed by PCR. We then re-confirmed the Neo removal by Southern blot in 2 clones. These were then used to generate chimeras and were crossed with C57/Bl6 mice. Offspring bearing the Mex3a targeted allele were confirmed by standard genotyping (**Figure 18C**) and the Mex3a cKO mouse colony was established for further crosses.

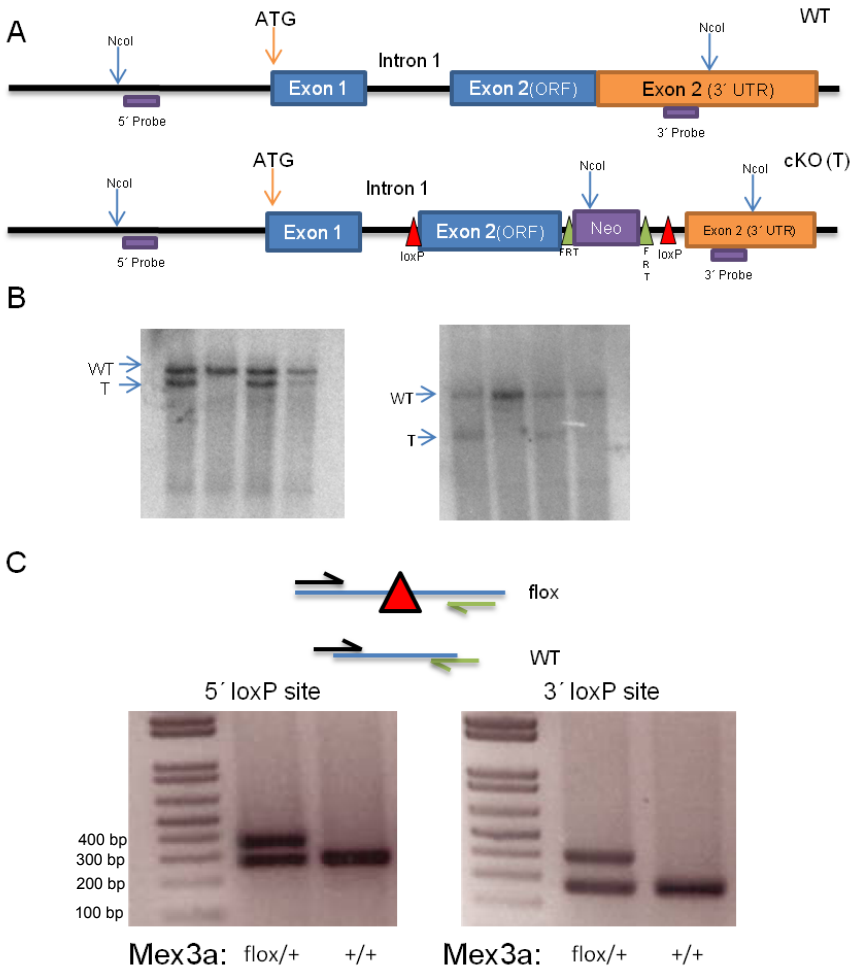

Figure 18: Generation of Mex3a cKO mice. A. Structure of the mouse Mex3a locus and the position of loxP sites. The Neo cassette was removed by transfecting an FlpO construct into ESCs before blastocyst injection. B. Southern blots of the 5´and 3´region of the Mex3a locus to assess the targeting. 5´and 3´probes were used to asses gDNA after NcoI digestion. C. Diagram of the PCR strategy to identify loxP sites. Lower panels show a representative genotyping of adult mice bearing the Mex3a cKO allele with both loxP sites present.

2.3.2 Conditional ablation of Mex3a in the intestinal epithelium

To ablate Mex3a expression in the intestinal epithelium we chose the well described Villin Cre-ER^{T2} transgenic mouse line. This Cre line allows robust and almost full deletion of a floxed gene in intestinal crypts and villi, including the ISC compartment (el Marjou et al., 2004). **Figure 19** shows the intestine-specific inducible deletion of exon 2 of Mex3a both at the level of gDNA and mRNA. Upon tamoxifen treatment the mRNA levels of Mex3a were reduced between 50 and a 100 fold compared to the Mex3a$^{+/+}$ littermate. At the protein level we have been unable to detect Mex3a by Western blot in full intestinal crypt extracts. We hypothesize that this is due to the low levels of expression of Mex3a. Furthermore, all commercially available antibodies detect by western blot several unspecific bands of diverse sizes in these extracts. In any case the strong decrease of Mex3a at the mRNA level suggests that the gene function is completely ablated in this mouse model.

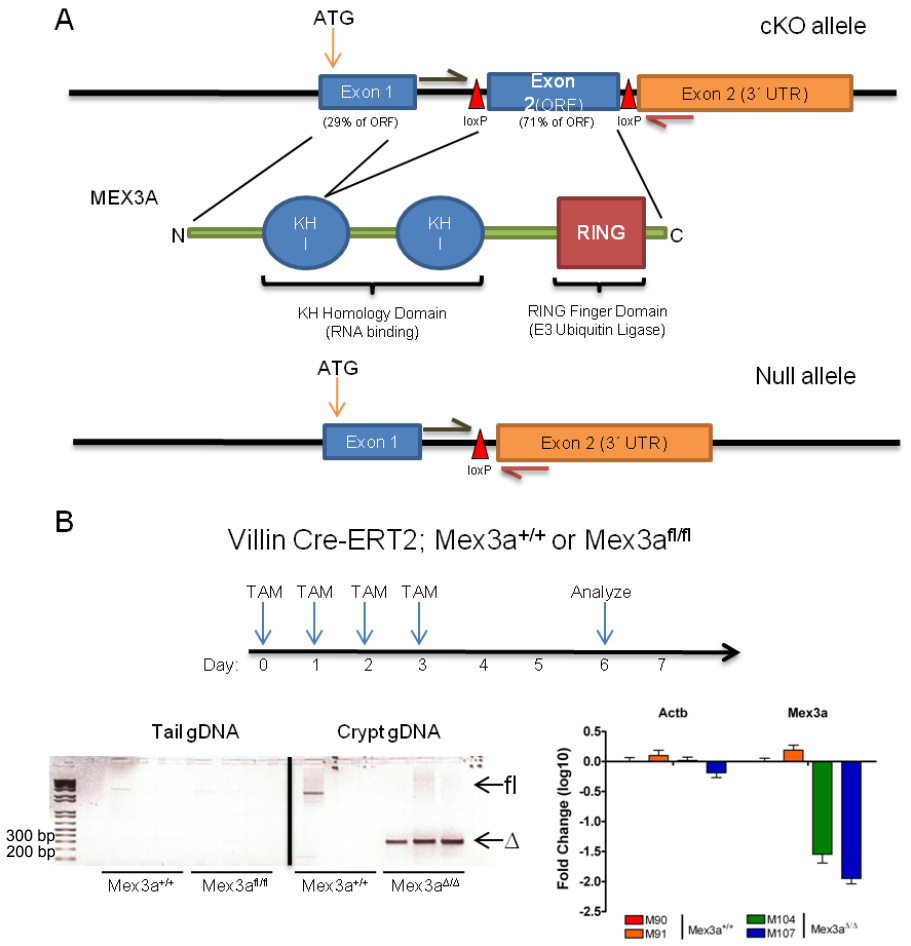

Figure 19: Intestinal deletion of Mex3a. A. Diagram of the cKO allele of Mex3a showing the contribution of both exons to the protein product (% of ORF in parenthesis). The lower diagram depicts the recombined allele and the PCR assay to detect the recombination. B. Analysis of Tamoxifen injected mice bearing the Villin Cre-ER^{T2} transgene and either the WT or floxed alleles of Mex3a. The left panel shows the PCR on gDNA to assess recombination and the right panel the mRNA levels of Mex3a in purified intestinal crypts. Analysis was performed 1 week after the initial Tamoxifen dose.

2.4 Cdx2 levels are not affected in Mex3a KO intestines.

With the validation of the intestine-specific knockout of Mex3a, we sought to test our hypothesis regarding the regulation of Cdx2. The transcription factor Cdx2 has been described to drive the expression of intestinal differentiation genes in cell lines and is required during development for intestinal specification (Boyd et al., 2010; Gao et al., 2009; Gross et al., 2008; Kakizaki et al., 2010).

We analyzed the expression of Cdx2 by immunohistochemistry in the small intestine and colon of Mex3a WT and KO mice. In WT mice, Cdx2 was expressed in all epithelial cells in an increasing gradient from the crypt base as previously described (Silberg et al., 2000; Verzi et al., 2010). By IHC we could not detect any significant difference in Cdx2 levels or expression pattern (**Figure 20A**).

In order to analyze if Mex3a KO intestines have subtle effects on Cdx2 expression we decided to analyze primary cultures of Mex3a WT and KO ISCs. For this, we cultured intestinal crypts in two conditions: either as organoid or as stem/progenitor enriched. The former represent a 3D organoid model of the intestinal epithelium with presence of both ISCs and differentiated cells (Sato et al., 2009). In the latter, the addition of exogenous Wnt3a blocks the majority of cells into an ISC/early progenitor phenotype (Sato et al., 2011).

By performing western blot we assessed if Cdx2 levels were modified in either condition after Mex3a in vitro deletion. The results demonstrate no major effects on Cdx2 levels after Mex3a deletion (**Figure 20B, C**). Overall, these results discarded our hypothesis on the regulation of Cdx2 by Mex3a.

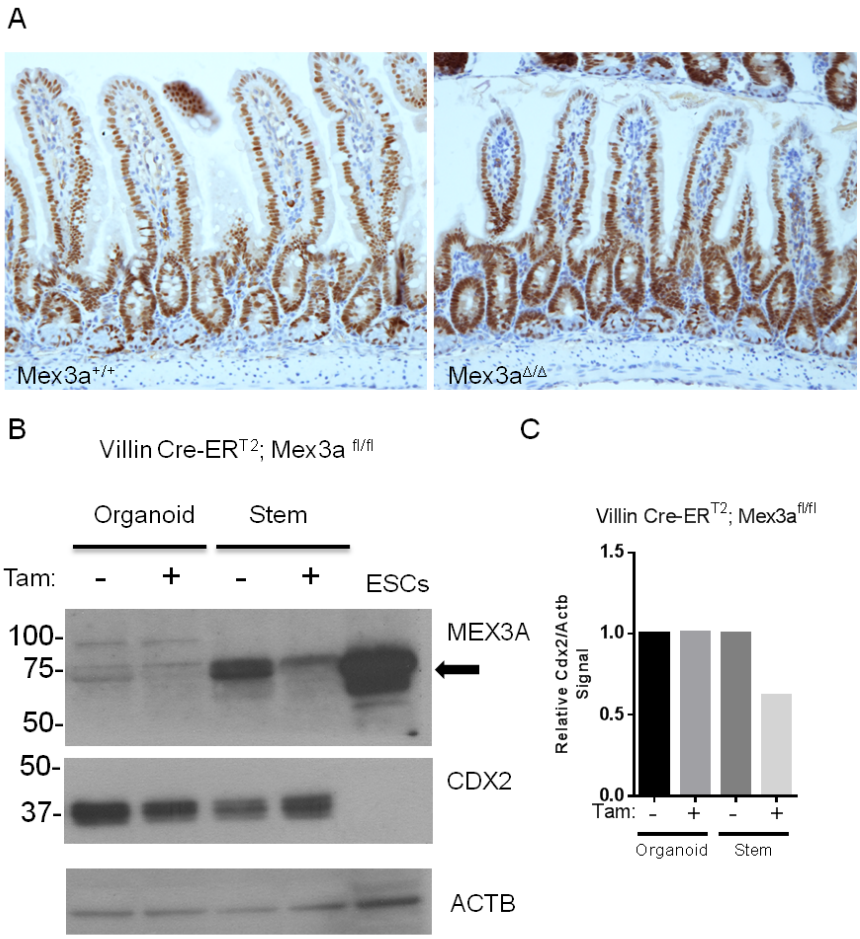

Figure 20: Intestinal deletion of Mex3a has no effect on Cdx2. A. Representative staining of Cdx2 in Mex3a WT and Mex3a KO small intestine. (Magnification 20X). B. Western blots of Mex3a and Cdx2 levels in primary ISC cultures. An ESC protein extract was used as a control for Mex3a expression and absence of Cdx2. The specific band in the Mex3a blot is highlighted with an arrow. C. Quantification of Cdx2 levels normalized to Actin.

2.5 Mex3a deletion has no overt effect on intestinal biology.

We studied the overall architecture and cell types present in the Mex3a KO intestines compared to WT intestines. We first analyzed the extent of Mex3a mRNA downregulation at different time points. We found that gene deletion is stable over 6 months, which suggested that Mex3a deficient ISCs do not suffer a negative or positive growth advantage (**Figure 21**).

At the histological level we could not find any obvious morphological or structural defects in Mex3a KO intestines when compared to their age and sex matched littermates (**Figure 22A**). Differentiation towards the secretory phenotypes was not altered as suggested by no differences in PAS/Alcian Blue staining (**Figure 22B**). Moreover, tuft cell frequency remained unchanged as shown by Dclk1 staining (**Figure 22C**). Importantly, numbers of stem cells were apparently unaltered upon Mex3a deletion as demonstrated through Olfm4 ISH (**Figure 23A**). Moreover, we could not detect major differences in the frequency of Paneth cells by lysozyme staining (**Figure 23B**).

We analyzed proliferating cells by phospho-histone H3 staining (pH3), which labels cells undergoing mitosis. We found that the ablation of Mex3a induced a mild reduction in the number of proliferative cells per crypt (**Figure 24A**). In a similar fashion, we analyzed the number of enteroendocrine cells by using the marker Chromogranin A. Interestingly, we could observe a mild increase in the number of $ChgA^{+ve}$ cells in the KO intestines (**Figure 24B**). Quantifications are shown in **Figure 24C**. Yet, when we analyzed ChgA and pH3 6 months after recombination we could not detect differences (data not shown). Overall, these results imply that Mex3a ablation only produce mild changes in the intestinal epithelium, which do not have apparent effects on intestinal homeostasis.

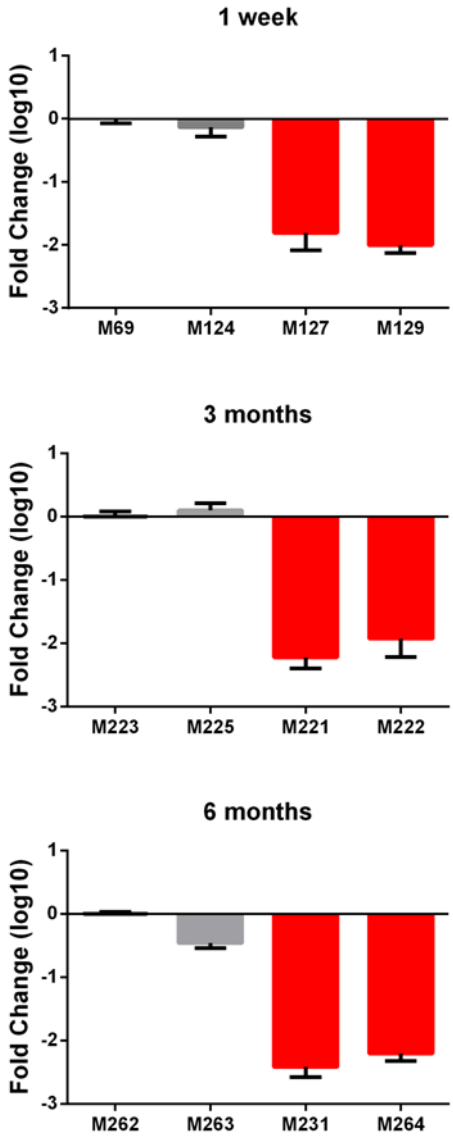

Figure 21: Mex3a KO crypts are not positively or negatively selected over time. Mex3a mRNA levels were quantified by RT-qPCR at different times after KO induction. The WT mice are shown in grey bars and the Mex3a cKO mice are depicted with red bars.

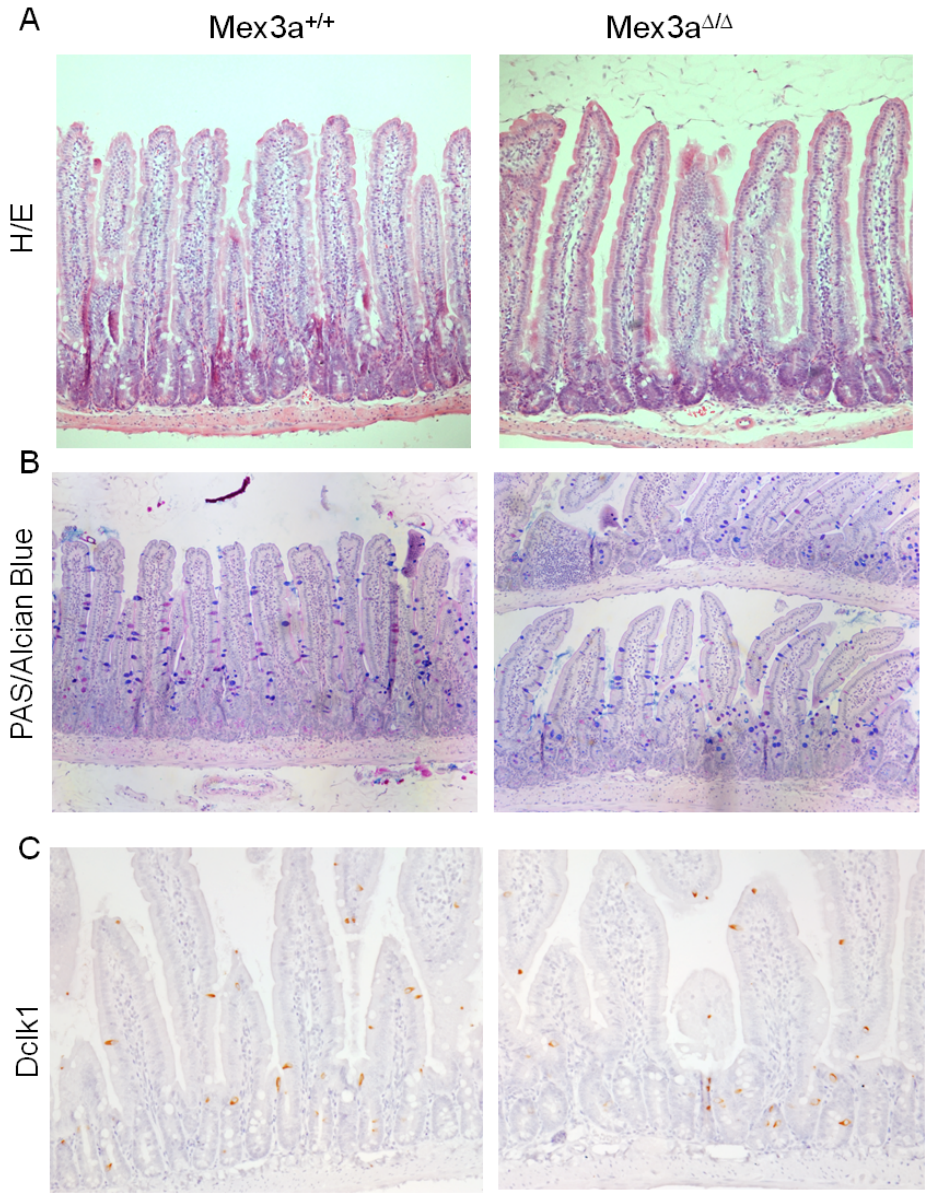

Figure 22: Mex3a deletion causes no gross changes in intestinal architecture. A. H/E staining of proximal small intestine of Mex3a WT and KO mice (Magnification 10X). B. PAS/Alcian Blue staining of mucosecretory cells (Magnification 10X). C. Dclk1 staining of tuft cells (Magnification 20X).

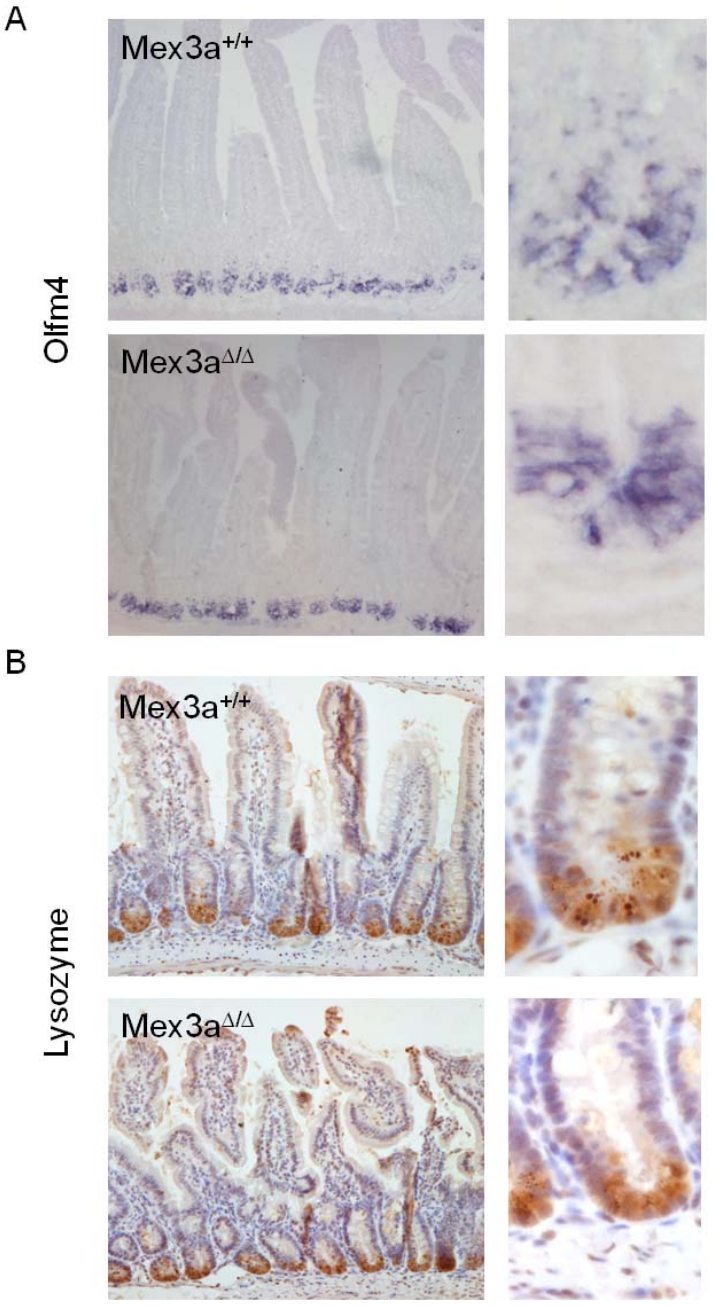

Figure 23: Mex3a deletion does not affect Olfm4 or Lysozyme expression. A. Representative pictures of Oflm4 ISH in WT or Mex3a KO intestines. B. Lysozyme staining on WT and Mex3a KO intestines. (Left panels are 20X and right panels are 40X).

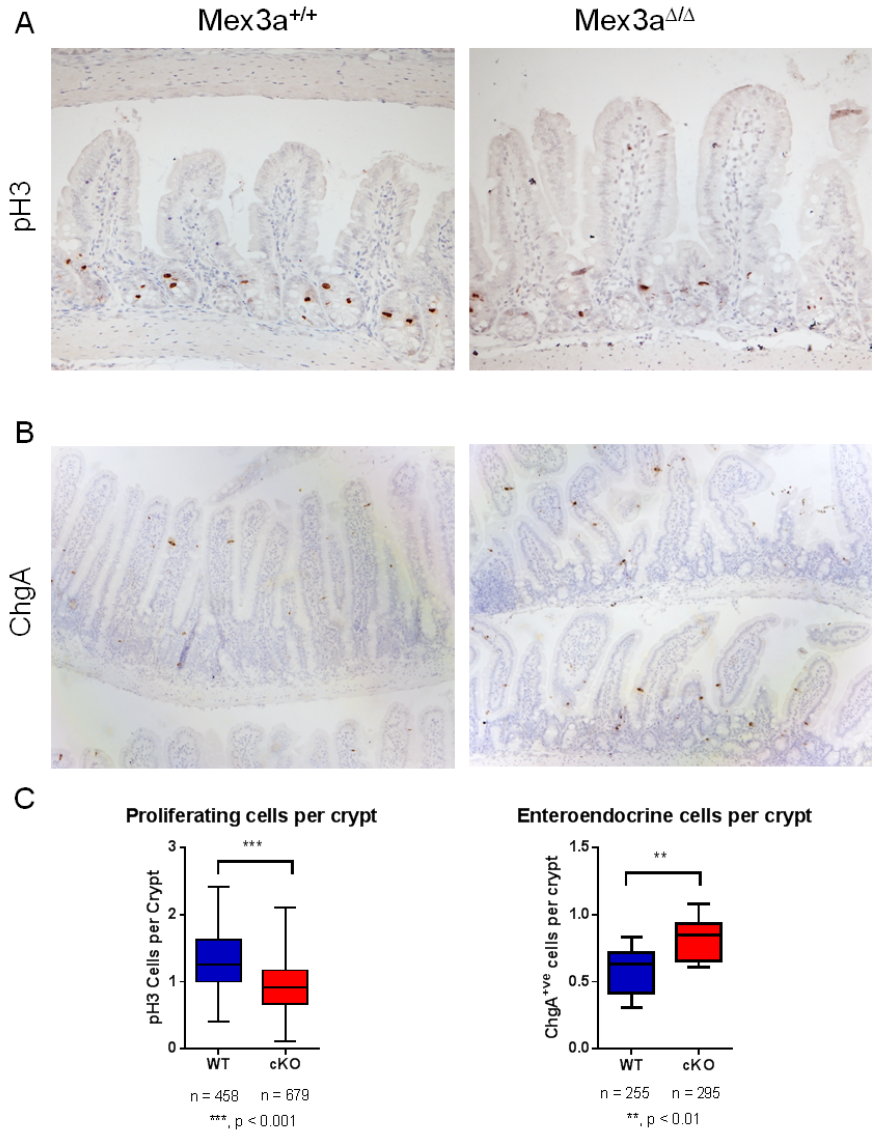

Figure 24: Mex3a KO intestines show mild changes in the number of proliferative and enteroendocrine cells. A. Representative images of pH3 staining of WT and Mex3a KO small intestine. B. ChgA staining of proximal small intestine of WT and Mex3a KO mice. (Magnification A and B 20X). C. Quantification of the pH3 and ChgA staining. The observations have been made in at least two mice of each genotype and analyzing at least 100 crypts of each mouse. Statistical differences were assessed by performing a t-student statistical test. The boxplots show the Min to Max and mean of each condition.

2.6 Mex3a null mice have reduced size during development and present perinatal lethality

Considering the lack of phenotype resulting from the conditional ablation of Mex3a in the adult intestine, we generated mice null for Mex3a in all tissues. To this end, we crossed $Mex3a^{fl/fl}$ mice with a transgenic Sox2-Cre line (Hayashi et al., 2002). This Cre line turned the conditional allele into a null allele in all the cells of the embryo including the germline. After selecting mice bearing the $Mex3a^{\Delta}$ allele, we crossed $Mex3a^{\Delta/+}$ to generate the Mex3a full KO mice ($Mex3a^{\Delta/\Delta}$). After genotyping 100 mice from these crosses we were only able to detect 2 adult Mex3a null mice and only one of these reached adulthood.

We looked into development to determine at which stage the Mex3a null mice were lost. We could detect $Mex3a^{\Delta/\Delta}$ mice by genotyping up to P1, but already at P3 there was a dramatic reduction in their number (**Table 2**). Of note, the penetrance of this phenotype is of over 97% (**Table 2**). The single surviving $Mex3a^{\Delta/\Delta}$ adult mouse showed a clear size reduction compared to its littermates, yet histopathological analysis showed no anatomical defects (data not shown).

Stage	WT observed (expected: 25%)	Het observed (expected: 50%)	Mut observed (expected: 25%)	Total (n)
E8.5	50%	33%	16%	6
E14.5	26.6%	40%	33%	15
E17.5	28%	50%	21%	14
P1	22%	53.6%	24.4%	82
P3	25%	72.2%	2.8%	36
Adults	33%	65%	2%	100

Table 2: Mex3a KO mice present perinatal lethality

When we analyzed the Mex3a null mice at different stages of development we found a size reduction evident from E14.5 up to P1. Despite this size difference there were no gross anatomical abnormalities in Mex3a KO P1 pups. **Figure 26** shows representative P1 mice either WT or null for Mex3a. As was observed during development, Mex3a null mice have reduced body size.

The reasons behind the mortality of these mice still remain to be determined, but we have observed reduced mobility and responsiveness to touch of the KO pups. A likely scenario is that there is culling of the KO mice, which is a behavior widely described for litters with weak pups (Turgeon and Meloche, 2009).

A simple readout of mouse physiology is the presence of liver glycogen, which is accumulated during the final stages of development prior to birth and its required for postnatal survival (Cifuentes et al., 2008). When we analyzed the postnatal livers of Mex3a KO mice, we found almost no traces of glycogen, suggesting either a severe starvation condition or a genetic deficiency in glycogen production (**Figure 26B**). Since these livers were analyzed several hours after birth, we analyzed P1 livers of mice delivered by cesarean birth in order to rule out the effect of postnatal starvation. **Figure 26C** shows that Mex3a KO mice have reduced yet detectable levels of liver glycogen, therefore showing that these mice are able to synthesize this molecule. This data implies that Mex3a KO mice may have metabolic issues.

Of note, both perinatal lethality and size reduction are commonly observed in knockout mice, thus they are not informative on the function of Mex3a (Turgeon and Meloche, 2009). Furthermore, the lethality precludes the analysis of adult stem cells, thus rendering the Mex3a full KO mice as a model suitable only to study embryo development.

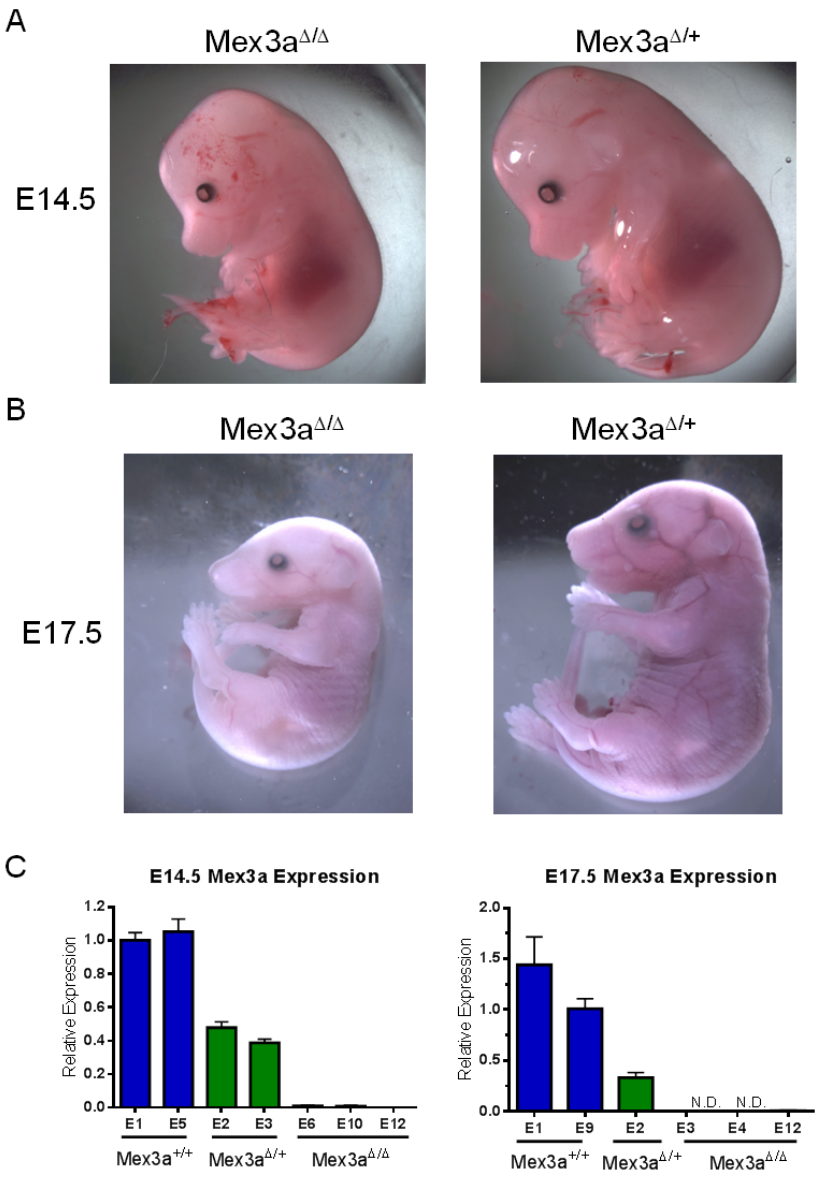

Figure 25: Mex3a KO mice have developmental defects and perinatal lethality. A. Representative images of E14.5 Mex3a$^{\Delta/\Delta}$ and Mex3a$^{\Delta/+}$ embryos. Note the smaller size of the KO embryo. B. E17.5 Mex3a$^{\Delta/\Delta}$ and Mex3a$^{\Delta/+}$ embryos show the same trend than E14.5 trend. C. Mex3a$^{\Delta/\Delta}$ mice have undetectable levels of Mex3a mRNA.

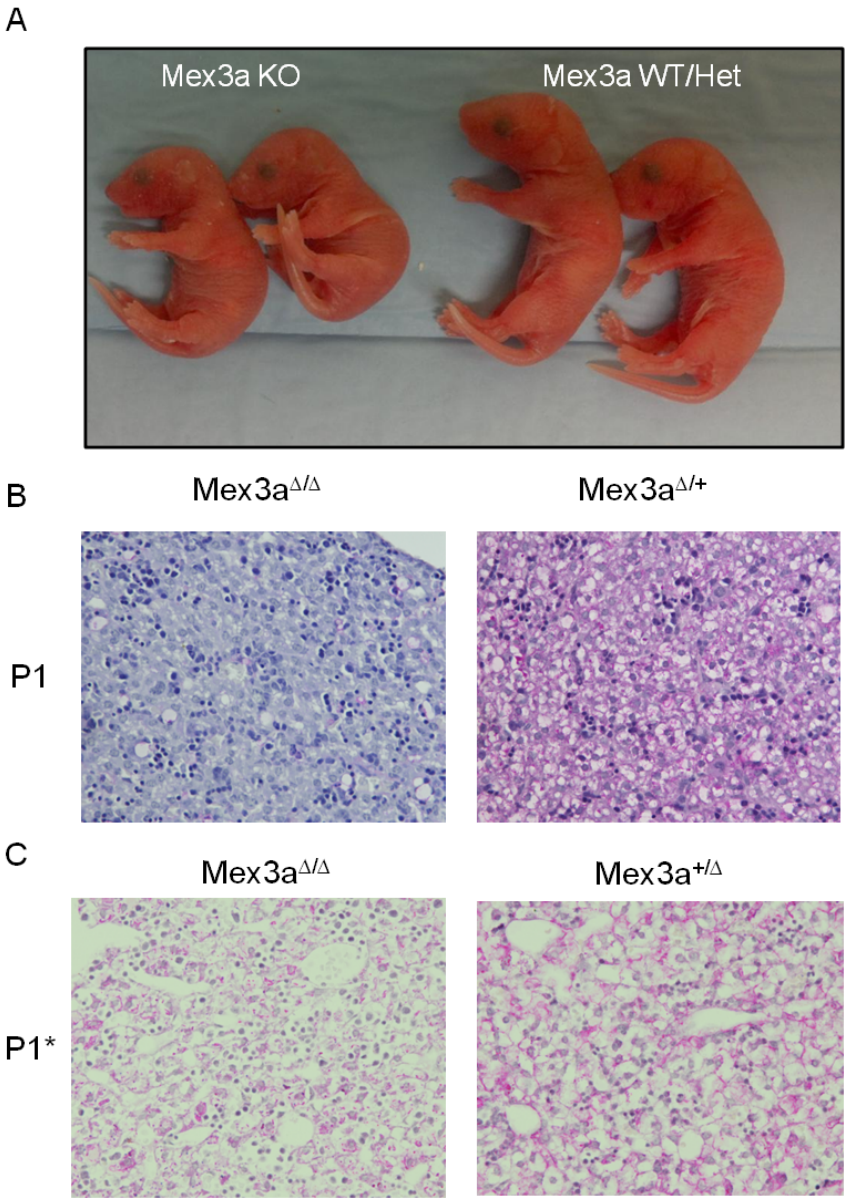

Figure 26: Mex3a KO mice have reduced liver glycogen. A. Picture of representative Mex3a KO P1 mice. Note the smaller size compared to the WT and Het littermates. B. PAS staining of liver sections from P1 mice several hours after birth. Note the lack of staining in the Mex3a$^{\Delta/\Delta}$ mouse. C. PAS staining of liver sections from P1 mice. *, P1 mice delivered by cesarean section. (Magnification of B and C 40X).

2.7 Generation of the Mex3a Knock In allele

We generated a construct bearing a transcriptional reporter for Mex3a consisting on a tdTomato (tandem dimer tomato), followed by a T2A sequence and the Cre-ER^{T2} protein. This reporter cassette was designed to be expressed as a single mRNA, yet the presence of the viral 2A sequence should result in the separation of the tdTomato and Cre-ER^{T2} proteins by promoting the skipping of the peptide bond formation by the ribosome (Hu et al., 2009). The rationale behind this approach was that the Mex3a-driven tdTomato would allow the sorting and profiling of the Mex3a^{+ve} cells in mouse tissues, whereas the Cre-ER^{T2} protein would allow for genetic analysis, including lineage tracing, gene ablation/activation or cell ablation, among other possibilities.

After the transfection of this cassette into ESCs, G418-resistant clones were selected and screened by long-range PCR for integration in the Mex3a locus by homologous recombination. We obtained 4/36 positive clones, 2 of which were later confirmed to bear single integrations in the correct genomic site by Southern blot. Subsequently the Neo cassette was excised by transfection of an FlpO bearing plasmid and clones were screened for the removal of the Neo cassette (3/79 screened). Finally, 2 of these Mex3a KI ESCs were re-confirmed by Southern blotting (**Figure 27B**). These two clones were used for blastocyst injection and chimeras were selected (all of which had over 70% chimerism). These chimeras were then bred with C57/Bl6 mice and the germline transmission of the allele was confirmed for all crosses. **Figure 27** depicts the overall design of the cassette, the final Southern Blot screening and a representative genotyping of a litter bearing the Mex3a KI allele.

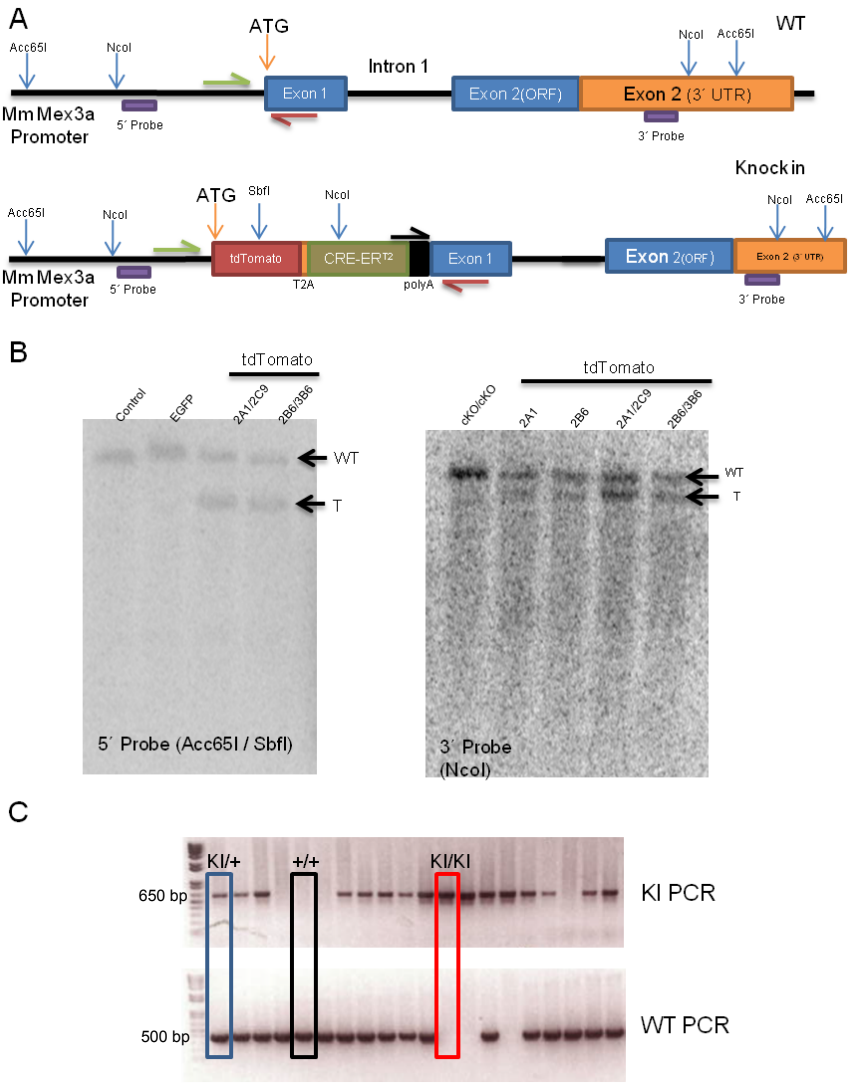

Figure 27: Design and generation of Mex3a KI mice. A. Scheme of the WT locus and the knock-in cassette. B. Southern blot of ESC clones to confirm targeting. The left panel shows the 5´ probe whereas the right panel depicts the 3´ probe of the targeted region. The enzymes used in each case are shown. C. Genotyping of mice bearing the KI allele. The blue box highlights a heterozygous mouse, the black box highlights a WT mouse and the red box points towards a double KI mouse.

2.8 Analysis of Mex3a^{+ve} cells in different tissues

2.8.1 Analysis of intestinal cells

We initially tested whether the Mex3a driven tdTomato was expressed in the intestine. To this end, we analyzed single-cell preparations of small intestines obtained from Mex3a$^{+/+}$, Mex3a$^{KI/+}$ or Mex3a$^{KI/KI}$ mice by FACS.

In order to ensure the detection of the potential Mex3a^{+ve} cells, we discarded debris and cell aggregates and selected for viable epithelial cells. As shown in **Figure 28A**, the intestine of Mex3a$^{KI/+}$ mice contained a population of tdTomato^{+ve} cells. As expected, the frequency of these cells was doubled in Mex3a$^{KI/KI}$ mice.

We then sorted cells with different levels of tdTomato expression (**Figure 28B**) and performed RT-qPCR. **Figure 28C** shows that tdTomato^{High} cells had higher mRNA levels of both Mex3a and Lgr5 than tdTomato$^{Low/Neg}$ cells, whereas the level of the proliferation marker Ki67 was enriched to a much lower extent. These results indicate that the Mex3a^{+ve} population is enriched in ISCs.

2.8.2 Analysis of hematopoietic cells

Analyzing the annotated expression of Mex3a in other tissues, we found that Mex3a was present in mouse bone marrow. We analyzed the existence of Mex3a^{+ve} cells in peripheral blood and bone marrow from Mex3a$^{+/+}$ and Mex3a$^{KI/+}$ mice. We could not detect any tdTomato cells in peripheral blood, yet a population of these cells was readily detectable in the bone marrow (data not shown).

To further characterize the Mex3a cells from bone marrow, we performed FACS staining of well-described hematopoietic surface markers. We analyzed the hematopoietic stem/progenitor cells by discarding lineage specific cells and selecting the cKit / Sca-1 double positive population (LSK cells) (**Figure 29**). We could observe that over 50% of these LSK cells were positive for

tdTomato (**Figure 29C**). This result is in line with the published expression of Mex3a in this system (Konuma et al., 2011) (**Figure 29D**). We analyzed the ability of Mex3a to identify LSK cells and found that 1 out of 7 (1238 / 9268) tdTomato^{+ve} cells were LSK cells. We performed this analysis with Sca-1 and found that 1 out of 22 (2072 / 46104) Sca-1^{+ve} cells were LSK. In comparison with Sca-1, Mex3a seems to be more specific of stem/progenitor cells of the hematopoietic system.

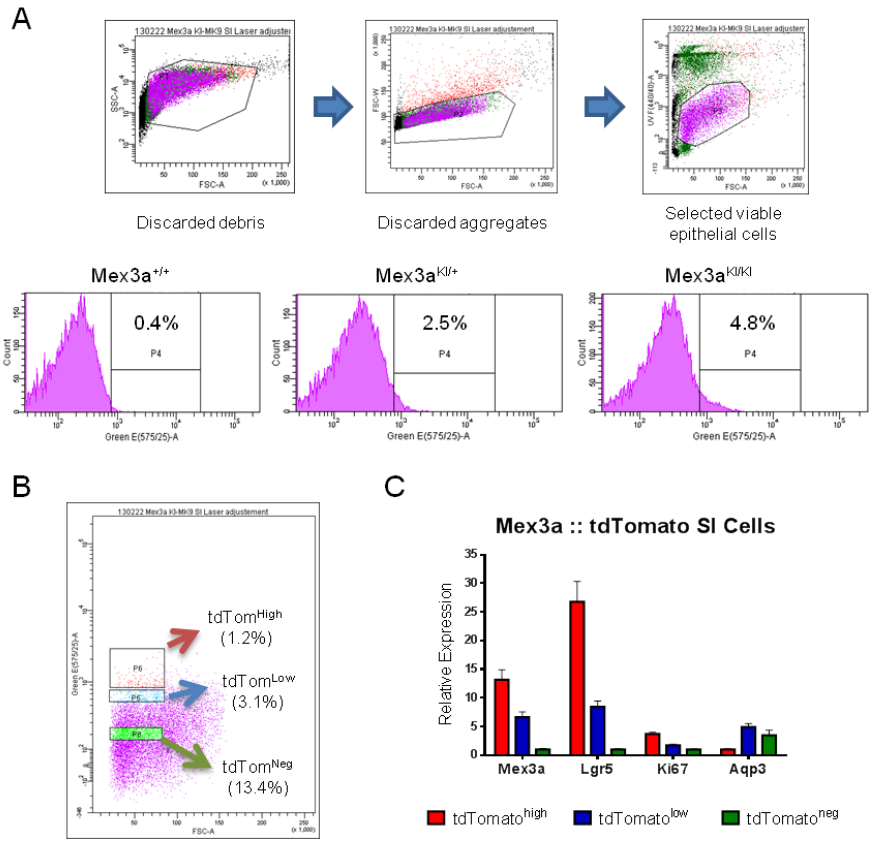

Figure 28: Mex3a::tdTomato cells in the small intestine. A. FACS gating scheme used to identify tdTomato cells in the small intestine cell preparations. B. Populations selected on the basis of size and expression of tdTomato in Mex3a$^{KI/+}$ mice. C. RT-qPCR data of tdTomato sorted cells for selected marker genes.

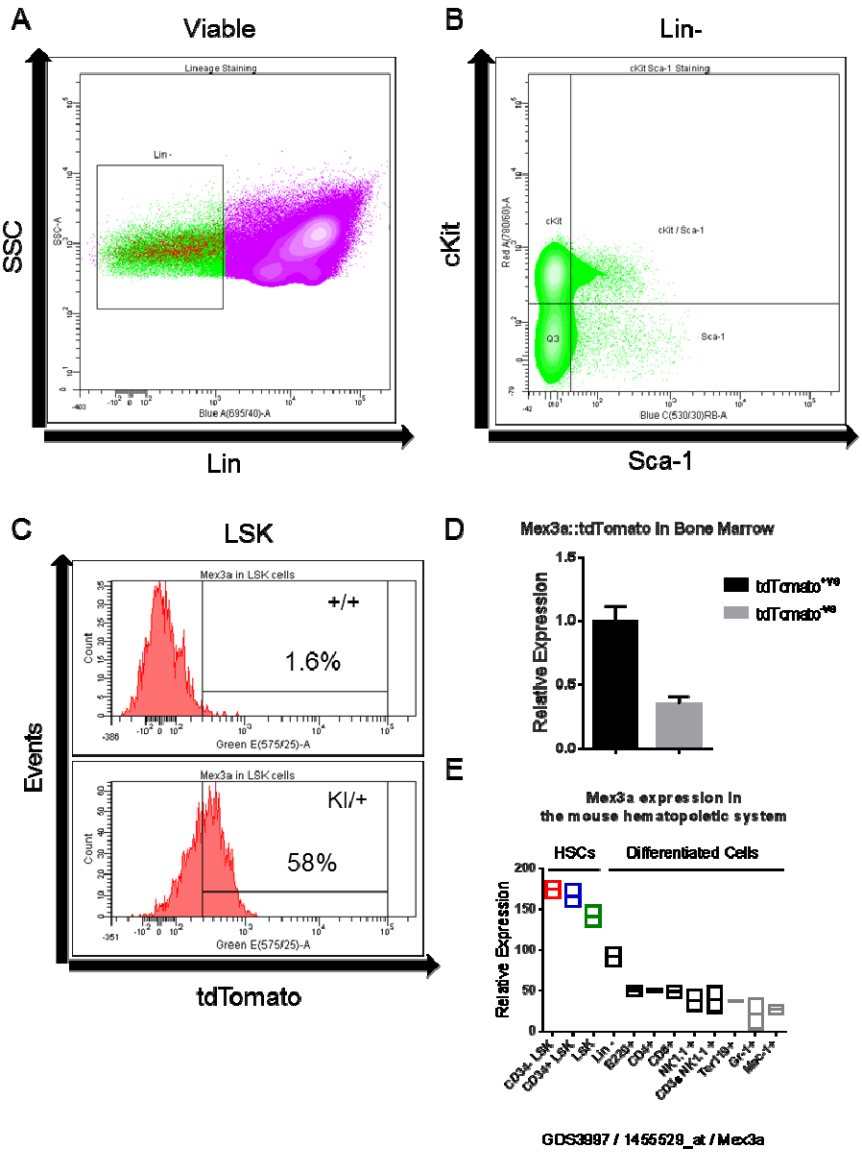

Figure 29: LSK cells express Mex3a. A. Lineage staining of bone marrow cells. The lineage markers used were CD3ε, Gr-1, B220 and Ter119. B. cKit and Sca-1 staining of the Lin$^-$ population from bone marrow. C. tdTomato expression of LSK cells in Mex3a$^{+/+}$ and Mex3a$^{KI/+}$ bone marrow. D. Mex3a expression in unstained bone marrow tdTomato^{+ve} vs tdTomato^{-ve} cells. E. Described RNA expression of Mex3a in different hematopoietic cells. Mex3a is enriched in Stem/Progenitor cells when compared to more differentiated cells. The GEO accession number and microarray probe are shown below the graph.

2.8.3 Analysis of embryonic stem cells

We analyzed the expression of Mex3a in embryonic stem cells. For this we took advantage of the clones bearing the Mex3a KI allele used to generate the Mex3a reporter mice. We could detect the Mex3a-driven tdTomato by fluorescence microscopy on live cultures (**Figure 30A**). This observation is in line with increased abundance of endogenous Mex3a at the mRNA and protein levels when compared to adult tissues (data not shown). By FACS we could detect that over 95% of ESCs were positive for tdTomato (**Figure 30B**).

Previous studies have shown that ESC cultures are actually heterogeneous populations containing cells with low yet detectable levels of differentiation (Marks et al., 2012). To investigate if Mex3a levels could separate cells with different commitment states we sorted tdTomato^{High} and tdTomato^{Low} cells from the Mex3a$^{KI/+}$ ESCs. We analyzed the expression of endogenous Mex3a to validate the reporter allele. To assess stemness we measured the levels of Oct4 and Sox2, as well as Gata6 and T (Brachyury) to measure differentiation. We could observe that the Mex3a allele enriched for the endogenous Mex3a as expected. Moreover, we could detect enrichment of both Oct4 and Sox2 in the tdTomato^{High} cells. Furthermore, the expression of the differentiation genes Brachyury and Gata6 were enriched in tdTomato^{Low} cells (**Figure 30C, D**). Our results show that Mex3a is expressed in ESCs and that its expression correlates with stemness genes in this system.

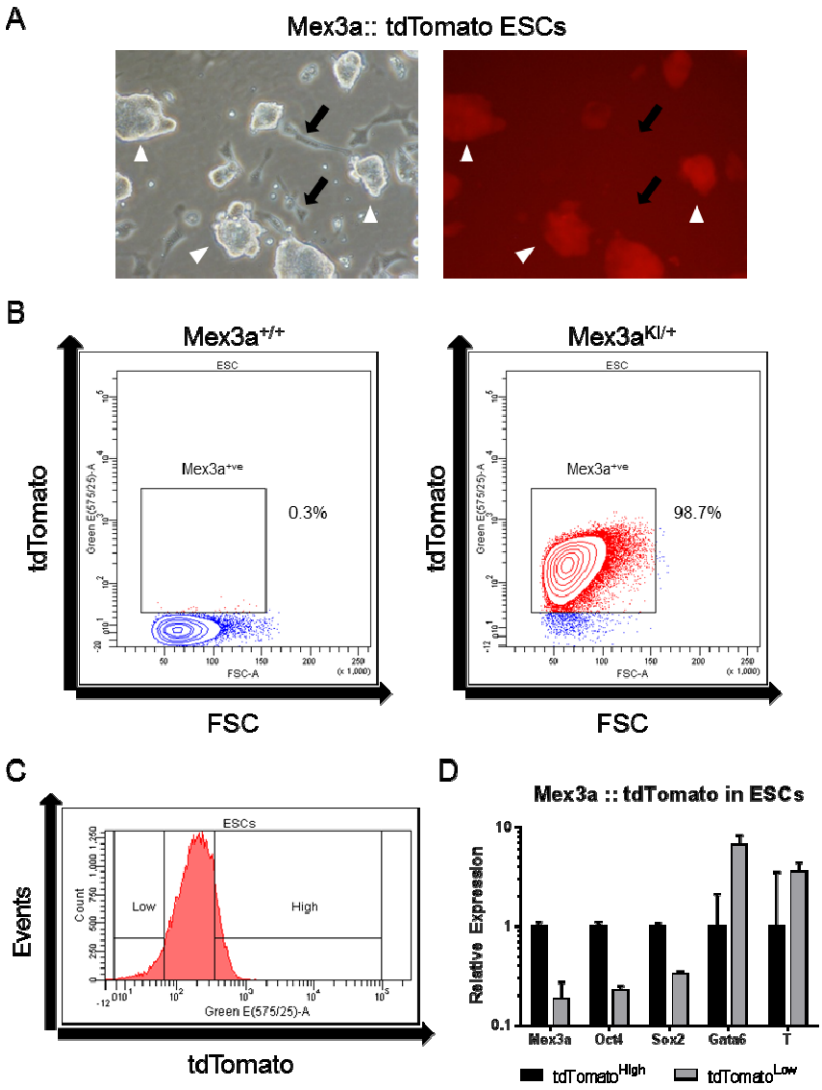

Figure 30: Mex3a is expressed in mouse ESCs and correlates with stemness markers. A. Bright field (left panel) and red fluorescence (right panel) images of live ESCs (white arrowheads) with contaminating feeder cells (black arrows). (Magnification 20X). B. FACS analysis of Mex3a$^{+/+}$ and Mex3a$^{KI/+}$ ESCs. Note that Mex3a is expressed in over 95% of ESCs. C. Sorting gates of tdTomato^{High} and tdTomato^{Low} cells from Mex3a$^{KI/+}$ ESCs (left panel). D. RT-qPCR analysis of stem and differentiation genes in tdTomato sorted populations.

2.9 Characterization of Mex3a^{+ve} cells of the small intestine

To further characterize the identity of intestinal Mex3a^{+ve} cells, we analyzed the transcriptome of tdTomato cells from Mex3a$^{KI/+}$ mice by microarray analysis. **Table 3** shows the genes most enriched in Mex3a^{+ve} cells. This list includes the ISC marker gene Lgr5 as one of most enriched genes in Mex3a^{+ve} cells yet the top positions of this list also contained many genes specific of the secretory lineage, particularly of enteroendocrine cells such as Gcg, Sst, Cck or ChgA (Habib et al., 2012).

The unexpected co-ocurrence of ISC and differentiated cell markers prompted us to further characterize the phenotype of these cells. To this end, we verified by GSEA the overall enrichment of the gene expression signatures that define particular cell types or compartments of the intestinal epithelium. We took advantage of gene signatures built-up from our lab and the Clevers lab in previous studies (van der Flier et al., 2009) and compared the EphB2-ISC, Lgr5-ISC, Proliferation and Late TA expression programs to that of Mex3a^{+ve} cells. As shown in **Figure 31**, Mex3a^{+ve} cells were enriched in ISC-specific genes as well as in expression of the proliferation program. Furthermore, this population is depleted from the late TA signature, which contains most differentiation markers. This data supports that Mex3a cells resemble ISCs despite the expression of endocrine-specific genes.

We also analyzed the Gene Ontology Biological Processes (GO BP) enriched in the Mex3a^{Hi} and in Mex3a^{Neg} cells (**Figure 32**). As expected, genes involved in DNA replication as well as Somatic Stem Cell Maintenance were enriched in Mex3a^{Hi} cells. On the other hand, genes involved in the tricarboxylic acid pathway and sodium ion transport were enriched in Mex3a^{Neg} cells. Overall, our transcriptomic data suggests that tdTomato^{+ve} cells are enriched in ISCs.

Gene Symbol	p-value (High vs. Neg)	Fold-Change (High vs. Neg)
Gcg	0,00	70,82
Afp	0,01	52,62
Sh2d6	0,00	50,75
Hck	0,00	45,88
Sst	0,00	39,75
Dclk1	0,00	34,22
Iapp	0,01	26,85
Rbp4	0,00	25,68
Siglec5	0,00	25,38
Cpe	0,00	23,83
Cck	0,00	23,80
Chgb	0,00	20,87
Tph1	0,00	20,43
Ghrl	0,00	20,23
Pnliprp2	0,00	20,02
Trpm5	0,00	19,48
Alox5ap	0,00	19,16
Lgr5	0,01	17,09
Gng4	0,00	16,91
Peg3	0,00	16,90
Pla2g2f	0,01	16,84
Vwa5b2	0,00	16,00
Thbs1	0,01	15,92
Nts	0,03	15,79
Spib	0,00	15,49
Chga	0,00	14,28

Table 3: Genes most enriched in Mex3a::tdTomato cells.

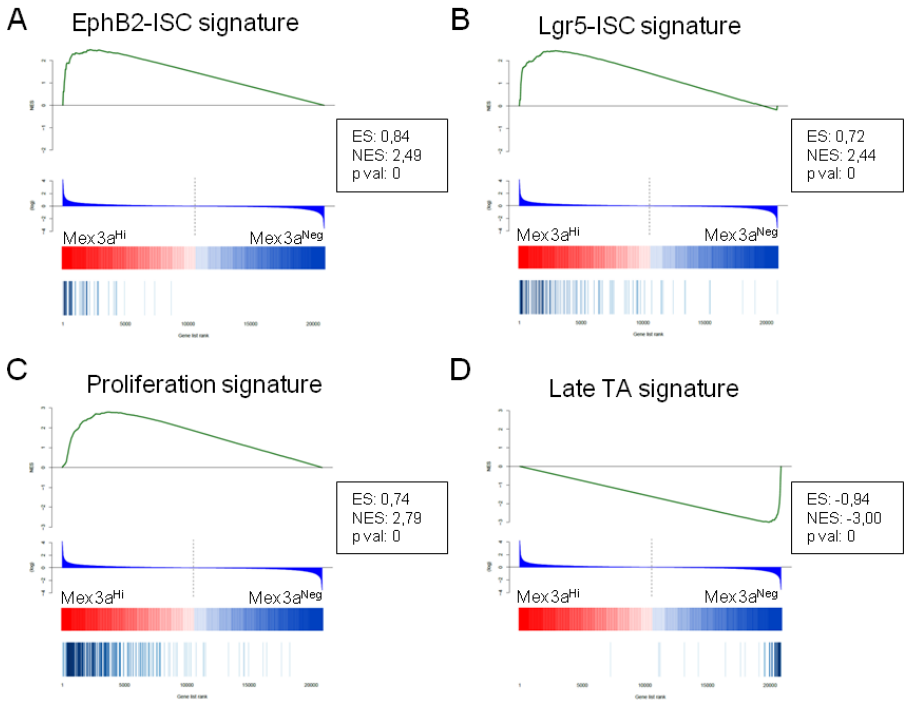

Figure 31: GSEA of Lgr5 and EphB2 derived signatures in Mex3a::tdTomato populations. A,B. Enrichment profile of the EphB2 and Lgr5 ISC signatures in Mex3a^{+ve} cells. C. The EphB2 derived proliferation signature is enriched in Mex3a^{+ve} cells. D. Late TA genes are depleted from Mex3a^{+ve} cells.

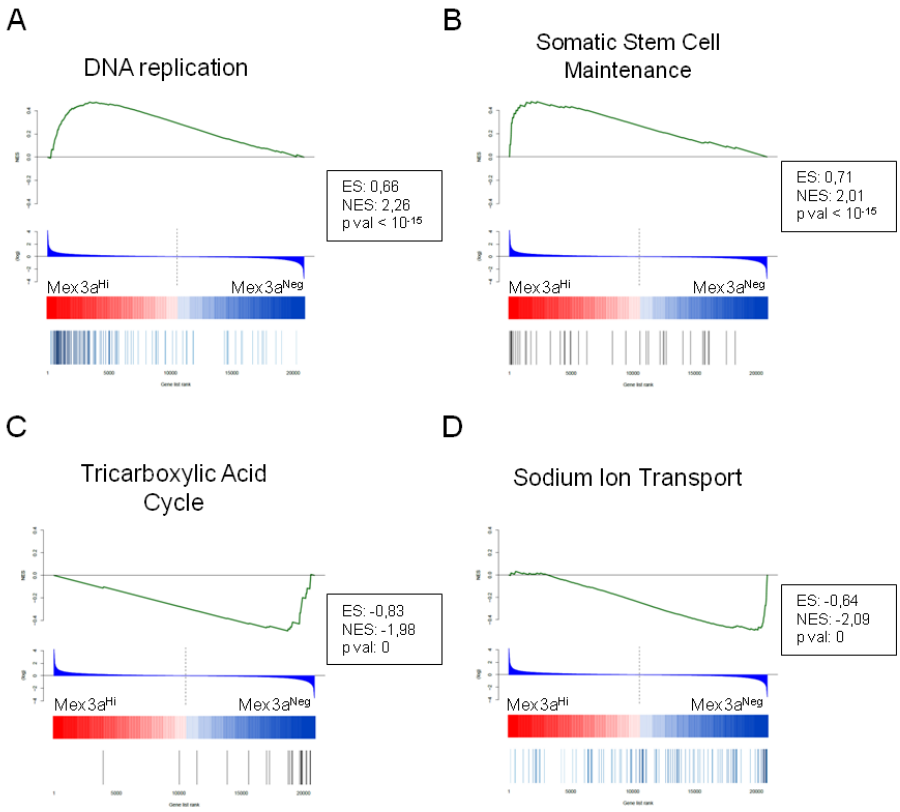

Figure 32: GSEA of Gene Ontology Biological Processes overrepresented in Mex3a^{Hi} and Mex3a^{Neg} cells. A. Enrichment in DNA replication genes in Mex3a^{High} cells. B. Enrichment of Somatic Stem Cell Maintenance genes in Mex3a^{High} cells. C. Enrichment of genes of the tricarboxylic acid cycle in Mex3a^{Neg} cells D. Enrichment of sodium ion transport genes in Mex3a^{Neg} cells.

2.9 Mex3a^{Hi} cells are enriched in LRC genes

A recent study by Doug Winton characterized the identity of intestinal label-retaining cells (LRCs) through the use of an H2B-YFP reporter gene (Buczacki et al., 2013). These cells were described to be a subpopulation of relatively quiescent Lgr5^{+ve} cells that have already committed to the enteroendocrine or Paneth cell lineage. Upon damage to the epithelium this cell population was able to revert to an ISC phenotype (Introduction Section 2.4).

As shown in **Table 3**, Mex3a^{High} cells express both ISC-specific and enteroendocrine-specific genes. This suggested a potential link of Mex3a cells to the aforementioned intestinal LRC. To test this possibility, we took advantage of the published data and defined a stringent LRC signature obtained from LRC cells (H2B-YFP^{+ve}) and comparing these to both purified Paneth cells (UEA-Lectin^{+ve}) as well as Low Crypt Cycling cells (LCCs) (H2B-YFP^{-ve}). The LRC genes were defined as those enriched at least 2 fold over Paneth cells and also at least 3 fold enriched over LCCs. This led to a final list comprised of 61 genes we defined as the LRC common signature.

We then analyzed by GSEA how these LRC genes were distributed in the different crypt cell populations: EphB2^{High} vs EphB2^{Med}, Mex3a^{High} vs Mex3a^{Low} and Lgr5^{High} vs Lgr5^{Low}. As shown in **Figure 33**, the LRC common signature was enriched in Mex3a^{Hi} cells and to a lower extent in EphB2^{Hi} cells. Interestingly, these LRC genes were randomly distributed in Lgr5^{Hi} and Lgr5^{Low} cells. From these results, we tentatively conclude that the EphB2^{Hi} cells encompass both Mex3a^{Hi} and Lgr5^{Hi} cells. On the other hand, LRC-specific genes are randomly distributed in the Lgr5^{Hi} and Lgr5^{Low} fractions. Finally, Mex3a^{Hi} cells are enriched in the LRC expression program.

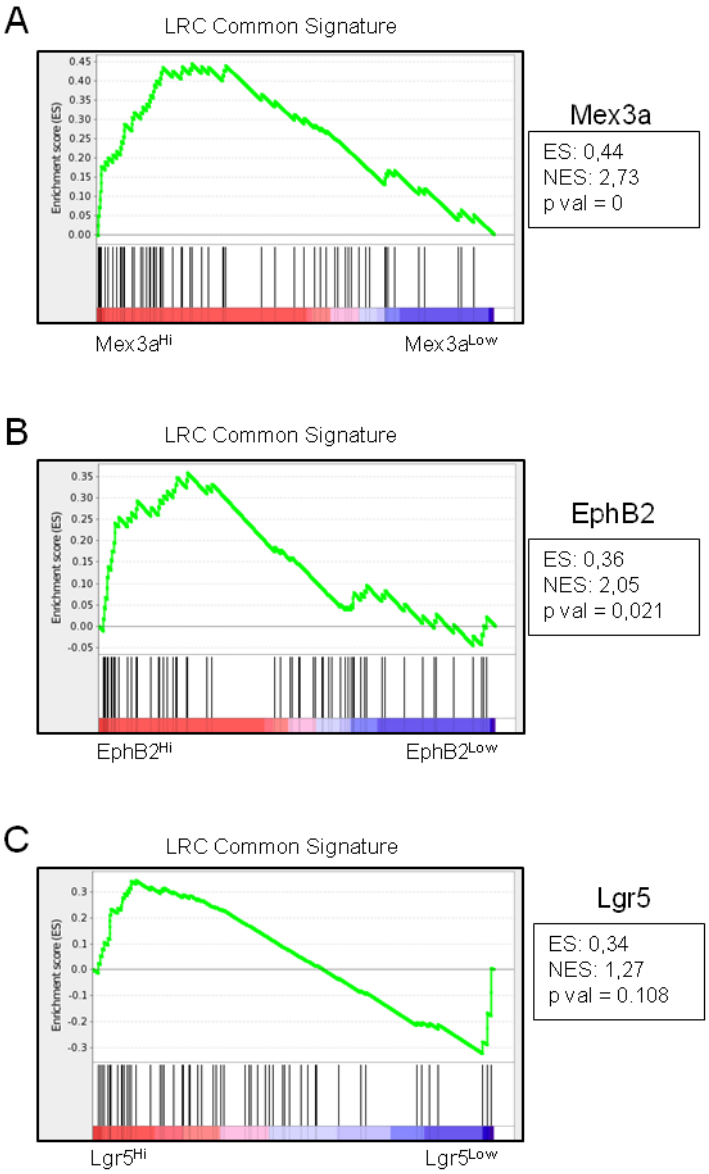

Figure 33: GSEA analysis of LRC common genes. GSEA of LRC common genes in Mex3a High vs Low signature (A), EphB2 High vs Medium signature (B) and Lgr5 High vs Low signature (C).

2.10 Mex3a and Lgr5 show differential behavior to stress

The link of Mex3a cells with LRCs led us to analyze their behavior under stress conditions. We treated mice with 6Gy of ionizing radiation (IR). This dose is sufficient to induce apoptosis to Lgr5^{+ve} cells (van Es et al., 2012; Yan et al., 2012) and trigger the phenotypic reversion of Dll1^{+ve} progenitor to ISCs (van Es et al., 2012).

72 hours after this regime, we quantified the number of tdTomato cells in the proximal small intestine. In parallel, we performed the same analysis on Lgr5 mice. As shown in **Figure 34,** Mex3a^{+ve} cells show an increased resistance to IR than Lgr5 at this dose. These data reinforce the notion that Mex3a cells comprise a population of relative radioresistant cells that behave differently than Lgr5^{+ve} cells. We speculate that Mex3a^{+ve} cells may hold similarities to LRCs.

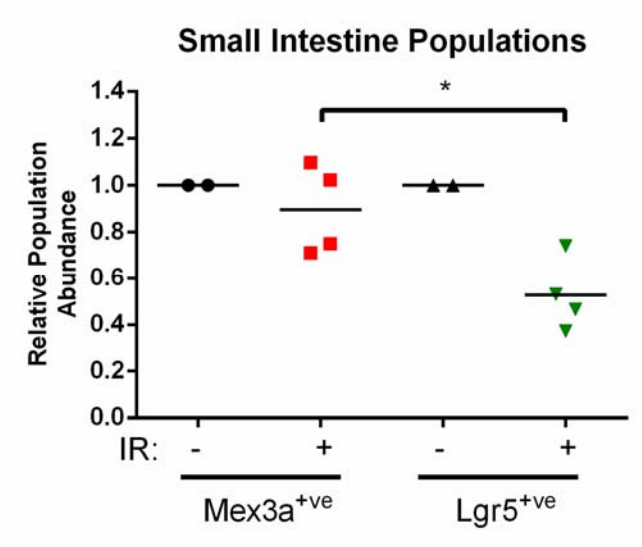

Figure 34: Response to IR of Mex3a and Lgr5 cells. Relative abundance of tdTomato^{+ve} or GFP^{+ve} cells 72 hours after a 6 Gy IR treatment. Populations were normalized to untreated mice. *, $p < 0.05$ in a one-way ANOVA statistical test.

2.11 Lineage tracing from the Mex3a knock in allele

In order to characterize the behavior of the Mex3a population, we performed lineage-tracing analysis by breeding Mex3a-KI with the ROSA-LSL-LacZ reporter mice. We analyzed the expression pattern of LacZ after Tamoxifen treatment and compared to that of Lgr5-Cre-ER^{T2}. Unfortunately, these experiments were not conclusive.

3 days upon treatment of Lgr5-Cre-ER^{T2} mice with Tamoxifen, we could observe the typical ribbon-like stainings from the crypt base to the villus tip that comprise stem cells and their progeny (data not shown). In contrast, we could not observe labeled cells or clones in Mex3a-KI mice at any time point. The exception was the sporadic observation of few LacZ labeled cells at the base of the crypt. One of the few positively stained crypts are shown in **Figure 35**. Yet, this staining was not consistent across all mice and time points, which precluded conclusion about the localization or behavior of the Mex3a population. We speculate that the Cre-ERT2 cassette knocked in the Mex3a locus may not be fully functional. Alternatively, not enough recombinase might be expressed to allow effective tracing due to the low transcriptional activity of the endogenous Mex3a locus.

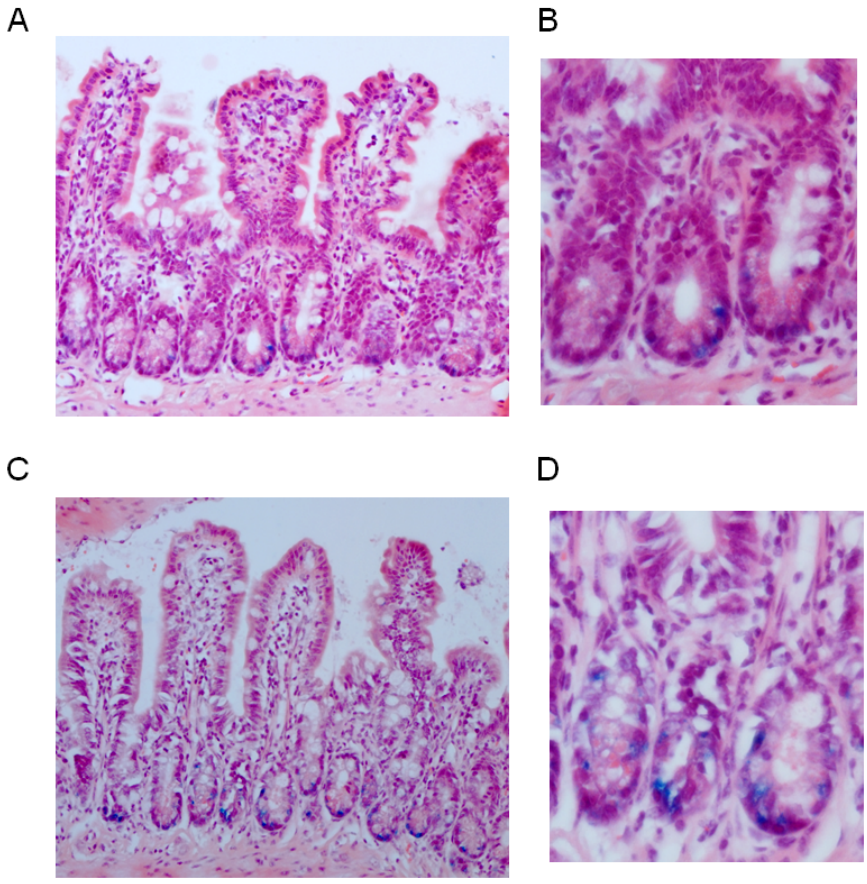

Figure 35: Mex3a-driven lineage tracing in the intestine. A,C. Representative images from a Mex3a-driven tracing 18 hours after tamoxifen induction. (Magnification 20X). B, D. Higher magnification images from A, C. Note that the labeled cells are only located in crypts (Magnification 40X).

2.12 Mex3a$^{KI/KI}$ mice have reduced levels of Mex3a and present growth impairment

To further characterize the role of Mex3a, we turned to the use of mice homozygous for the Mex3a KI allele. By analyzing the mRNA levels of Mex3a in intestinal crypts derived from these mice we demonstrated a strong reduction (>50 fold) when compared to heterozygote mice. Of note, sorted Mex3a::tdTomato cells from the KI/KI mice still express some levels of Mex3a mRNA implying that the coding region is transcribed to some extent despite the insertion of the reporter cassette at the ATG (**Figure 36A**). This leakage could be explained by the presence of an in-frame ATG in codon 8 that could drive translation from any read-through transcription after the polyA of the cassette.

Mex3a$^{KI/KI}$ mice were viable with only a slight reduction in the expected Mendelian ratios (**Figure 36B**). These mice presented size reduction in a fashion reminiscent to the observed for the Mex3a full KO pups (**Figure 36C**). This phenotype was present in around 50% of KI/KI mice. Despite the reduced body weight, the residual production of Mex3a protein in Mex3a$^{KI/KI}$ mice appears to be sufficient to rescue the perinatal lethality observed in the full KO mice (Section 2.6, Table 2). We concluded that the Mex3a$^{KI/KI}$ mice behave as hypomorphs of the Mex3a function.

We used the Mex3a$^{KI/KI}$ mice to explore the function of Mex3a. We purified tdTomato^{+ve} cells and obtained their expression profiles. Of note, since Mex3a$^{KI/KI}$ mice have 2 copies of the reporter allele, we adjusted the sorting gates to select the equivalent population we sorted from Mex3a$^{KI/+}$ mice. **Table 4** shows the genes most differentially expressed between Mex3a$^{KI/+}$ and Mex3a$^{KI/KI}$ cells. The loss of Mex3a seems to induce the upregulation of cell cycle related genes as well as mitochondrial genes. These observations suggest a potential role for Mex3a in the regulation of proliferation and metabolism. As noted before, Mex3a cells express LRC-specific genes and LRCs are a slow dividing subpopulation of Lgr5^{+ve} cells. These observations prompt us to speculate that Mex3a might regulate genes that affect the proliferation rate and metabolism of LRCs.

A

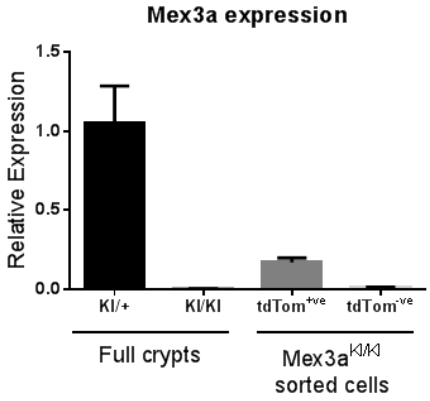

B

WT (25%)	Het (50%)	Mut (25%)	Total (n)
38%	45%	17%	122

C

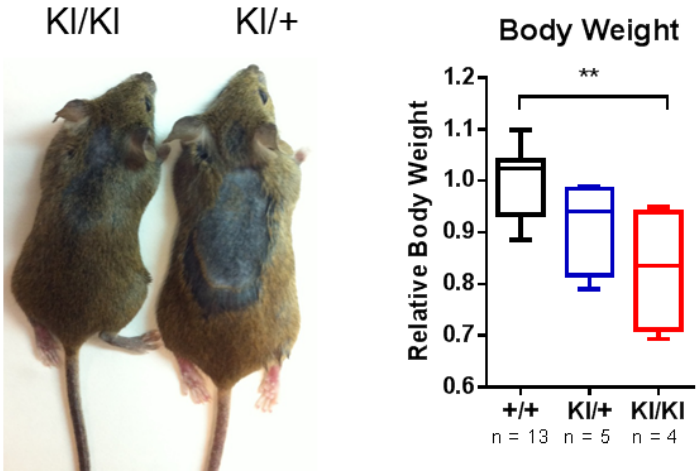

Figure 36: Mex3a Kl/Kl mice have a reduced body size. A. Expression levels of Mex3a in intestinal tissue. The full crypts of Mex3a$^{KI/KI}$ mice have very low levels of Mex3a, yet the sorted Mex3a::tdTomato cells have detectable levels. B. Mex3a KI mice are viable albeit with slightly reduced Mendelian ratios. C. Mex3a$^{KI/KI}$ mice present a reduction in body weight and overall size. **, p value < 0.01 in a one way ANOVA.

Gene Symbol	p-value	Fold-Change (WT High vs. Mut High)
Serinc3	0,01	4,88
Cyp2b10	0,03	4,59
Zbtb16	0,02	3,22
Gpt2	0,01	3,07
Adcy5	0	3,04
Dclk1	0,02	2,83
2010012P19Rik	0	2,73
Siglec5	0,03	2,65
9430012M22Rik	0,03	2,61
Aldh1l2	0,02	2,6
Mrpl54	0	2,59
Basp1	0,01	2,56
Gm9930	0	2,54
Mapk1ip1l	0	-3
Fubp3	0,01	-3,1
Plk4	0,02	-3,11
Pdzd8	0,01	-3,14
Ndufab1	0	-3,17
Snrpf	0,01	-3,18
Chchd6	0,04	-3,23
Klhl9	0	-3,26
Ppp1r2	0,01	-3,28
Dfna5	0,02	-3,38
Slc25a32	0,01	-3,38
Dars	0,01	-3,38
Yme1l1	0,01	-3,38
Hspa9	0	-3,49
Tsn	0,02	-3,52
Hddc3	0	-3,57
Vamp7	0,01	-3,71
Tial1	0,03	-4
Foxn2	0,02	-4,11
Scn2b	0	-4,14
Dkc1	0,03	-4,26
2810417H13Rik	0,01	-4,44
Ndufab1	0	-6,12
Hist1h2ab	0	-22,6

Table 4: Genes differentially expressed in tdTomato^{High} Mex3a$^{KI/+}$ and Mex3a$^{KI/KI}$ cells.

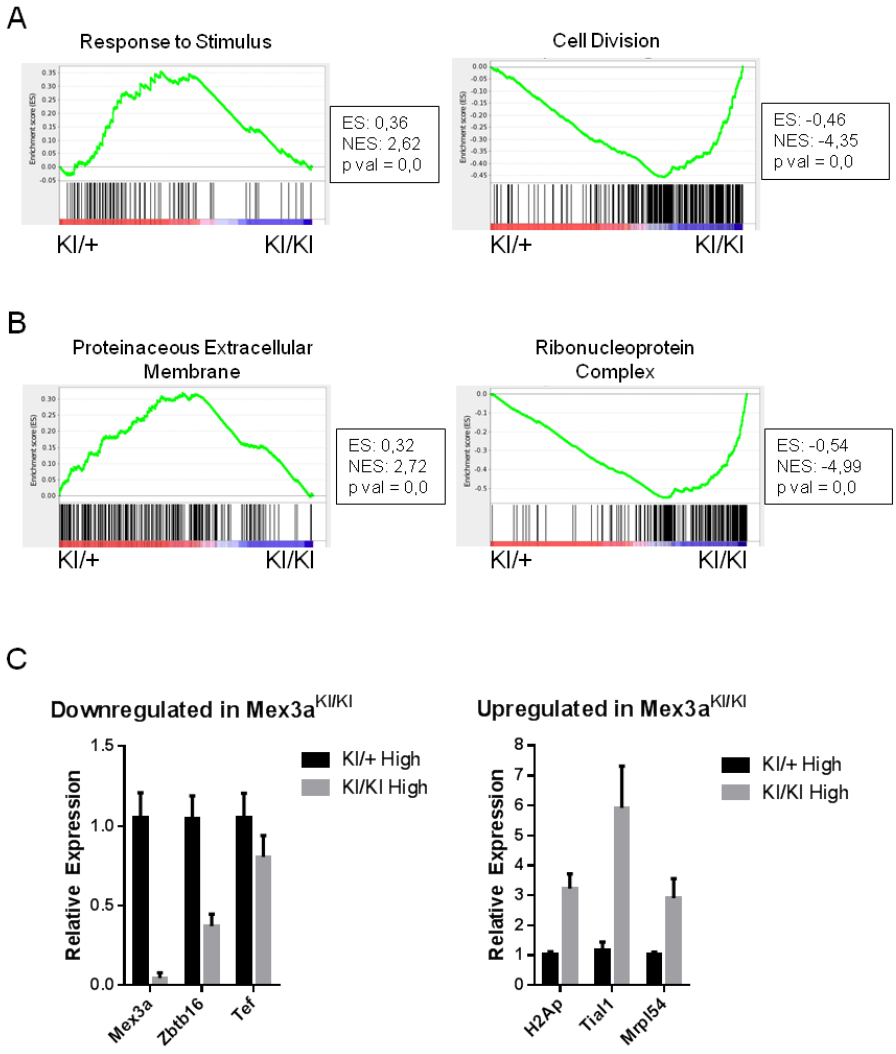

Figure 37: GSEA analysis of genes deregulated in Mex3a deficient cells. A,B. PreRanked GSEA of the top GO Biological Processes and Cellular Components enriched in Mex3a$^{KI/+}$ and Mex3a$^{KI/KI}$ cells. C. RT-qPCR validation of selected genes differentially expressed in the microarrays from Mex3a$^{KI/+}$ and Mex3a$^{KI/KI}$ cells.

2.13 Mex3a is required for efficient *in vitro* ISC self-renewal

Having not found an evident phenotype in Mex3a deficient intestines, we turned to a system more amenable to manipulation. We took advantage of the possibility of expanding ISCs *in vitro* (Sato et al., 2009). In these culture conditions, mouse ISCs generate organoids composed of all differentiated cell types (Intestinal Organoid culture) as described in Chapter 1.

A variation of this method consists in enhancing Wnt signaling through the addition of Wnt3a conditioned media. This produces a shift of the culture towards a stem/progenitor phenotype (Stem/Progenitor Culture) (**Figure 38A**). These Stem/Progenitor conditions generate spheroid-like cultures similar to that of Apc-mutant ISCs (Sato et al., 2011).

When we analyzed the expression of Mex3a in the Stem/Progenitor cultures, we observed an increase at both the mRNA and protein level compared to the Intestinal Organoid system (**Figure 38B, C**). We reason that this effect is the consequence of the increased frequency of ISCs induced by Wnt3a supplementation.

We then cultured Villin Cre-ER^{T2}; Mex3a$^{+/+}$ or Villin Cre-ER^{T2}; Mex3a$^{fl/fl}$ ISCs from age and sex-matched mice. Stem/Progenitor cultures were then treated with 1 μM 4-OH Tamoxifen for 48h, and then passaged by mechanical disaggregation. The cultures were then followed from 48h to 96h and their re-seeding capacity was assessed by quantifying the number of stem-like spheroids growing in WT and KO conditions.

In these conditions, we observed a reduction of around 3 fold in the frequency of stem-like spheroids expanded from Mex3a deficient cells. Considering the variability of the system and the inherent inaccuracy of the 3D culture models, we performed all experiments at least in triplicate per condition in at least 4 biological replicates (**Figure 39**).

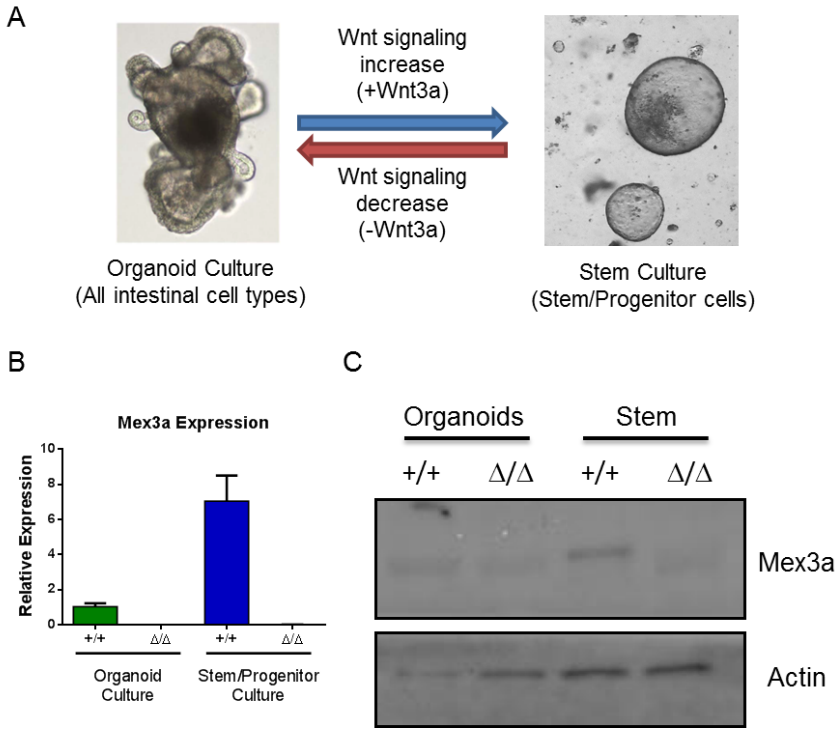

Figure 38: *In vitro* models for ISC studies. A. Diagram of the culture conditions that either mimic the intestine (organoid) or enriches in stem/progenitor cells through the increase in Wnt signaling in the media. The organoid culture picture is adapted from (Sato et al, 2010). B. Mex3a expression increases in stem conditions at the mRNA level. C. Mex3a protein is enriched in stem cultures.

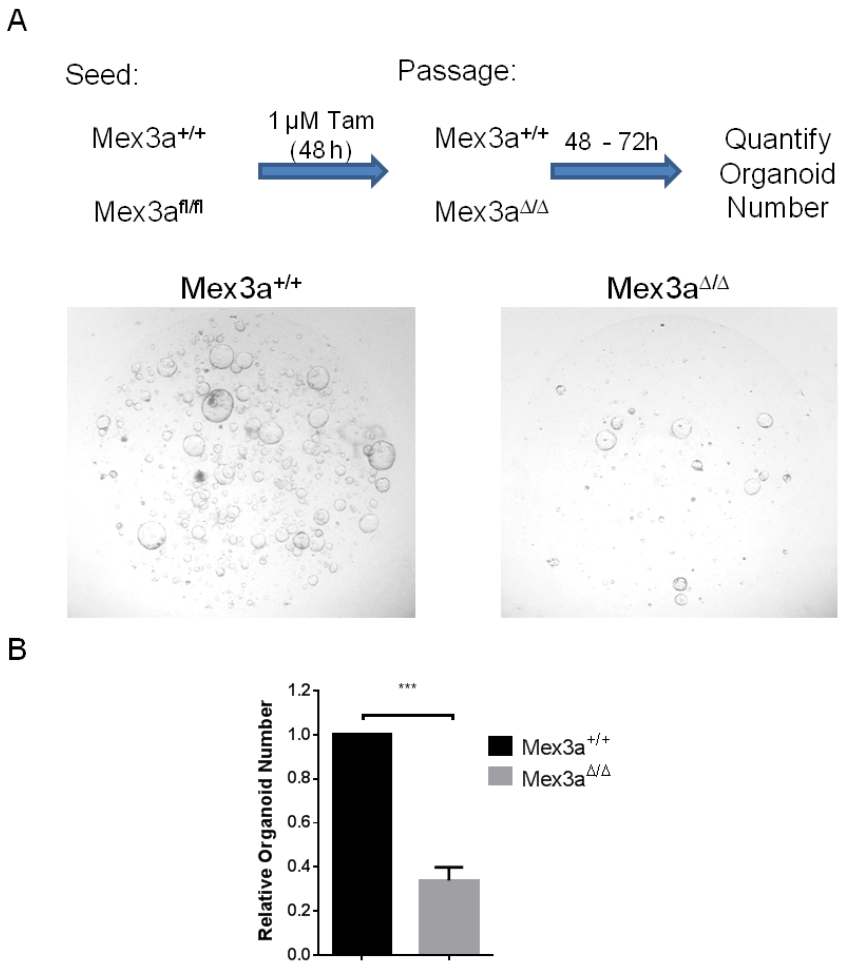

Figure 39: Loss of Mex3a reduces the ability of ISCs to propagate *in vitro*. A. Experimental setup to determine the effect of Mex3a ablation on ISC cultures. The lower panels are representative images of the WT and KO ISC cultures at the time of quantification. B. Quantification of organoid number in WT and KO ISC cultures (10X magnification). The data represents the normalized number of organoids in 4 different experiments with at least 3 matrigel drops of each genotype per experiment. ***, p value < 0.01

To understand the molecular basis of the ISC impairment caused *in vitro* by Mex3a deletion, we analyzed the transcriptome and proteome of the ISC cultures after tamoxifen treatment. To determine the more direct effects of Mex3a deletion, this analysis was performed at early time points before growth impairment was evident. The transcriptomic changes after Mex3a deletion were analyzed by microarrays and the top genes up and downregulated are shown in **Table 5**. Our analysis indicated that several of the top downregulated genes upon Mex3a deletion are ISC genes (e.g. Lgr5, Ptpro, Rgmb). We tentatively concluded that either Mex3a deficiency causes reduced expression of ISC genes or that the Mex3a null cultures contained decreased number of ISCs. This effect occurs without triggering intestinal differentiation.

Downregulated mRNAs in Mex3a KO ISCs

Gene Symbol	p-value (KO vs. WT)	Fold-Change (KO vs. WT)
Lgals6	0,004836	-32,10
2810417H13Rik	0,039915	-3,19
Esrrg	0,048149	-2,33
Ifitm1	0,048247	-2,24
Nfia	0,012349	-2,22
C1ra	0,028825	-2,07
Galc	0,009006	-1,97
B4galnt4	0,034241	-1,96
Rgmb	0,039597	-1,93
Lrig1 (intron)	0,012135	-1,89
Mex3a	0,047175	-1,88
C79468	0,037335	-1,81
Bhlha15	0,001493	-1,79
Qser1	0,022936	-1,79
Lass4	0,032978	-1,79
Dscc1	0,029830	-1,78
Casp8ap2	0,039813	-1,77
Lgr5	0,025639	-1,72
Glcci1	0,031735	-1,70
Ptpro	0,029072	-1,70
Klhl23	0,013273	-1,70
Srl	0,004245	-1,70
Mcm10	0,024157	-1,69
Slco3a1	0,017882	-1,69
Enpp4	0,038088	-1,66

Upregulated mRNAs in Mex3a KO ISCs

Gene Symbol	p-value (KO vs. WT)	Fold-Change (KO vs. WT)
Ctgf	0,003891	3,86
Krt4	0,028616	2,97
Tpm2	0,013385	2,67
Tspan2	0,039462	2,56
8430408G22Rik	0,040833	2,44
Ly6c1	0,006922	2,37
Slc25a48	0,046250	2,33
Hspa1b	0,040291	2,29
Ahnak	0,044755	2,20
Amotl1	0,013663	2,12
Mtap9	0,024319	2,11
Col4a1	0,024630	2,08
5830408B19Rik	0,007360	2,07
Samd5	0,009358	2,04
Serpinb9b	0,039731	2,00
Slc7a11	0,044957	1,99
Stxbp1	0,026853	1,98
Cadm1	0,049218	1,96
Tnfrsf23	0,031261	1,95
Fetub	0,005096	1,91
Plod2	0,022873	1,85
Ldhd	0,030518	1,83
Basp1	0,005401	1,83
S100a14	0,009107	1,83
Serpinb5	0,001437	1,80

Table 5: Transcriptomic changes 48 hours after Mex3a deletion in ISC cultures.

2.14 Proteomic analysis of Mex3a KO ISC cultures

Mex3a is an RNA binding protein with not known nuclear function (Buchet-Poyau et al., 2007; Courchet et al., 2008). Thus, we reasoned that all the transcriptomic effects observed *in vitro* upon deletion of Mex3a are only indirectly linked to the loss of Mex3a activity. In order to identify events directly regulated by Mex3a we performed proteomic analysis (**Table 6**).

Control and Mex3a KO ISC cultures established from age and sex-matched mice were treated in parallel. We identified about 1000 proteins in each sample, yet only 652 of them were present in all triplicate samples of the experiment. Of these common proteins, 38 of them were differentially expressed after comparing Mex3a WT and KO cultures. Upon a preliminary analysis, it was evident that most of these proteins were involved in mitochondrial biology and metabolic processes. It is important to point out that the proteomic approach used is biased to highly abundant proteins, therefore it is likely that changes in lowly expressed genes were not detected.

Downregulated proteins in Mex3a KO ISCs

Uniprot ID	p.value	Fold change
ATPK_MOUSE	0,00476	-3,12
VDAC1_MOUSE	0,02703	-2,76
H4_MOUSE	0,01724	-2,56
ODPB_MOUSE	0,02238	-1,91
PROF1_MOUSE	0,02075	-1,79
GALK1_MOUSE	0,02933	-1,73
PPBI_MOUSE	0,01473	-1,69
MTAP_MOUSE	0,02360	-1,64
PLCB3_MOUSE	0,00916	-1,59
LAMC1_MOUSE	0,01660	-1,36
CADH1_MOUSE	0,01045	-1,32
IF6_MOUSE	0,01908	-1,14
IMPA1_MOUSE	0,03354	-1,13

Upregulated proteins in Mex3a KO ISCs

Uniprot ID	p.value	Fold change
DEST_MOUSE	0,04126	2,38
BAX_MOUSE	0,02185	2,30
ERO1A_MOUSE	0,02252	2,26
PGM1_MOUSE	0,04442	1,99
VDAC3_MOUSE	0,00560	1,84
ARF3_MOUSE	0,01562	1,79
STML2_MOUSE	0,00927	1,60
ALDH2_MOUSE	0,03321	1,58
VASP_MOUSE	0,02568	1,48
TLN1_MOUSE	0,00284	1,47
RAB1A_MOUSE	0,00310	1,47
EF1G_MOUSE	0,04744	1,46
ERLN2_MOUSE	0,00218	1,42
PDC6I_MOUSE	0,01943	1,40
ARP2_MOUSE	0,01253	1,39
TOM7_MOUSE	0,04170	1,35
RL18A_MOUSE	0,04584	1,35
C1TC_MOUSE	0,02580	1,33
1433G_MOUSE	0,01641	1,32
TCPD_MOUSE	0,02527	1,29
ACADL_MOUSE	0,00231	1,29
EFTU_MOUSE	0,01889	1,29
CATA_MOUSE	0,01892	1,28
PLAK_MOUSE	0,00266	1,24
SRSF1_MOUSE	0,03680	1,23

Table 6: Proteomic changes 48 hours after Mex3a deletion in ISC cultures.

2.15 Generation of Mex3a-inducible colon cancer cell lines

To dissect the function of Mex3a in detail we turned to cell lines. We used the well-studied cell line LS174T. These cells share several features with normal ISCs at the transcriptional level (Van de Wetering et al., 2002) (Whissell and Batlle, unpublished).

We generated stable cell lines bearing doxycycline-inducible versions of TAP-tagged WT and mutant Mex3a (**Figure 40A**). In particular, we disrupted the two putative functions of Mex3a: RNA binding and E3 ubiquitin-ligase activity. To disrupt the RNA binding of Mex3a we generated the G240D point mutation that targets a residue in the second KH domain and is conserved in the C elegans mex-3 protein. To disrupt the E3 ligase domain we generated the C469G mutation that disrupts the first cysteine of this domain. The C469G mutation should disrupt the binding of one of the Zn^{+2} ions required for the E3 ligase activity (Deshaies and Joazeiro, 2009). Finally, we generated a truncated version of Mex3a that spans from the start codon to the end of the second KH domain (we refer to this truncated protein as ΔRING).

We analyzed the performance of our system in basal conditions and observed comparable expression of Mex3a between parental, control vector and uninduced cells (data not shown). 16 hours after doxycycline induction we could detect the increase in Mex3a mRNA (**Figure 40B**) as well as exogenous Mex3a protein (**Figure 40C**). Interestingly, we found that Mex3a mutants G240D and C469G had reduced levels of expression when compared to WT and ΔRING forms of Mex3a.

We studied the kinetics of WT Mex3a accumulation and assessed protein cellular localization by immunofluorescence (**Figure 40D**). Exogenous Mex3a was readily detectable after 16 hours of induction and was localized in the cytoplasm of cells. It was evident that Mex3a was present in granules of varying size and intensity (**Figure 40E**). In contrast, the Mex3a mutant forms displayed diffused patterns in the cytoplasm.

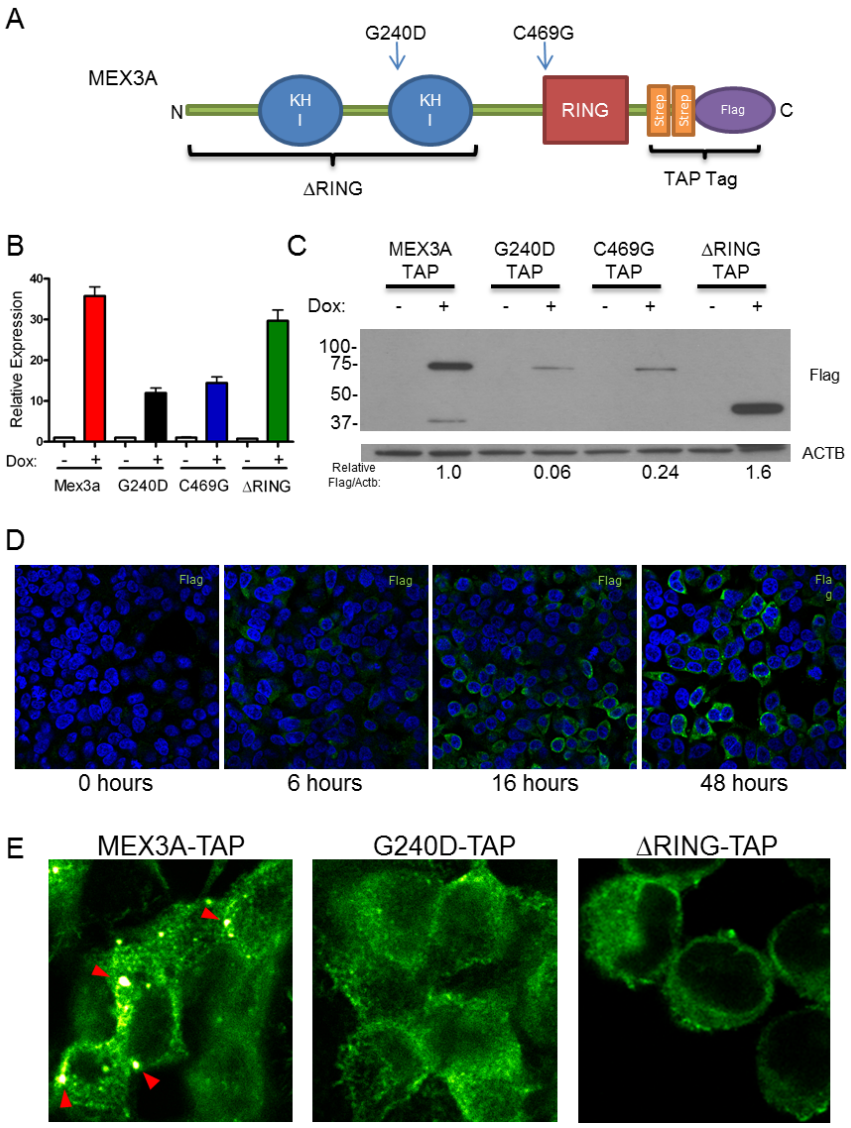

Figure 40: Generation of an inducible system for Mex3a WT and mutant expression in CRC cells. A. Diagram of the Mex3a protein designed with the C terminal TAP Tag. The arrows point towards two point mutations: G240D (RNA binding mutant) and C469G (RING finger mutant). A truncated version of Mex3a was also generated (named ΔRING TAP). B. mRNA induction of the different constructs after 16 h induction with 1 µg/mL Dox. C. Western blot of flag tag for the same conditions shown in B. D. Induction kinetics of WT Mex3a-TAP assessed by IF. Note that by 16 hours the protein is readily detectable in the cytoplasm of cells and apparently excluded from nuclei. Magnification 40X. E. Higher magnification pictures of flag immunofluorescence for WT MEX3A, G240D and ΔRING overexpression.

Note that WT Mex3a forms granular structures (red arrowheads) not present in the mutant forms. Magnification 100X.

2.17 Mex3a acts as a translational enhancer in tethering assays

To study whether Mex3a has a role in translational regulation we performed tethering assays. This assay is based on the interaction of the MS2 coat protein (MS2cp) with the MS2 RNA loop. With this system we analyzed the effect of chimeric MS2cp-MEX3A on the post-transcriptional regulation of the Firefly luciferase (FLuc) reporter fused to MS2 RNA loops in the 3´UTR.

We cloned both the WT human Mex3a protein and the RING finger mutant (C469G) in frame with a C-terminal TAP Tag and the MS2 coat protein (MS2cp) (**Figure 41 A, B**). Both the WT and C469G fusion proteins were expressed to similar extent (**Figure 41C**). We then tested the ability of these constructs to modify the activity of the FLuc reporter compared to the MS2cp and/or luciferase reporter alone. **Figure 41D** shows that WT Mex3a enhanced FLuc activity and that this enhancement required an intact RING finger.

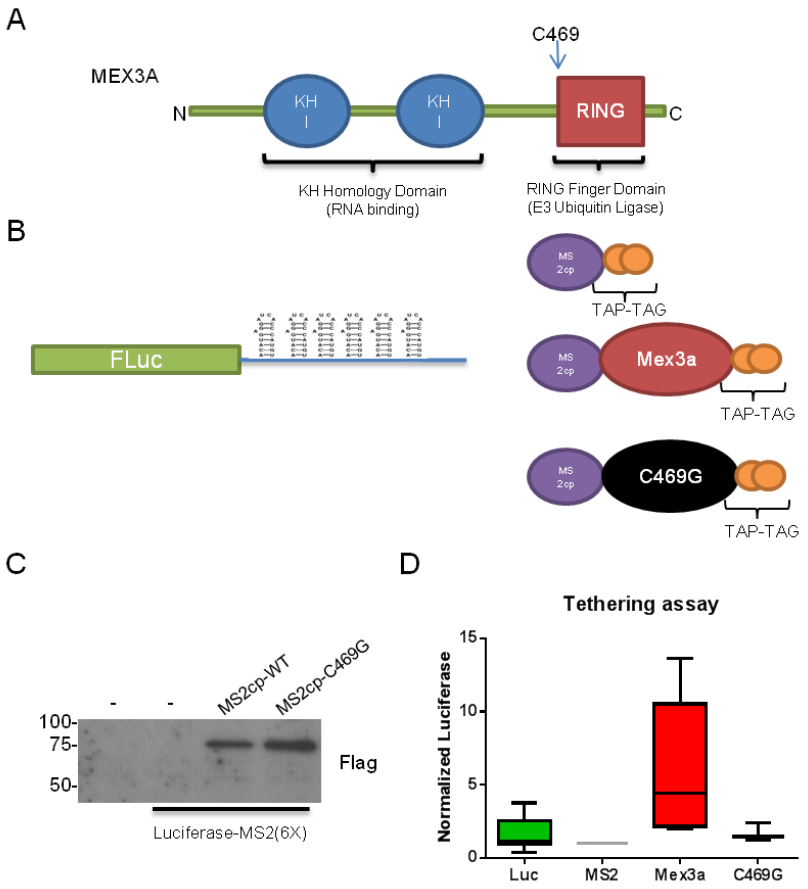

Figure 41: Mex3a acts as a translational activator in 293T cells. A. Diagram of the Mex3a protein highlighting the C469 residue present in the first Zn finger of the RING domain. B. Scheme of the MS2 based tethering assay. MS2 loops are cloned in the 3´ UTR of the firefly luciferase and exposed to fusion proteins of the gene of interest (WT or mutant) and the MS2 coat protein. The interaction between the coat protein and the RNA loop will recruit the protein of interest to the 3´UTR of the luciferase gene. C. Western blot showing that the MS2cp fusion proteins are expressed in 293T cells to a similar extent after transfection. D. Relative luciferase activity when the assay is performed with the constructs shown in B (n = 6).

2.18 Mex3a-bound mRNAs in colon cancer cells

We decided to study the potential mRNA targets of Mex3a. To this end we performed RNA-binding protein immunoprecipitation (RIP) as described for other RNA binding proteins (RBPs) (Keene et al., 2006; Tenenbaum et al., 2002).

The protocol follows steps similar to that of a standard immunoprecipitation, but varying the lysis protocol and introducing RNAse free conditions. After the pulldown the RNA bound to Mex3a is purified and used for cDNA synthesis or other applications.

Our experimental setup consisted of 3 conditions: LS174T induced control cells (Control + Dox), LS174T uninduced Mex3a cells (Mex3a – Dox) and LS174T induced Mex3a cells (Mex3a + Dox). We performed RIP of these samples and extracted their corresponding input samples. The RNAs bound to Mex3a as well as the control RIPs and inputs were hybridized to Human Exon Arrays to generate a more accurate idea of the overall mRNA regions bound by Mex3a. As described for most RNA binding proteins, Mex3a binding was considerably enriched towards the 3´UTR of its targets compared to the enrichment found in the ORF or 5´UTR of the mRNAs (data not shown).

Figure 42A shows the top mRNAs bound by Mex3a. It is to be noted that the enrichments are normalized to the corresponding input of each pulldown. Only those RNAs bound specifically to the LS174T pTRIPz Mex3a + Dox condition (but not the control conditions: Control + Dox and Mex3a – Dox) are considered for all subsequent analysis. We validated several of our microarray data targets by repeating the RIP experiment and analyzing by RT-qPCR the enrichment to WT Mex3a and the G240D mutant as a negative control (data not shown).

We performed GSEA of all GO categories. We found that several aspects of RNA biology as well as DNA damage response are over-represented in the Mex3a targets (**Figure 42B**).

A

Probeset ID	Gene Symbol	Fold Enrichment (RIP vs Input)
3343229	EED	95,691
3537830	ACTR10	64,883
3340725	UVRAG	61,910
2566652	MITD1	60,995
3137881	GGH	60,545
2862752	GFM2	56,266
2812307	PPWD1	49,173
3103511	TMEM70	49,168
3521584	UGGT2	48,465
3598819	SMAD6	48,034
2546299	TRMT61B	47,571
3214380	AUH	47,555
3185090	UGCG	47,487
2348936	CDC14A	47,408
2866563	CETN3	47,105
3430403	C12orf23	44,857
3591050	HAUS2	44,562
3898231	ESF1	44,126
2551705	PIGF	44,101
2866552	CETN3	43,640
3139964	LACTB2	41,443
3282607	MPP7	40,607
3625398	DYX1C1	40,117
2456811	BPNT1	39,859
2734081	AGPAT9	39,342
3137896	GGH	38,836
3280005	PTPLA	38,774
3493438	C13orf34	38,740
2566662	MITD1	37,475
3150805	MRPL13	37,228
2382380	DEGS1	37,072
3106299	OSGIN2	36,613
2704219	PDCD10	36,120
2566660	MITD1	35,936
3629582	PARP16	35,849
2709793	BCL6	35,848

B

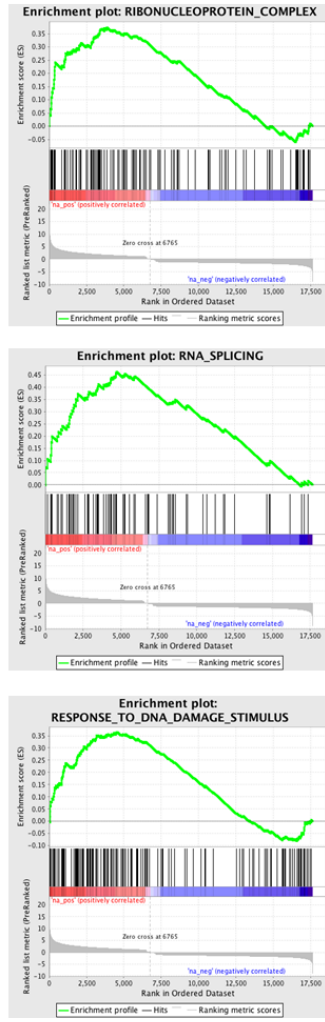

Figure 42: Mex3a targets in LS174T colon cancer cells. A. Table listing the top mRNAs bound by Mex3a in LS174T cells. The fold change refers to the RIP vs input. All targets shown have specific enrichment to Mex3a and no enrichment in the control conditions B. GSEA analysis of GO categories enriched in Mex3a RIP targets. Three representative plots are shown.

2.19 Mex3a regulates EED at the protein level

The top target of Mex3a in LS174T cells is the gene EED. This gene is a central member of the PRC2 (polycomb repressive complex 2), which establishes the H3K27me3 repressive mark on chromatin (Margueron et al., 2009; Margueron and Reinberg, 2011; Montgomery et al., 2005; Montgomery et al., 2007). This protein complex has been shown to be essential in ESC multipotency (Montgomery et al., 2005) and also in hair-follicle stem cell biology (Ezhkova et al., 2009).

The regulation of EED is complex and it has been described that the EED mRNA is able to generate 4 isoforms of EED termed EED1, EED2, EED3 and EED4 (Montgomery et al., 2005; Montgomery et al., 2007). These are the product of alternative translation initiation sites which include non-canonical valines for EED1 and EED2 (Kuzmichev et al., 2004). The different EED proteins have been described to form variations of the PRC2 chromatin remodeling complex (Kuzmichev et al., 2004; Kuzmichev et al., 2005). Despite these observations, no functional differences have been found in KO models of each EED isoform (Ura et al., 2008).

We validated the interaction of Mex3a with the Eed mRNA by RIP followed by RT-qPCR. We used the G240D mutant as a control for the specificity of this binding (**Figure 43A**).

When we analyzed the EED protein in our cell culture system we could detect all 4 isoforms (**Figure 43B**), yet the relative abundance of the isoforms was cell line-dependent (data not shown). We then knocked down Mex3a with an inducible shRNA and saw an effect on a single isoform of EED, EED2 (**Figure 43B**). This was not due to differences in EED mRNA levels (**Figure 43C**).

We analyzed the predicted subcellular localization of these isoforms by using different algorithms. Interestingly, we found that MitoProtII predicted the mitochondrial localization of EED2, but not for the other isoforms (**Figure 44A**). We performed mitochondrial enrichment from LS174T cells and assessed the levels of EED in

Mex3a control and knockdown cells. We found that EED2 was enriched in mitochondria in a Mex3a-dependent manner (**Figure 44B**). Of note, a recent publication validates our observations by showing that EED has mitochondrial localization through its interaction with the mitochondrial kinase PINK1 (Berthier et al., 2013).

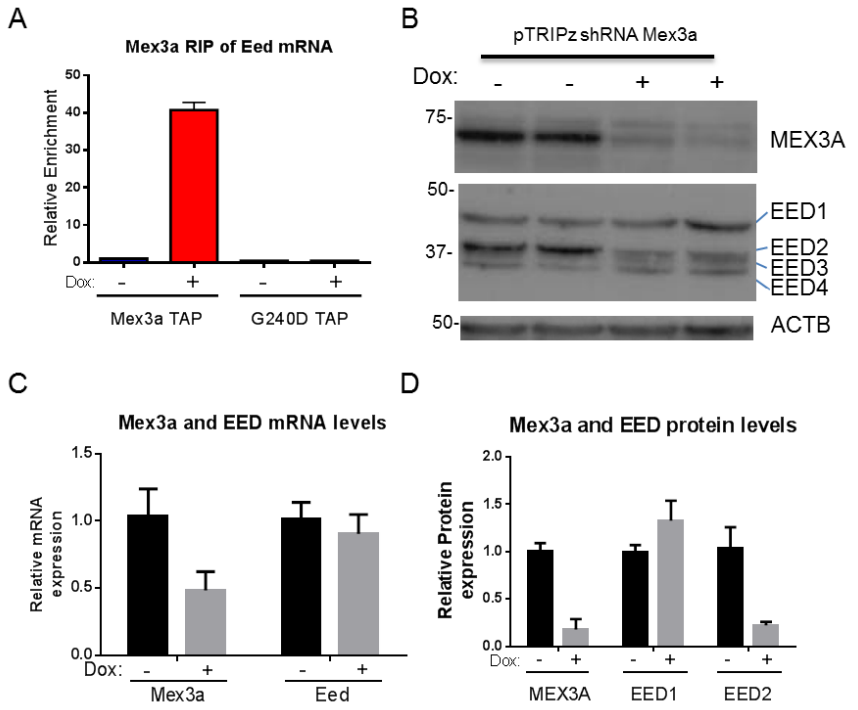

Figure 43: EED2 is regulated by Mex3a. A. RT-qPCR of RIP performed from WT and RNA binding deficient (G240D) Mex3a. Note the specific enrichment in the WT pulldown when Mex3a-TAP is expressed. B. Mex3a knockdown cells show reduced levels of the second isoform of EED. C. Mex3a knockdown does not affect Eed mRNA levels when analyzed by RT-qPCR in LS174T cells. D. Quantification of the western blot from panel B. Values are normalized to actin.

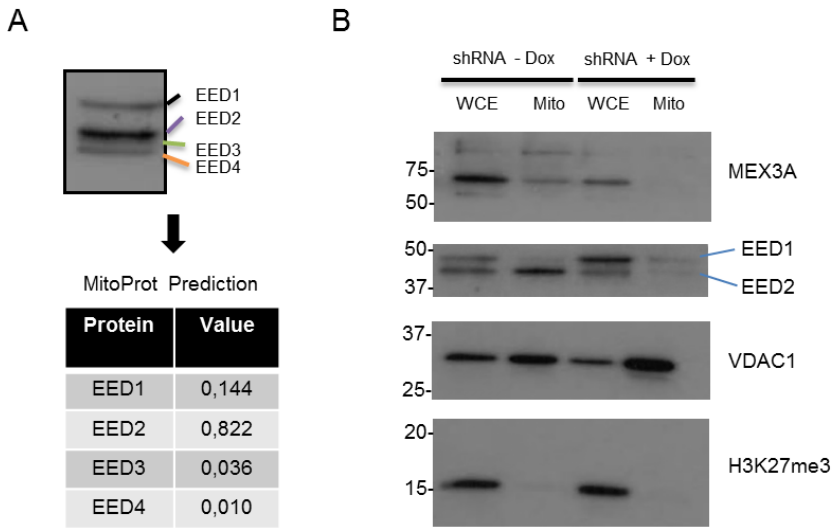

Protein	Value
EED1	0,144
EED2	0,822
EED3	0,036
EED4	0,010

Figure 44: **EED2 is a mitochondria-enriched protein with Mex3a-dependent expression.** A. MitoProtII prediction of the different EED isoforms. The upper panel shows a representative western blot where all EED isoforms are visible. The lower panel shows the predict MitoProtII scores (Value > 0.5 indicates mitochondrial localization). B. Western blots of EED in Mex3a control and knockdown cells. Note that in these conditions only EED1 and EED2 are visible. VDAC1 is a mitochondria-specific protein and H3K27me3 is a nuclear-specific protein. WCE: whole cell extract. Mito: mitochondria-enriched extracts.

2.20 Searching for Mex3a interactors

We next probed the potential protein interactors of the Mex3a protein. To this end, we performed a standard streptactin pulldown of the Strep-Tagged Mex3a protein in LS174T cells and analyzed by mass spectrometry the co-eluting peptides as previously described (Gloeckner et al., 2007; Gloeckner et al., 2009).

We considered Mex3a interactors those proteins with at least 2 unique peptides present in our pulldown (Mex3a + Dox condition) that in turn were absent in the control pulldown (Control + Dox condition). **Table 7** shows the most reliable interactors detected through our approach. The putative interactors of Mex3a were several well-described RNA binding proteins (e.g. HuR/Elavl1, UPF1 and XRN2) and components of the mitochondrial translation machinery (e.g. DAP3, ICT1 and MRPS27). The interaction with UPF1 would suggest that Mex3a is in P bodies and may have a function related to non-sense mediated decay. On the other hand the link with the mitochondrial translation machinery is potentially interesting when put into context with the proteomics data of the Mex3a KO ISC cultures.

		Unique Peptide Count	
Protein ID	Gene Symbol	CV	Mex3a-TAP
A1L020	MEX3A	0	27
B4DP59	DAP3	0	5
Q15717	ELAVL1	0	5
Q92552	MRPS27	0	5
Q92900-2	UPF1	0	5
Q9H0D6	XRN2	0	4
E9PN17	ATP5L	0	3
Q13895	BYSL	0	3
Q9H9J2	MRPL44	0	3
F5H0B8	SART3	0	3
B4E241	SFRS3	0	3
O95994	AGR2	0	2
F8VPD4	CAD	0	2
A6NKA3	COPE	0	2
E7ESJ9	DLAT	0	2
Q9BS26	ERP44	0	2
P31942-3	HNRNPH3	0	2
Q14197	ICT1	0	2
P42704	LRPPRC	0	2
Q9HCE1-2	MOV10	0	2
Q9Y3B7	MRPL11	0	2
P49406	MRPL19	0	2
Q9NWU5-2	MRPL22	0	2
Q9BYD3-2	MRPL4	0	2
F8VZJ2	NACA	0	2
Q9Y2X3	NOP58	0	2
Q8WWY3-3	PRPF31	0	2
F8WF32	RPN1	0	2
G3XAL9	SLC12A2	0	2
Q9Y5L4	TIMM13	0	2
F5H0B0	TPD52	0	2
Q6UXN9	WDR82	0	2

Table 7: Interactors of Mex3a in LS174T cells

2.21 Mex3a interacts with HuR

Our top interactor in the mass spectrometry analysis was HuR (Elavl1). This protein is a RBP involved in stress response and has been shown to have both positive and negative effects on the mRNAs that it binds. These effects occur at various levels such as splicing, translation and RNA stability (Mukherjee et al., 2011).

Analysis of HuR knock-out mice indicates that HuR deficiency is deleterious to progenitor cells of both the hematopoietic system and small intestine. This phenotype is due to the ectopic activation of p53 in the absence of HuR, which regulates Mdm2 levels (Ghosh et al., 2009). Of note, $HuR^{\Delta/+}$ mice had an increased sensitivity to DNA damage, providing a link to stress responses.

Given the interesting characteristics of HuR, we decided to validate the interaction of this gene with Mex3a. For this purpose we performed immunoprecipitation of Mex3a and probed for the presence of HuR. As can be observed in **Figure 45A**, exogenous Mex3a is able to interact with endogenous HuR, thus confirming our mass spectrometry data.

When we tested the interaction of HuR with mutant forms of Mex3a we saw a clear loss of binding with the G240D mutant, suggesting that the interaction between Mex3a and HuR is mediated by RNA (**Figure 45B**). Alternatively, the mutation of this residue may alter the structure of the KH domain of Mex3a and alter its binding to HuR.

It is tempting to speculate that the presence of targets involved in DNA-damage response found in the RIP assays could be related to the interaction of Mex3a and HuR as the latter has been involved in regulating the levels of several genes involved in the response to stress (Masuda et al., 2011).

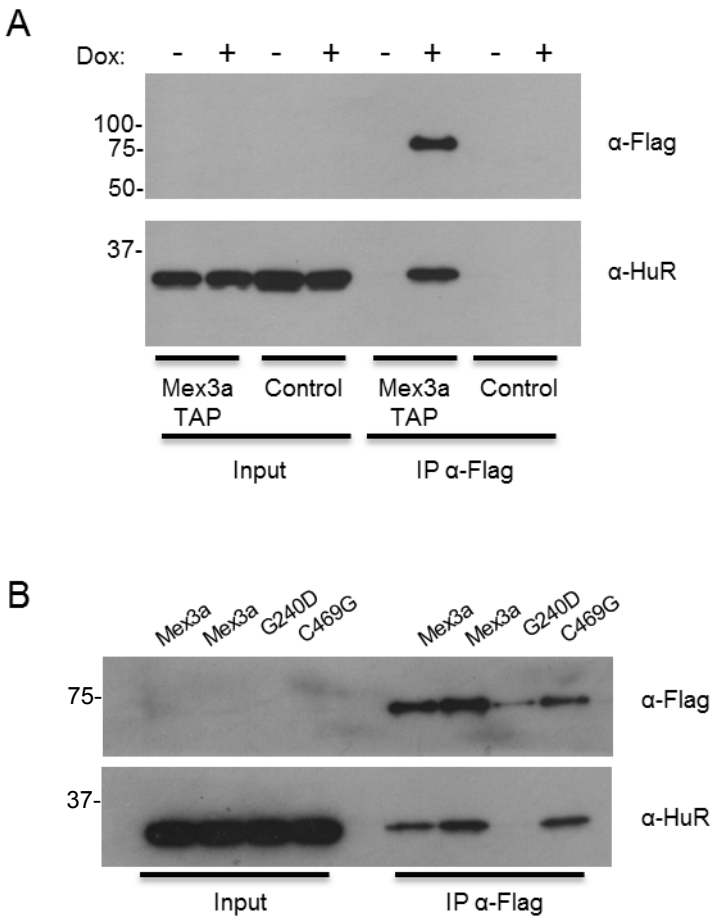

Figure 45: Mex3a interacts with HuR in colorectal cancer cells. A. Confirmation of the binding of Mex3a-TAP to HuR. B. The interaction between ectopic Mex3a and endogenous HuR seems to depend on RNA binding. Duplicate pulldowns with WT Mex3a were used and compared to the RNA binding deficient (G240D) and the RING finger deficient (C469G).

2.22 Mex3a is upregulated in colon cancer and mouse models of intestinal adenomas

In Chapter 1 we have described that ISC genes are co-opted by colon cancers and that tumors with high ISC levels are more resistant to therapy (Merlos-Suarez et al., 2011).

When we analyzed the expression of Mex3a in APC mutant cells from mouse small intestine we found a strong induction of Mex3a (**Figure 46A**). Furthermore we analyzed publicly available datasets and we observed that the expression of Mex3a is increased in cohorts of human colon cancer when compared to matched colon normal tissue (**Figure 46B**).

Besides our analysis in colon cancer, we analyzed the described genomic alterations of the Mex3a locus. Interestingly, we observed that over 15% of lung adenocarcinomas present amplifications of this gene. Other tumor types showing alterations in Mex3a are breast, ovarian and uterine tumors. Whether these alterations in gene expression or copy number are relevant for tumor biology remains to be shown (**Figure 46C**). Our preliminary data suggests that Mex3a might be a relevant player in different types of cancer.

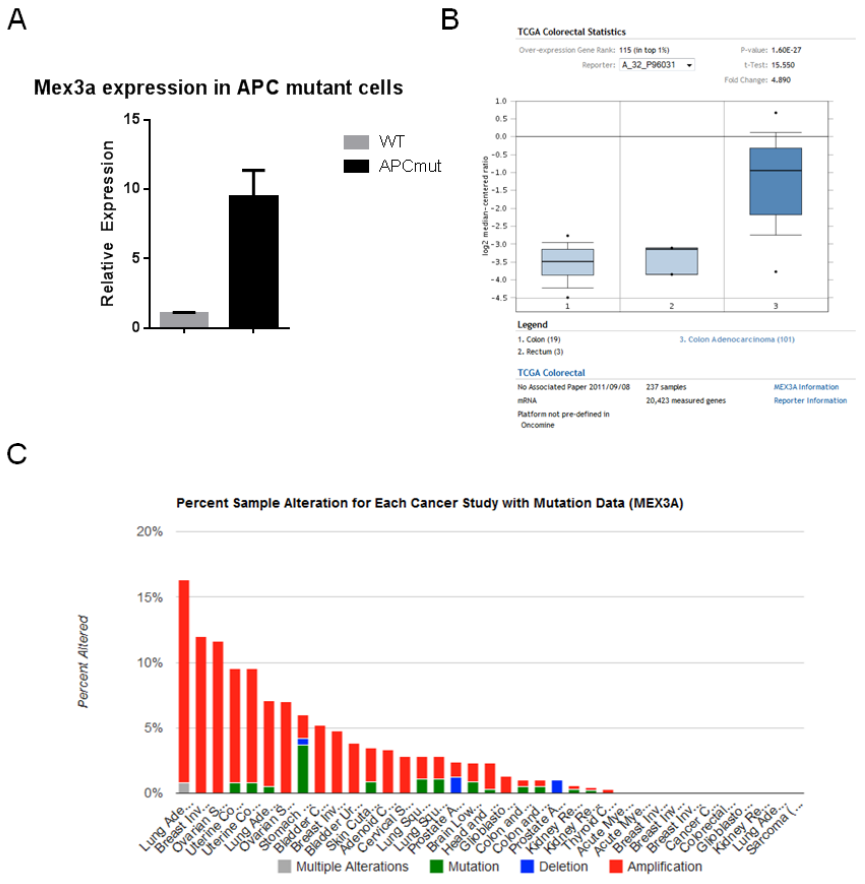

Figure 46: Mex3a is upregulated in human colorectal cancer and mouse adenomas. A. Mex3a expression from the TCGA dataset of colorectal cancer (graph obtained from Oncomine). B. Expression levels of Mex3a in WT and APC mutant cells. C. Genomic alterations of the Mex3a locus in human cancer (graph obtained from cBIO Portal).

Discussion

Chapter 1 Discussion: Identification of the ISC signature and its relationship with colon cancer

Purification of intestinal population based on Lgr5-GFP versus surface EphB2 levels

In Chapter 1 we have identified the transcriptional landscape of the mouse small intestine through our EphB2-based sorting method. Unlike other methods to purify crypt cells which are based on markers of specific populations, EphB2 separates cell types according to the position that they occupy within the crypt axis. Compared to the method developed by the Clevers lab using Lgr5-GFP KI mice, EphB2 surface levels allows the interrogation of more differentiated populations, ranging from ISCs to fully differentiated cells. In contrast, the Lgr5-GFP knock in allele cannot be used to isolate differentiated cells given its mosaic expression in the intestine (i.e. only a small percentage of crypts express the GFP reporter allele and therefore the GFP-negative population comprises both differentiated cells as well as unlabeled ISCs) (Barker et al., 2007a; van der Flier et al., 2009). The other advantage of our technique is the ability to purify intestinal cells types from mice that have not been genetically modified. It is worth mentioning that at the time of performing these experiments, there were no reliable anti-Lgr5 antibodies available. Finally, the major advantage of our approach is that it can be used to purify human intestinal stem cells as we have shown in an independent publication (Jung et al., 2011).

The ISC signature is enriched in advanced CRCs and predicts the risk of developing recurrent disease

Our first observation was regarding the enrichment of the average expression of the ISC signature in metastatic tumors (stage III – IV). A similar finding was made for mammary stem cell signature in breast cancer (Pece et al., 2010). Our observation implies that either the ISC-like phenotype is selected as colon cancer progresses or that mutations arising in more advanced tumors co-opt part of the ISC signature. Whichever is the mechanism, it has been well documented that late stage CRCs are more aggressive and resistant to therapy, features which could be directly linked to ISC-specific genes expressed in tumors. To date, tumor staging is the most powerful predictor of clinical behavior for CRC. Our data demonstrates that the ISC signature may capture some of these features included in the staging system, but also predict features the staging system does not capture. Indeed, the levels of the ISC signature directly correlate with an increased probability of tumor relapse after therapy independently of staging as shown by multivariate analysis. Considering that ISCs are long lived and mediate the regeneration of the normal tissue throughout the life of the individual, CRC cells may have co-opted the genetic program of these cells to perform similar functions in tumors. Of note, the correlation of a normal stem cell signature with clinical outcome has also been identified for acute myeloid leukemia (Eppert et al., 2011), which broadens our observations and argues in favor that several tumor types co-opt traits from the stem cells of the their tissue of origin.

An important caveat that arises is that our approach does not allow us to distinguish whether CRC samples displaying different levels of each signature are the consequence of increased abundance of tumor cells of a particular phenotype within a given CRC or rather the consequence of upregulation of the levels of the signature´s genes in particular cell populations. Increased numbers of ISC-like tumor cells, as defined by our signatures, will increase the probability that these cells survive the adjuvant therapy. Alternatively, overexpression of particular ISC genes may also facilitate the process of metastasis and relapse.

Another fact to highlight is that the proliferation signature was inversely correlated with the ability of tumors to relapse. It is tempting to speculate that slow proliferating cells may be more resistant to standard chemotherapeutic treatments. Our finding has been corroborated in several studies. Of note, this feature seems specific to colon cancer since in breast cancer proliferation is directly correlated to disease progression and recurrence. Would this imply that ISC-like tumors do not proliferate or have lower proliferation rates? A possible interpretation is that the ISC and proliferation signatures are measurements of different biological aspects. This idea argues that, as was observed for the normal intestinal mucosa, stemness is a feature that goes beyond the mere capacity of cells to proliferate and encompasses several other biological functions such as long term self-renewal capacity. In the case of the healthy intestinal epithelium, ISCs express both the ISC-specific genes and proliferation program, whereas TA cells only express the proliferation signature. We speculate that the same principles may apply in CRCs. In favor of this view, tumor cells that express distinct EphB2 surface expression (i.e. ISC, TAs and differentiated tumor cells) had comparable levels of proliferation genes, yet their tumor initiation abilities correlate with expression of ISC-specific genes.

A prediction that follows from the above ideas is that differentiated-like tumors should have a better prognosis. The lack of predictive power associated to the differentiation signature is puzzling. A possible interpretation is that CRC cells do not undergo a canonical differentiation and therefore the signatures derived from normal tissue do not completely capture the abundance of this population in tumor samples.

Colon tumors have a structure reminiscent of the normal colon epithelium

One of the major findings in our publication from Chapter 1 is that CRC architecture and cell heterogeneity is reminiscent of the normal colon epithelium. Our results show the presence of at least

two mutually exclusive phenotypes based on the expression of genes that segregate normal ISCs (i.e. Lgr5, EphB2 and Olfm4) and normal differentiated cells (i.e. Krt20). Besides IHC, we performed expression profiling of selected ISC, proliferation and differentiation genes in the EphB2 populations. These results reinforced the observations made in tissue sections.

It is important to mention that, with our current data, we are unable to conclusively rule out that the ISC-like and differentiated-like populations may represent different cells clones each carrying subsets of genetic alterations that confer different phenotypes. Yet, the close proximity of the $Lgr5^{+ve}$ and $Krt20^{+ve}$ cells within tumors argues in favor of a common clonal origin (Siegmund et al., 2009). Additionally, the Clarke lab has recently performed transcriptional profiling of single tumor cells purified from human samples and identified three tumor cell populations in CRCs; ISC-like, enterocyte-like and secretory-like (Dalerba et al., 2011). Future lineage tracing experiments within tumors will conclusively demonstrate the relationship between these populations.

Another aspect worth mentioning is the existence of tumor cells negative for both Lgr5 and Krt20. Our current hypothesis is that these cells comprise an intermediate state between the ISC-like and differentiated-like cells although this hypothesis is difficult to prove with the current technologies. Another possibility is that these cells have silenced EphB2 expression. Our lab has shown that EphB2 plays a tumor suppressor role in the intestinal epithelium by compartmentalizing the expansion of tumor cells, (Batlle et al., 2005b; Cortina et al., 2007a). Several independent works have shown that CRCs with low expression of EphB2 have a worse prognosis compared to those with elevated expression (Guo et al., 2006a). Silencing of EphB2 occurs mainly at the invasion fronts and in areas of poor differentiation (Guo et al., 2006a). On the contrary, the tumor bulk is generally composed of glandular structures containing patches of $EphB2^{+ve}$ tumor cells that display an ISC-like phenotype intermingled with $EphB2^{-ve}$ cells that are differentiated-like.

Fitting with these previous observations, a recent publication by the Medema lab (de Sousa et al., 2011) indicates that silencing of a

subset of Wnt target genes, including EphB2, correlates with disease relapse in CRC. Several of these Wnt target genes are included in our ISC signature. They argue that silencing occurs by methylation of these genes in a subset of tumors. We have investigated this possibility but could not corroborate the data by Medema and colleagues. Neither EphB2 nor the other Wnt-ISC-specific genes appear to be highly methylated (Whissell et al., submitted). Instead, we discovered that tumor hypoxia downregulates expression of Wnt target genes in most aggressive CRCs (Whissell et al., submitted). This phenomenon occurs prominently at invasion fronts.

Despite these caveats, all the functional data collected from our laboratory after analyzing many different CRC samples have shown that EphB2^{High} cells are enriched in tumor-initiating cells (TICs). An interpretation that would reconcile all these paradoxical findings is that that the absolute level of EphB2 in the overall tumor is readout of the differentiation degree or tumor grade compared to other tumors, whereas the relative levels of EphB2 within the same tumor would identify cancer stem cells compared to their differentiated progeny.

EphB2 identifies tumor initiating cells in CRCs

The functional proof that high levels of EphB2 identifies cancer stem cells comes from assessing the tumor initiation potential of this population through transplantation assays combined in limiting cell dilutions. These experiments demonstrated that the tumor initiating potential is present in the EphB2^{High} population. In addition, this ability is retained over serial passaging. Tumors derived from EphB2-high cells that were serially transplanted in mice retained the overall structure and expression profiles of the original tumor. Unbiased clonal analysis of colon cancer by lentiviral marking has identified that cancer cell populations exist with either ISC-like and TA-like behavior (Dieter et al., 2011). This finding agrees well with our observations.

An aspect worth commenting is that the TIC frequencies observed in our experiments are much higher than that observed in the original studies by John Dick´s, Ruggero de Maria's and Mike Clarke´s labs (Dalerba et al., 2007c; O'Brien et al., 2007; Ricci-Vitiani et al., 2007a). This discrepancy may be simply explained by technical issues such as the initial cell viability, presence of cellular aggregates and efficiency of antibody staining which would impinge in the absolute number of TICs (Shackleton et al., 2009). However, the major difference between these studies and our work is the use of different surface marker genes to identify CRC-SCs. These initial studies make use of CD133 or CD44. In our hands, CD133 does not perform well to separate ISC-like tumor cells in CRCs. The expression of pattern of CD44 overlaps with that of EphB2 in some CRCs, yet EphB2 appears to be a more consistent maker for ISC-like cells in different tumor samples. Of note, the described staining pattern for CD44 in normal mucosa is broader that the EphB2 high populations, an observation that supports our experiments of expression profiling of tumor samples (Morral et al. work in progress). The inability of these other TIC markers to purify ISC-like cells argues that either the populations we define using EphB2 are included within the populations defined by CD44 or CD133 or that EphB2 segregates tumor cells with a distinct biological features (van der Flier et al., 2007a).

In any case, the arguments claiming that high abundance of cancer stem cells invalidates the fact that they could be relevant for disease progression are not correct (Kelly et al., 2007). Cancer stem cells must be solely defined by their ability to self-renew and differentiate into different tumor lineages and their abundance is not related to these two properties. Moreover, our data goes in line with the published estimates for CSC frequency in colon cancer assessed by unbiased analysis of DNA methylation (Siegmund et al., 2009).

Colon CSCs and the cell of origin of metastasis

One aspect that we are unable to test with our current experimental setting is the ability of the EphB2 populations to metastasize. Our prediction is that cancer stem cells represent the population capable of initiating metastasis. It is important to point out that in CRCs the overall organization of the metastasis is similar to that of the primary tumor. We report that metastasis also contain ISC-like and differentiated-like tumor cell populations. This observation may suggest that the cell of origin of metastasis has regenerated the cell hierarchies present in the primary tumor.

It is possible that metastasis-initiating cells represent a subfraction of the CSC population, which has been shown for pancreatic cancer (Hermann et al, 2007). What could determine if a CSC initiates metastasis or not? One possibility is the appearance of a mutation in a subset of CSCs that confers them an advantage in distant organ colonization. Another not mutually exclusive possibility is that environmental cues such as hypoxia, metabolic stress or stromal interactions directly induce tumor cell colonization. This does not imply that only CSCs are migratory, but among all migratory tumoral cells, the CSCs hold the features to regenerate a tumor at the targeted organ.

Overall, our evidence favors the hierarchical model of tumor growth more than the model of clonal evolution. Initially these two models were thought to be mutually exclusive, yet the most recent evidence points towards that both possibilities can co-exist (Clevers, 2011; Dalerba et al., 2007a; Driessens et al., 2012; Gupta et al., 2009; Jordan et al., 2006). The reconciliation of these models lay in the fact that clonal evolution would only affect tumor biology when mutations occur in cancer stem cells.

The origin of tumor cell heterogeneity in CRC

The first evidence suggesting the presence of ISC-like cells in CRCs came from a study by the Clevers lab demonstrating that the cell of origin of adenomas is indeed the ISC. By performing the inactivation of the Apc gene in different cell compartments, Barker et al demonstrated that only $Lgr5^{+ve}$ cells give rise to adenomas. Although this observation does not show evidence for cancer stem cells, the authors noticed heterogeneity within the adenomas in the expression of Lgr5 in a subset of cells (Barker et al., 2009). This already suggested the potential existence of stem-like cells in mouse adenomas. Definite proof for the presence of stem-like cells in mouse adenomas was recently put forward by the use of lineage tracing within adenomas. This work showed unequivocally that $Lgr5^{+ve}$ adenomas cells self-renew and give rise to Paneth-like tumor cells (Schepers et al., 2012). Another recent publication has also hinted on the relevance of Lgr5 cells in fueling the growth of adenomas. This study focused on the observation that the tracing from a Dclk1 Cre is able to stain complete adenomas. This gene is normally labeling differentiated Tuft cells, yet upon inactivation of Apc, a subset of Lgr5 cells express this marker. The authors went on to show that the elimination of the $Lgr5^{+ve}$/$Dclk1^{+ve}$ cells was enough to fully stop the growth of adenomas (Nakanishi et al., 2013).

Initial observations in late stage CRCs suggests that differential activation of the Wnt signaling pathway in CRCs may confer stem or differentiation properties to genotypically identical cell populations (Vermeulen et al., 2010). The organization in tumors shows ISC-like cells in close proximity to the stromal cells suggesting the existence of a CRC-SC niche. This niche may define the behavior or phenotype of ISC-like cells, including the degree of activation of the Wnt signaling pathway.

An intriguing notion is that the ISC-like phenotype maybe entirely linked to the ability of cells to recruit and activate the stroma. Non-epithelial tumor cells will then confer the self-renewal and multipotency to the cancer stem cells. Likewise, ISC-like cells may be the only cell population able to activate the stroma. Considering

that the results dissecting the cancer-stroma interface are based mainly in cell lines, it still remains to be shown that cancer stem cells have a specific connection with stromal cells.

Plasticity of tumor cell phenotypes and the relevance for therapy

In the normal intestinal mucosa, progenitor cells such as LRCs can revert their phenotypes and reacquire ISC features in certain contexts, particularly upon damage of the ISC pool by irradiation or drugs. As CRC are caricatures of the normal colonic mucosa, it is likely that this plasticity may also exist in tumor cell populations. The question is whether cell fates represented within tumors are invariable or if there is a fixed equilibrium that will restore itself even after disruption of a particular population? Evidence for tumor cell plasticity in late stage CRC awaits the development of genetic tools that allow lineage tracing of all the cell populations present in a tumor. All of the evidence commented so far directly implies that cancer stem cells are relevant for tumor regeneration, yet the single most important observation to establish the relevance of tumor hierarchy for CRC therapy is missing: will the eradication of cancer stem cells have therapeutic relevance? Proof of concept experiments in adenomas have shown that ablation of adenoma stem cells is sufficient to induce tumor collapse (Nakanishi et al., 2013). These experiments suggest that there is no plasticity in adenomas although there are several experimental caveats related to this work, including the fact that the toxin used to delete adenoma stem cells was also expressed in non-CSC at later stages of induction. In human late stage CRCs, a likely scenario is that the mere ablation of cancer stem cells will not be enough to completely eliminate the tumor. Therefore, future cancer stem cell-directed therapy will probably be used as an adjuvant to conventional treatments.

Chapter 2 Discussion: Characterization of Mex3a as a novel ISC gene

The second Chapter of this thesis focuses on the ongoing work to characterize Mex3a, a novel stem cell gene. Its expression closely follows stem cell traits in several systems and we predict that its function could be a new feature of general stemness. We will now discuss the current evidence we have gathered for this novel RNA binding protein and the future directions we will pursue to understand its potential function in stem cell biology.

The function of Mex3a in the intestine

Our initial hypothesis was that Mex3a would repress the translation of Cdx2 in ISCs, thus allowing for the maintenance of the stem cell phenotype. At the time this project was conceived, all published data suggested that Cdx2 was one of the major transcription factors driving intestinal differentiation. Furthermore, there were several reports suggesting that the expression of Cdx2 was regulated at the post-transcriptional level since the mRNA was distributed all along the crypts villus axis, yet the protein was reported to be expressed solely in differentiated cells. Despite these observations, we were unable to confirm that Cdx2 is differentially expressed in crypts compared to villi and that the removal of Mex3a had an effect on the protein or RNA levels of this transcription factor. Our data is in clear contrast with a recent publication that found that Mex3a is a negative regulator of Cdx2 in the Caco2 cell line, and that this led to defects in differentiation (Pereira et al., 2013). The reasons behind these differences can be varied:

-First, the effects described of Mex3a on Cdx2 may be mild and would be difficult to detect *in vivo*.

-Second, the data in Pereira et al is largely based on overexpression of Mex3a in the CRC cell line Caco2.

-Third, the phenotype of the Cdx2 KO mouse has been described both during development and in the adult intestine. These mice lacked colon specification and there was a general anteriorization of the intestinal epithelium into a stomach-like stratified epithelium (Gao et al., 2009). This phenotype was similar, although milder, when Cdx2 was ablated in the adult intestine (Stringer et al., 2012). The genetic data shows that Cdx2 is not required for ISC differentiation as was expected from the results of Pereira et al, but rather it is required for the specification of the intestinal vs stomach lineages.

Besides Cdx2, we looked into the phenotypes that may arise from the deletion of Mex3a in the adult intestine. After Mex3a knockout, the overall architecture and structure of the small intestine and colon had no gross alterations, which again imply that it is unlikely that Mex3a deficiency leads to alterations in Cdx2 expression. These data also show that Mex3a is dispensable for adult intestinal physiology during homeostasis.

Why is there no obvious phenotype in Mex3a mutant intestines? A plausible explanation is the existence of redundancy between Mex3 family members. Mex3a is part of a family of genes that also includes Mex3b, Mex3c and Mex3d. All four genes share very high homology in their RNA binding domains, as well as the C-terminal RING finger domain. All the Mex3 genes are expressed in the intestine (albeit at different extent), yet Mex3a is the only isoform displaying an ISC-specific expression pattern. In addition, the analysis of the detailed protein sequence of the RNA binding domains of all 4 genes demonstrated that Mex3a was the most phylogenetically distant isoform (data not shown). Furthermore, Mex3a and Mex3b share the most similarities as both are able to localize to cytoplasmatic RNA granules, whereas Mex3c has a diffuse cytoplasmatic expression (Buchet-Poyau et al., 2007). Mex3d in turn has been described to have a nuclear localization (Donnini et al., 2004). Of note, Mex3b has been shown to be expressed in mucous-secreting cells of the small intestine (Buchet-Poyau et al., 2007), yet our Mex3a signatures from the KI allele do not suggest that Mex3a is expressed in these cells.

Compensatory increases of redundant genes have been postulated to contribute to incomplete penetrance (Burga et al., 2011), yet after Mex3a deletion we were unable to detect any upregulation of Mex3b, Mex3c or Mex3d (data not shown). This argues against redundancy but does not preclude that the endogenous levels of these genes are enough to cover for the loss of Mex3a.

Besides redundancy, the lack of an overt phenotype in the intestine suggests that Mex3a is not required for stem cell maintenance in homeostasis. Because the relative radioresistance of Mex3a^{+ve} cells after irradiation and the resemblance to intestinal label retaining cells, it is tempting to speculate that Mex3a may play a role in stress conditions (see below).

We also used in vitro models of intestinal organoids to study the function of Mex3a given their easier manipulation in different experimental conditions. In contrast to the results in vivo, we could observe that acute deletion of Mex3a in organoid cultures led to a decrease in clonogenic capacity after passaging. This observation suggests that impaired self-renewal of stem cells after Mex3a deletion, which was not evident in the *in vivo* setting. A possible explanation this discrepancy is that a 2-3 fold difference in ISC numbers induced by Mex3a deletion *in vitro* would be hardly noticeable with our current techniques to assess intestinal function *in vivo*. We are currently generating mice where we can track by FACS Lgr5-GFP^{+ve} cells after ablation of Mex3a with the Villin Cre-ER^{T2} allele to analyze if this difference of Mex3a KO cells can be seen *in vivo* as well.

Another possibility to account for the discrepancy between the *in vitro* and *in vivo* results is that there might be *in vivo* redundancy of the function of Mex3a which would apparently not be present in the *in vitro* setting. The reason for this phenomenon is unclear but it may include compensation by the stromal compartment which is not present in the organoid culture system. Alternatively, the differences observed arise from the increased stress that ISCs face in culture conditions such as hyperoxia, increased metabolic activity and potentially the lack of a niche factor not present in the culture conditions. Some of our preliminary data suggest that Mex3a may play a role in the adaptation of ISCs to stress.

Characterization of Mex3a^{+ve} cells

Unlike intestinal Lgr5^{+ve} cells (Munoz et al., 2012; van der Flier et al., 2009), Mex3a^{+ve} cells appear to encompass not only ISC genes but also enteroendocrine lineage markers. We speculate that this could be due to either a mix of stem and differentiated cells or the existence of cells co-expressing these genes. Our approach does not allow us to differentiate between single cells co-expressing markers or if two different populations are Mex3a positive.

Intriguingly, enteroendocrine progenitors have recently been described as the label retaining cells (LRCs) in the intestine by the Winton lab. They generated a genetic model to trace from label retaining cells and showed that after damage, the LRCs are able to regenerate the population of Lgr5 ISCs. From the data gathered so far it seems that intestinal LRCs are a subpopulation of relatively quiescent Lgr5^{+ve} cells that express markers of enteroendocrine and Paneth cells.

By GSEA we found that the LRC common signature we defined was highly enriched in Mex3a^{High} cells. To verify the specificity of this observation we repeated this analysis with the EphB2 and Lgr5 populations. This showed that Mex3a has a higher enrichment of LRC genes than EphB2. Intriguingly, the Lgr5 cells had a random distribution of this LRC signature. These observations can be explained by considering that the EphB2 population includes both Mex3a and Lgr5 cells. On the other hand, these LRC genes would be equivalently distributed between the Lgr5^{Hi} and Lgr5^{Low} cells. In the light of our Mex3a data, it would fit that Mex3a^{+ve} cells encompass both ISCs and LRCs, making this a new genetic marker for these populations.

The enrichment of Mex3a^{+ve} cells in LRC genes prompted us to analyze the behavior of Mex3a and Lgr5 cells upon ionizing radiation (IR). Our preliminary results point towards a differential response of these two populations to stress. We observed that Mex3a cells had higher resistance to IR than Lgr5 cells. Whereas

we need to expand these observations to different dosages of radiation and times, they support that Lgr5 and Mex3a mark distinct populations of cells. The enhanced resistance of Mex3a cells also reinforces the idea that Mex3a may be expressed by LRCs.

With respect to the markers to the postulated alternative ISC population (e.g. Bmi1, Tert, Hopx and Lrig1), we did not find an obvious connection between Mex3a and these other putative ISC marker genes. Importantly, a recent publication by the Clevers lab has described that all of these genes are expressed in Lgr5 cells. For some of these genes, it has been shown that the expression of lineage tracing alleles knocked in the respective locus does not reproduce the expression of the endogenous gene. For instance, in the case of Bmi1, by ISH and IHC it has been shown that it is expressed in the ISC and TA compartments (Munoz et al., 2012), yet the tracing results from different lines have yielded completely different results (Sangiorgi and Capecchi, 2008; Yan et al., 2012). The reasons behind this incongruence remain unknown but a potential explanation is that the alleles used are introducing artifacts in the expression of the Cre. The same has been suggested for the Tert-driven Cre-ER^{T2} allele (Montgomery et al., 2011).

The precise identity and behavior of the Mex3a^{+ve} population could have been investigated by means of the tdTomato reported and Cre-ER^{T2} driver knocked in the locus. Whereas tdTomato levels have been sufficient to purify this cell population by FACS, we have been unable to detect tdTomato in intestinal cells by microscopy. Likewise, the experiments of lineage tracing have not been consistent. We speculate that the failure to perform these assays is due to low levels of expression of the Mex3a locus in this tissue. The failure to use these reporter cassettes has represented a major limitation to investigate the role of Mex3a. We are currently testing variations of the experimental protocols and conditions that would allow taking advantage of these tools to study the Mex3a population.

Is Mex3a a marker of additional types of stem cells? The expression of Lgr5 allows identifying several populations of adult stem cells in a wide range of tissues: small intestine, colon, stomach, skin, liver and kidneys (Barker et al., 2010b; Barker et al., 2012a; Barker et al., 2007a; Huch et al., 2013; Jaks et al., 2008). Of note, Mex3a expression is enriched in $Lgr5^{High}$ cells of the stomach (data not shown). These observations led us to start investigating the possibility that Mex3a may also represent a general marker gene of adult stem cells in several tissues.

For instance we can detect $Mex3a^{+ve}$ cells in bone marrow, yet no $Mex3a^{+ve}$ cells are present in peripheral blood. Although further phenotypic characterization of these bone marrow $Mex3a^{+ve}$ cells is required, our results show that stem/progenitor cells express Mex3a. Furthermore, the specificity of Mex3a as a marker for LSK cells seems higher than that of Sca-1. Our results are in agreement with the published expression of Mex3a mRNA (Konuma et al., 2011).

We also observed that endogenous Mex3a is highly expressed in mouse ESCs. In this system we could detect tdTomato by microscopy, a finding that agrees with our observations that endogenous Mex3a is expressed in ESCs at much higher levels than adult tissues. The ability of the tdTomato reporter to identify $Oct4^{High}$ and $Sox2^{High}$ cells in ESC cultures argues in favor of this gene as a marker of stemness in this system. Indeed, a recent study has described Mex3a to be part of the ESC-specific RNA binding protein repertoire (Kwon et al., 2013). Furthermore, Mex3a expression is downregulated when ESCs are induced to differentiate to embryoid bodies (Liu et al., 2011).

Importantly, Lgr5 is not expressed in HSC or ES cells implying that its expression does not completely overlap that of Mex3a. Lgr5 has been shown to be a robust Wnt target (Hatzis et al., 2008; van der Flier et al., 2009) and its function if to act as a receptor of Rspo1, a well described Wnt agonist (de Lau et al., 2011). Thus, Lgr5 segregates stem cell populations based on its use as readout of active Wnt signaling. We do not understand yet which signals regulate Mex3a expression but our investigations have revealed no link to Wnt signaling. In particular, we and others have generated

comprehensive studies of Wnt targets and there is no evidence of binding of TCF7L2/TCF4 to the Mex3a promoter (Hatzis et al., 2008; van der Flier et al., 2007a), nor that Wnt blockade generates a consistent decrease in Mex3a expression (Whissell and Batlle, unpublished results).

We are currently exploring expression patterns of Mex3a tissues other than the intestine and blood. It would be particularly interesting to find out whether Mex3a^{+ve} cells of different tissues express common genetic programs or display similar features. In this regard, it is worth pointing out that one of the top genes enriched in the intestine Mex3a-specific signature is Peg3. This gene is a maternally imprinted transcriptional repressor shown to be involved in p53 and TNFα signaling, and regulates muscle satellite cells (Nicolas et al., 2005). Peg3 has been shown to be expressed in hematopoietic stem cells (HSCs), muscle satellite cells, undifferentiated cells from testis and in neural stem cells (Besson et al., 2011). Neither EphB2^{-high} nor Lgr5^{+ve} cells enrich for Peg3, whereas the Mex3a and LRC signatures are characterized by high levels of this gene. This observation also reinforces the notion that Mex3a labels a cell population different from Lgr5 cells.

The role of Mex3a during embryonic development

Mex3a null mice have a clear reduction in size (evident from E14.5 onwards), an observation that is reminiscent to the observed for Mex3a KI homozygotes. Despite these severe phenotypes, the histopathological analysis yielded no gross abnormalities in the major organs suggesting that Mex3a does not play morphogenic roles during development. Moreover, the lethality of Mex3a null mice indicates that this gene plays non-redundant roles during development. The only mouse genetic model for the other Mex3 members is the gene trap of Mex3c. These mice show background-dependent perinatal lethality, most probably due to respiratory distress. The authors show that in C57/Bl6 background the lungs of the newborn Mex3c$^{tr/tr}$ mice have increased cellularity and that these mice appear cyanotic (Jiao et al., 2012a). In the 129 background Mex3c mutant mice are viable, although a clear size reduction was also evident. The authors show that the levels of

IGF-I in these mice were reduced and that this might explain most of the size differences. In a follow up manuscript, the authors show that Mex3c deficiency leads to reduced adiposity and increases energy expenditure although no mechanism is postulated (Jiao et al., 2012b).

In the case of Mex3a, we have not assessed the levels of IGF-1, yet the KO mice do not show signs of respiratory problems nor cyanotic aspect. Our preliminary analysis of Mex3a null mice showed that they lacked hepatic glycogen. This phenotype could be due to lack of food intake in these mice since we have never observed the characteristic milk spot in their stomachs. To rule out starvation, we analyzed P1 mice right before birth. We could detect glycogen in KO mice, yet at reduced levels. These results may relate to metabolic alterations that might impinge in their ability to keep energy reserves. These findings could potentially explain the size reduction and perinatal lethality characteristic of Mex3a full KO mice. We are currently studying the alterations present in Mex3a deficient mice and how they may relate to the role of Mex3a in stem cells.

Speculating about the cellular functions of Mex3a

We have expressed WT and mutant versions of Mex3a with a doxycycline inducible lentiviral vector. We observed that point mutants of Mex3a reach much lower induction levels at both the mRNA and protein level. These mutations abolish the ability of Mex3a to bind RNA (G240D) or disrupt the C terminal RING finger domain (C469G). Considering that these vectors are different from the WT version by a single nucleotide, it seems unlikely that these differences in expression are due to problems in virus packaging or infection. Our data suggests that Mex3a protein stability requires its ability to bind RNA. This could be due to degradation signals that are present in the protein that are masked upon RNA binding through protein complex formation. In the case of the C469G mutant, it could be that Mex3a is actively degrading a negative regulator of itself. When we analyzed a truncated version of Mex3a consisting of only the N-terminus with the RNA binding domains, the protein showed a stability equivalent to that of the WT version. This suggests that the putative degradation signal is encoded in the region that lies between the second KH domain and the RING finger, which contains several predicted ubiquitination and phosphorylation sites.

To investigate the activity of Mex3a, we decided to make use of mRNA tethering assays. These experiments yielded, unexpectedly, that Mex3a can act as a translational activator. The data in C. elegans had shown the role of *mex-3* only as a translational repressor (Huang et al., 2002; Schoppmeier et al., 2009), yet several RNA binding proteins have been shown to have dual activities depending on the target and the cellular context used (Noubissi et al., 2006; Volk et al., 2008).

Our tethering approach shows that the activity of the C terminal RING finger domain is required for the translational activation effect of Mex3a. So far, there is no conclusive evidence showing that this domain has E3 ubiquitin ligase activity; although by structure prediction it seems to be very likely. In the case of Mex3c, the C terminal domain is required for the downregulation of the MHC-I mRNA and acts as a E3 ubiquitin ligase (Cano et al., 2012).

The evidence from these results could be suggestive that Mex3a may be involved in different protein complexes bound to different target mRNAs. Depending on the interaction partners, it could be that through its E3 ligase activity Mex3a degrades proteins bound to the 3'UTR either required for activating or repressing the translation of a target mRNA.

An alternative mechanism could be that the ubiquitination by Mex3a is not involved in the proteosomal degradation of a target, but rather on the modulation of its levels and activity. All of these hypotheses remain speculative until further evidence is gathered on the effect of Mex3a on endogenous targets.

Preliminary evidence for a role of Mex3a in coordinating the cellular response to stress

We were able to capture the proteins interacting with exogenous WT Mex3a protein by performing a TAP pulldown and analyzing by mass spectrometry the bound peptides. Interestingly, we found several RNA binding proteins that interacted with Mex3a. Among these the protein HuR (Elavl1), was one of the most strongly associated, alongside UPF1 and XRN2. The confirmation of the interaction data by co-immunoprecipitation shows that ectopic Mex3a is able to interact with endogenous HuR, and that this binding requires an intact RNA binding domain. This implies that Mex3a and HuR are binding a subset of the same mRNAs and might have synergistic or antagonistic roles in the stability or translation of these common targets.

HuR has been shown to be involved in several aspects of RNA metabolism: splicing, mRNA export, mRNA stability and translation (Mukherjee et al., 2011). Moreover, HuR has been reported to be a central regulator of the stress response by modulating the mRNA stability of p21 upon phosphorylation by the stress-activated p38 MAPK (Lafarga et al., 2009). Another interesting aspect of HuR is that the adult KO of this protein leads to the rapid loss of progenitors in the hematopoietic and intestinal systems (Ghosh et al., 2009).

Considering that Mex3a is also a phosphoprotein, it can be speculated that Mex3a and HuR are part of the same stress-sensing complex, activated by stress responsive kinases. Alternatively, the phosphorylation of HuR could be the main link of Mex3a with the stress response. Of note, the major localization of HuR is nuclear, whereas Mex3a is strictly cytoplasmatic in our model. The shuttling of HuR from the nucleus to the cytoplasm is regulated by stress conditions (Lafarga et al., 2009), and this may imply that Mex3a interacts only with the subset of HuR protein that is shuttling out of the nucleus (i.e the stress responsive pool of HuR).

A recent publication has shed light to a new layer of regulation of HuR function. This study addressed the interaction of HuR with the p97/UBXD8 complex and showed that these proteins recognize an ubiquitinated form of HuR and remove it from mRNP complexes (Zhou et al., 2013). It is worth noting that the ubiquitination of HuR was non-degradative, and that the E3 ligase responsible for this modification has not been described. This observation opens the possibility that Mex3a is the E3 ligase able to induce this modification on HuR and modulate its ability to bind target mRNAs.

The relative radioresistance of Mex3a^{+ve} cells and their enrichment in LRC-specific genes together with the interaction of Mex3a with HuR is strongly suggestive of a role for Mex3a in coordinating the response of ISCs to stress. We are currently testing this hypothesis by exposing the *in vitro* and *in vivo* models developed during this thesis to different stress conditions including irradiation and metabolic stress.

Connecting Mex3a to mitochondrial biology.

Because Mex3a controls RNA translation, all transcriptional modulation observed upon Mex3a deletion *in vitro* are most likely indirect effects of changes in mRNA translation. To study the mRNAs directly controlled by Mex3a, we turned to analyzing directly the proteins regulated by deleting Mex3a in ISC cultures. We found the main proteins affected were mitochondrial and involved in metabolism.

We also used RIP to characterize the direct targets of Mex3a in LS174T cells. Gene Ontology analysis of Mex3a targets revealed enrichment in RNA metabolism, DNA damage response and mitochondrion. Indeed, the list of RIP targets included several bona-fide regulators of mitochondrial biology. For instance, one of the top targets of Mex3a in LS174T cells is Uvrag which has been described as a central regulator of autophagy (Liang et al., 2006). As several targets of Mex3a, Uvrag is present in the mitochondria where it regulates the levels of Bax (Yin et al., 2011). Uvrag is also involved in the DNA damage response and centrosome regulation (Zhao et al., 2012).

Mex3a also binds to the Tmem70 mRNA. This gene is integral to the mitochondrial membrane and is required for the proper formation of the mitochondrial complex V (i.e ATP synthase). Children carrying mutations in this gene have encephalocardio-myopathy and early neonatal death (Cizkova et al., 2008). Interestingly, TMEM70 itself is not part of complex V, but it is required for its proper assembly and function through mechanisms still unknown.

The Eed mRNA is the top target of Mex3a in LS174T cells. The function of this gene has been widely described as an essential member of the PRC2 complex involved in chromatin modification (Hansen et al., 2008; Margueron et al., 2009; Montgomery et al., 2005; Montgomery et al., 2007). When we probed for the interaction between Mex3a and the PRC2 we could not find changes in H3K27 methylation. Instead, we found by subcellular localization prediction that one of the isoforms of EED (i.e. EED2), had a canonical mitochondrial localization signal. When we analyzed mitochondria-enriched fractions we could detect EED2 in a Mex3a-dependent manner. A recent publication has described a PINK1-dependent localization of EED in mitochondria, which supports our observations (Berthier et al., 2013). From a functional perspective only one previous work has put forward the connection of mitochondrial genes with EED (Kawamura, 2012), yet no mechanism was postulated behind this observation. Our results with EED show an involvement of Mex3a in regulating the translation of EED2 since Mex3a knockdown affects EED2

specifically, without altering the mRNA levels of EED or the protein levels of EED1, EED3 and EED4. The role of EED2 in the mitochondria remains to be elucidated.

The Mex3a interactions discovered by proteomics of Mex3a pull down as well as the experiments in ISC cultures suggest a link to mitochondrial biology. These experiments indicate that Mex3a is bound to 3 mitochondrial proteins that interact directly to each other: DAP3, ICT1 and MRPS27 (Miller et al., 2008; Mukamel and Kimchi, 2004; Richter et al., 2010). These proteins are part of the mitochondrial ribosome. This observation leads to speculate that Mex3a may modulate the translation of nuclear-encoded mitochondrial genes. In favor of this view, overexpressed Mex3a is present in mitochondria-enriched fractions although no mitochondrial import signal is predicted (data not shown). A possible explanation to this finding could be that Mex3a is present in the mitochondrial periphery and the proteins being pulled down are due to an indirect purification of mitochondria. It is noteworthy that at least 50% of the nuclear-encoded mitochondrial mRNAs are differentially localized to the mitochondrial periphery (Devaux et al., 2010), yet the mechanisms for transcript targeting in mammals are still unknown. One of our current hypotheses is that Mex3a is aiding translation in the mitochondrial periphery.

Finally, whereas the data described above suggest a role for Mex3a in controlling mitochondrial biology, we still lack a proof that parameters of mitochondrial function are altered after in vivo depletion of Mex3a. Our in vivo data shows that whatever may be the function of Mex3a in mitochondria, it is not essential for intestinal homeostasis. We are currently analyzing whether perinatal lethality in Mex3a null mice may be related to defects in mitochondrial function. We are also investigating the possibility that Mex3a regulates sensitivity to stress via regulation of mitochondrial genes.

Mex3a in tumorigenesis

The data we have gathered in regard of the function of Mex3a suggests a role in mitochondrial biology and stress. These observations have prompted us to analyze Mex3a in different settings such as stress conditions or tumorigenesis.

Regarding the role of Mex3a in tumorigenesis, we are currently generating mouse models were we simultaneously delete the tumor suppressor gene Apc in background WT o mutant Mex3a context. In mouse intestinal adenomas, there is a 10-fold increase in the levels of Mex3a. We found a similar upregulation in human CRCs. Considering that Mex3a is not a Wnt target gene in cell lines, Mex3a upregulation probably reflects the expansion of the stem cell compartment in the tumors. A recent publication has shown that $Dclk1^{+ve}/Lgr5^{+ve}$ cells are responsible for the maintenance of mouse adenomas (Nakanishi et al., 2013). Considering that Mex3a cells in normal mouse tissue purify cells positive for both of these marker genes, it is tempting to speculate that $Mex3a^{+ve}$ cells may represent mouse adenoma stem cells. Another possibility is that $Mex3a^{+ve}$ might be labeling tumoral LRCs involved in regenerating the tumor after therapy.

We also found that the Mex3a locus is largely amplified in several tumor types, being the most prominent lung adenocarcinomas, invasive breast cancer and hepatocellular carcinoma. These observations may suggest additional roles for Mex3a in these other tumor types and may open new interesting research avenues.

Perspective and Future directions

The unifying theme behind this thesis has been to understand stemness in the intestine, and how this is related to homeostasis and disease. Defining stemness is not a trivial issue since this entails understanding the sum of functions encoded within ISCs and how they are essential in maintaining self-renewal and multipotency.

In Chapter 1 we undertook a top-down approach to answer this issue and were able to identify, isolate and characterize the defining features of ISCs at the transcriptional level. Furthermore, we were able to ascertain that these ISC features are intricately linked to CRC biology.

In the light of our study and others, the major issue in the CSC field is whether the ablation of these cells gives an actual survival benefit to patients. We envision that tumor heterogeneity and cancer cell plasticity will pose the greatest challenges to answer this central issue, but we are actively pursuing new strategies to overcome these matters. If indeed CSCs are a valuable therapeutic target, the following challenge will be to identify the differences between colon CSCs and ISCs to generate tailored therapies.

In Chapter 2 we have attempted to dissect intestinal stemness features in a bottom-up approach. By studying Mex3a, a largely unknown gene intricately connected to SCs, we expected to uncover new principles of stemness regulation in homeostasis and disease.

In this sense, this project has posed a challenge due to the complete lack of tools and information available, but has led us to completely unexpected research avenues to explore in SCs. Although we still require finding a biological context where we can clearly uncover the function of Mex3a, our preliminary data shows that this gene has essential functions in mouse development and potential connections to ISC biology at the level of cell cycle and metabolism.

Overall, we expect that through the understanding of Mex3a we will identify new general principles of stemness that can be applied to normal and cancer SC biology in the intestine and other tissues. While the current state of the project is preliminary, so far our findings suggest that that Mex3a may be involved in stem cell biology. **Figure 47** summarizes our working hypothesis regarding the function of Mex3a based on our results.

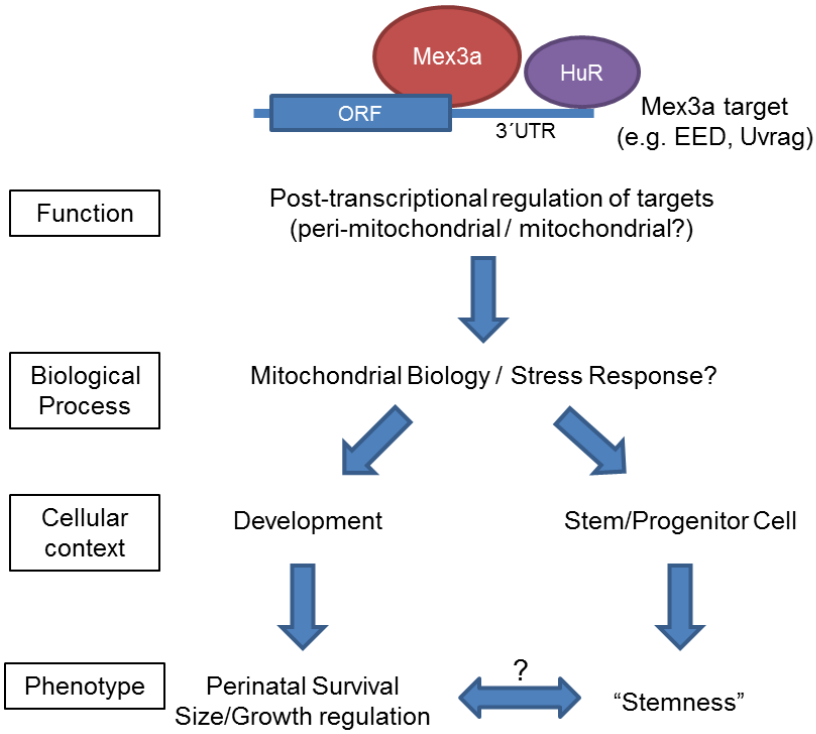

Figure 47: Working hypothesis for the biological function of Mex3a. Mex3a forms protein complexes with HuR and other RBPs and regulate the translation of nuclear-encoded mitochondria regulatory genes. These genes in turn regulate mitochondrial biology and stress response, which are necessary for development and stem cell maintenance upon stress.

Conclusions

Chapter 1

1. An expression gradient of the EphB2 tyrosine-kinase receptor characterizes intestinal cells at different stages of differentiation. Intestinal stem cells, transit-amplifying cells and differentiated cells of the intestinal epithelium can be purified according to decreasing EphB2 surface levels.

2. We have generated gene expression signatures that define stem cells, proliferative cells and differentiated cells of mouse small intestinal epithelium.

3. The expression levels of the ISC-specific signature are increased in late stage colorectal cancers. High expression levels of the ISC signature predict colon cancer relapse.

4. Human late stage colon cancers show at least two phenotypically distinct cell populations: ISC-like and differentiated-like tumor cells. These phenotypes are mutually exclusive.

5. Tumor cells are organized in a manner reminiscent to the normal colon epithelium. Generally, ISC-like cells are in close contact with the stroma, whereas differentiated-like cells are towards the tumor lumen.

6. EphB2^{High} tumor cells express markers of normal intestinal stem cells. This tumor cell population is enriched in tumor initiating cells as shown by their ability to propagate the disease in transplantation assays.

7. EphB2^{High} tumor cells self-renew and produce differentiated progeny.

8. Colon cancers are organized in a hierarchical structure reminiscent of that of the normal colon epithelium.

Chapter 2

9. The ISC signature encodes several genes whose function might be essential for stemness. One of these genes is Mex3a, which is enriched in all stem cell populations tested so far.

10. The ablation of Mex3a in the adult intestine in homeostatic conditions does not generate any overt effect. The disruption of Mex3a is stable over time and does not alter Cdx2 levels or particular cell lineages.

11. Mex3a fully deficient mice present reduced size and perinatal lethality.

12. Mex3a^{+ve} cells in the intestine express both ISC and enteroendocrine specific genes. These cells are enriched in the expression of intestinal label retaining cell (LRC) –specific genes.

13. Mex3a^{+ve} cells are more radioresistant than Lgr5^{+ve} cells.

14. Mex3a interacts with HuR (Elavl1).

15. The mRNAs bound by Mex3a are enriched in mitochondrial and cell cycle related genes.

16. EED2 is a novel mitochondrial protein whose expression requires Mex3a.

17. Mex3a expression is elevated in hematopoietic LSK cells as well as in ES cultures.

18. Mex3a expression is increased in mouse adenomas as well as in several types of human cancer.

Methods

Standard Cell culture

All cell lines were cultured in standard conditions in DMEM (Gibco), supplemented with 10% FBS (Gibco). For the lentivirus-transduced cells, puromycin (Invivogen, 2 µg/mL) was added to the standard media to select the stable expression of the transgenes. For transgene induction Doxycycline (Sigma-Aldrich) was used at 1 µg/mL and left in the culture media for the intended time of the experiment. All the cell lines used in this study were obtained from the ATCC (i.e. 293T, LS174T, SW948, SW403 and L-cells).

Cloning of Human and Mouse Mex3a

All PCR reactions involved in cloning were performed with the PFU Turbo polymerase (Agilent) following the manufacturer's instructions. All Gateway reactions were done following the manufacturer´s protocol (Invitrogen).

Human Mex3a was cloned by exons and these were ligated taking advantage of an AgeI site in the 5´ of exon 2. Briefly, exon 1 was amplified adding the initial segment of exon2 (including the AgeI site) in the reverse primer. This PCR product was cloned into the pIRES2-DsRedExpress2 vector. After this step, the same was done for exon 2, which was ligated in frame to exon 1 through the abovementioned AgeI site. After confirming the correct sequence, the entire Mex3a ORF was amplified removing the stop codon and adding a NotI site. This PCR product was cloned in frame (through the NotI site) to a pcDNA3.1 with a C-terminal TAP tag (consisting in two tandem strep tags followed by a flag tag). The Mex3a-TAP construct was then amplified with Gateway adaptors and recombined into the pDONR221 vector. Finally, the Mex3a TAP was recombined into the lentiviral inducible vector pTRIPz Gateway.

Site directed mutagenesis

In order to generate mutant versions of Mex3a, site directed mutagenesis was performed. 40 – 50 nt primers (forward and reverse) were designed to have the desired mutation in the center of the primer. 10 ng of pDONR221 Mex3a TAP was used as template of a PFU PCR program were the entire plasmid was amplified. After amplification, 10 µL of the reaction were used to visualize if the PCR worked. If so, the rest of the material was digested with DpnI at 37 ºC for 6 hours. 5 µL of digested PCR product where then transformed into E. coli competent bacteria (Lucigen) and plated. 3 colonies were grown and sequenced to verify the presence of the desired mutation. When confirmed, the pDONR221 mutants were cloned into pTRIPz to generate stable cell lines.

Lentiviral production and infection protocol

HEK293T cells were seeded at 80% confluence and after 8 - 16 hours, were transfected with third generation lentiviral packaging plasmids RTR2, VSV-G, KGP1R and pTRIPz in a ratio 1:1:3:5. 24 hours post transfection, the media was changed. After another 24 hours cell media was collected. This media was supplemented with 10% FBS and polybrene and sterilized by passing through a 0.22 µm filter. This was added to recipient cells (e.g. 293T, LS174T, SW403, SW948) seeded at low confluence (20 – 30%). This procedure was repeated with the media from 293T cells 24 hours after the initial infection to ensure a higher viral infection. After the infection, viral media was removed and cells were incubated in normal media for 24 hours. Finally, infected cells were trypsinized and seeded in media containing puromycin (2 µg/mL) and left under selection to obtain a stable resistant population with a doxycycline inducible cassette.

RNA extraction, cDNA production and RT qPCR analysis

RNA extractions from cultured, FACS sorted or isolated cells were done with the Trizol reagent (Invitrogen). The RNA from the aqueous phase was then purified with the RNA PureLink Kit (Ambion) and quantified by Nanodrop. cDNA was produced with

the High-Capacity cDNA Reverse Transcription kit (Applied Biosystems) following the manufacturer´s instructions.

To assess changes in expression of selected genes RT-qPCR was done with their respective TaqMan probes or primers for SYBR Green. For TaqMan assays the TaqMan Universal PCR Master Mix (Applied Biosystems) was used. In the case of SYBR Green reactions the Power SYBR Master Mix (Applied Biosystems) was used. To calculate gene expression to a normalization gene the comparative threshold cycle method was used.

Western Blot Analysis

Cells were lysed using 1:1:1 buffer (1 mM EDTA, 1 mM EGTA, 1% SDS) supplemented with protease and phosphatase inhibitors (Sigma Aldrich) and heated at 99 ºC for 10 min. After this heating step, cell lysates were pipetted several times to break up gDNA and later centrifuged at 13200 rpm for 15 min. The supernatant was kept as the protein extract. Protein content was quantified with the Protein Assay (BioRad), based in the Bradford method. Equal amounts of protein per sample were separated by standard SDS-PAGE and transferred to PVDF membranes. The membranes were incubated in TBS-T 0.1% supplemented with 5% milk for 30 min at RT to block unspecific antibody binding. Primary antibodies were incubated overnight at 4 ºC (See **Table 8** for antibody details). Secondary antibodies were diluted 1/10000 and incubated for 1 hour at RT with the membranes. After antibody incubations membranes were washed at least 3 times with TBS-T 0.1% for 10 min. Immuno-complexes were visualized with ECL (Amersham).

Ribonucleoprotein complex immuno-precipitation (RIP)

RIP was performed following the protocol described by Keene et al (Keene et al., 2006; Tenenbaum et al., 2002). Cells were seeded and after 24 hours, doxycycline (1 µg / mL) was added. After an overnight induction, cells were washed twice with ice cold PBS. After the washes, cells were scraped in PBS and centrifuged at 1200 rpm for 5 min at 4 ºC. The cells were then resuspended in one pellet volume of polysome lysis buffer (100 mM KCl, 5 mM $MgCl_2$, 10 mM HEPES pH 7.0, 0.5% NP40, 1 mM DTT, 100 units/mL RNAse OUT, 400 µM VRC, Protease Inhibitors). The cells

were lysed on ice for 5 min and then stored at -80 ºC for at least 1 hour. The lysate was then thawed and centrifuged at 13200 rpm for 15 (4 ºC). The supernatant was kept for the IP. Magnetic anti Flag M2 beads (Invitrogen), were washed 5X with NT2 buffer (50 mM Tris HCl pH 7.4, 150 mM NaCl, 1mM $MgCl_2$, 0.05% NP40). Half of the lysate (normally around 150 µL) was supplemented with NT2 buffer (up to 1 mL) and with RNAse Inhibitors (200 units/mL RNAse OUT, 400 µM VRC, 1 mM DTT and 20 mM EDTA). 50 µL of washed beads were added to each lysate, mixed briefly and 100 µL of the mix were kept as 10% of input for each IP. The rest of the IP was left for 2 hours at RT with orbital shaking. After this incubation, the supernatant was discarded and the beads were washed 4 times with ice cold NT2 buffer. After the final wash was done, all liquid was removed from the beads and 1 mL of Trizol reagent was added to these as well as the inputs. RNA extraction was performed as described above. In the case of the RIP Chip experiment, 25 ng of RNA were hybridized to Human Exon Arrays (Hu Ex 1.0, Affymetrix). The samples analyzed were RIP and Input of CV + Dox, Mex3a TAP– Dox and Mex3a TAP + Dox. To generate the list of targets, RIPs were compared to their respective Inputs and a probe was considered a target when the enrichment in Mex3a TAP+ Dox RIP vs Input was over 10 fold and not enriched in either Mex3a TAP– Dox RIP vs Input and CV + Dox RIP vs Input. To independently validate the targets, the experiment was repeated and SYBR green RT qPCR was used to assess enrichment mRNAs to Mex3a TAP. Relative enrichments were calculated by assessing the RIP against its respective input, Gapdh was used as the reference gene (for primers used in RIP assays see **Table 10**).

Tandem Affinity Purification (TAP)

TAP was performed as previously described (Gloeckner et al., 2007; Gloeckner et al., 2009). LS174T pTRIPz Mex3a TAP and CV cells were seeded and after 24 hours, doxycycline (1 µg / mL) was added. After an overnight induction, cells were washed twice with ice cold PBS. After the washes, cells were scraped in PBS and centrifuged at 1200 rpm for 5 min at 4 ºC. The pellet was then lysed in 1 mL of lysis buffer (TBS, 0.5% NP40, Protease and

Phosphatase Inhibitors) for 20 min on ice. Lysates were then sonicated for 15 min with a Bioruptor sonicator (Diagenode), with cycles of 30s ON / 30s OFF set at the highest intensity. After this step, lysates were cleared by centrifugation at 13200 rpm for 15 min (4 ºC). Protein extracts were quantified with the Protein Assay (BioRad) and 10 mg of each sample was used per IP in a total volume of 1 mL. To this extract 100 µL of streptactin resin (IBA) was added to each IP and incubated for 1 hour at 4 ºC with orbital rotation. After this step, the IP was loaded to a microspin column (GE Healthcare) and 3 washes were done with wash buffer (TBS, 0.1% NP40, Protease and Phosphatase Inhibitors). Washes were performed by adding the buffer to the column, and centrifuging at 800 rpm for 15 s and discarding the flow-through. After the washes, the proteins were eluted with 500 µL of 5X desthiobiotin elution buffer (IBA) for 20 min on ice. The flow-through was then collected and concentrated using an Amicon Ultra centrifugal filter (Millipore). The concentrated flow-through was then analyzed by mass spectrometry (CRG facility). Mex3a interacting proteins were defined as proteins with at least 2 peptides that were solely present in the Mex3a + Dox IP or were at least enriched 2 fold over the CV IP.

Mex3a interactors were independently confirmed by repeating the TAP protocol using the anti-Flag M2 magnetic resin. For this 1 mg of lysate was loaded in each IP and the protein elution was performed with 20 µL of 5X Laemmli buffer on the magnetic beads and incubated at 99 ºC for 5 min. After elution, the western blot protocol was followed as described above.

Immunofluorescence of cultured cells

Cells were seeded in glass slides (BD Falcon). After induction or treatment, the cells were fixed for 10 min with 4% PFA at room temperature. After this, 3 washes with PBS were done and glycine 20 mM (in PBS) was added for 10 min at room temperature to block the PFA. After this, 3 washes with PBS were done as before and the cells were incubated with Triton X-100 0.25% (in PBS) for 20 min at room temperature. Once again 3 washes were done with PBS and the cells were blocked with PBS-BSA 1% for 30 min at room temperature. Primary antibodies were diluted in PBS-BSA 1%

and added to the cells overnight at 4ºC. After this incubation the cells were washed with PBS 3 times and the secondary antibody was added (in PBS-BSA 1%) and incubated at room temperature for 90 min in the dark. Finally, cells were washed twice with PBS, stained with DAPI, washed once again and mounted for viewing by confocal microscopy in a Leica SP5 microscope.

Tethering assays

Tethering assays were performed as previously described (Novoa et al., 2010). Mex3a TAP and mutant versions were PCR amplified and cloned in frame with the MS2 binding protein. The empty, chimeric MS2-TAP or chimeric MS2-Mex3a-TAP (WT or C469G mutant) were transfected into 293T cells alongside a pLUC MS2 6X (bearing 6 tandem repeats of the MS2 loop in the 3´UTR of the Firefly luciferase gene) and a pCMV-RNL plasmid (containing the Renilla luciferase gene). 48 hours after transfection the firefly luciferase activity was analyzed relative to the renilla luciferase activity. All samples were normalized to the MS2-TAP transfected cells and the relative activity of WT and mutant MS2-Mex3a-TAP constructs was measured.

Mitochondrial enrichment protocol

Cells were washed twice with ice cold PBS and scraped. They were centrifuged at 1200 rpm for 5 min (4ºC). The cells were then resuspended in 10 packed volumes of NKM buffer (1 mM Tris HCl pH 7.4, 0.13 M NaCl, 5 mM KCl, 7.5 mM $MgCl_2$) and centrifuged at 1200 rpm for 5 min (4 ºC). This step was repeated twice. The pellet was resuspended in 6 packed cell volumes of mitochondrial homogenization buffer (10 mM Tris HCl pH 6.7, 10 mM KCl, 0.15 mM $MgCl_2$, 1mM DTT and protease inhibitors) and incubated on ice for 10 min. This suspension was then transferred to a tissue grinder (Kimble Chase) and cells were broken with 40 strokes of a large pestle. After homogenization, the lysate was transferred to a tube containing 1 packed cell volume of 2M sucrose and centrifuged at 3700 rpm for 5 min (4 ºC). The pellet was discarded and the supernatant was transferred to a new tube containing 1 packed cell volume of 2M sucrose. This procedure is repeated twice. The obtained supernatant is centrifuged at 8700 rpm for 10 min (4 ºC)

to pellet mitochondria. The supernatant was kept as the cytoplasmatic fraction. The mitochondrial pellet was resuspended in 3 packed cell volumes of mitochondrial suspension buffer (10 mM Tris HCl pH 6.7, 0.15 mM $MgCl_2$, 0.25M sucrose, 1 mM DTT and protease inhibitors). The mitochondrial suspension was centrifuged at 10200 rpm for 5 min (4 ºC). Finally, the mitochondrial pellet was lysed with 1:1:1 buffer and analyzed by western blot as previously described.

Immunohistochemistry

Immunohistochemistry was performed as previously described in Chapter 1 (Merlos-Suarez et al., 2011).

Generation of the Mex3a conditional KO (cKO) mouse model

To ensure the deletion of Mex3a, loxP sites were designed to flank the coding region of exon 2. The targeting vector was generated by Genebridges. The vector was verified by restriction enzyme digestion as well as sequencing. The vector was electroporated into W4 mouse embryonic stem cells (mESCs) and stably transfected cells were selected with G418. After this, single colonies were picked and triplicate plates were generated of resistant clones. The clones were then screened by long range PCR by using the Sequal Prep Kit (Invitrogen). Positive clones were then expanded and further analyzed by Southern Blot (as described in Barker et al, Nature, 2008) to assure correct and unique genomic integration. The clones verified by southern were then transfected with an FlpO-bearing plasmid to remove the Neomycin resistance. Single clones were picked and screened by PCR for recombination and presence of both loxP sites. Positive clones were then expanded and analyzed by Southern once again to ensure the appropriate integration of the cassette, as well as to independently confirm the deletion of the Neomycin resistance cassette. Finally, positive clones were selected and blastocyst injection was done to generate chimeras. The chimeras with successful germline transmission were bred with C57Bl6 mice and the offspring were used to generate the final colonies of mice.

Generation of the Mex3a knock-in mouse model

A cassette bearing a tdTomato/T2A/Cre-ERT2/bGH polyA was inserted in frame with the Mex3a start codon in exon 1. The

targeting protocol followed was the same as described for the cKO mouse model.

Organoid Culture

ISC organoid cultures were done as described in Chapter 1 (Merlos-Suarez et al., 2011). Besides the standard culture conditions, the Stem Organoid media was used by replacing 50% of the Advanced DMEM/F12 with Wnt3a conditioned media. Apc media was used to culture Apc mutant organoids (the culture conditions being exactly the same as the basic media, but removing Rspo1 and recombinant Noggin as well). For Cre induction, cultures were supplemented with 500 nM of 4-OH Tamoxifen (Sigma) for 48 hours, after this period it was removed from the cultures and after different times the cells were collected.

Transcriptomics and Proteomics of Stem Organoids

Proximal duodenum of 3 $Mex3a^{+/+}$ and 3 $Mex3a^{fl/fl}$ mice (all age and sex-matched and bearing the Villin Cre-ER^{T2} transgene) were used to obtain crypts and put in culture in stem conditions. After 72 hours the cultures were expanded and treated with 500 nM of 4-OH Tamoxifen for 48 hours. After this treatment 1 matrigel drop was collected in Trizol for each mouse and checked for deletion of Mex3a at the RNA level. The remaining drops were pooled together for each animal and treated with cell recovery solution (BD Biosciences) for 1 hour on ice. After this, the cells were washed twice with HBSS and resuspended in lysis buffer for mass spectrometry (SDS 4%, 0.1 M DTT, 0.1M Hepes). After the lysis, cells were vortexed and incubated at 95 ºC for 3 min. Finally, the lysates were then sonicated with a Bioruptor for 15 min with cycles of 30s ON / 30s OFF. The samples were stored at -80 ºC and submitted for mass spectrometry analysis. The transcriptomic data was obtained by hybridizing 25 ng of RNA to M430_2 microarrays (Affymetrix) of 2 $Mex3a^{+/+}$ and 2 $Mex3a^{fl/fl}$ mice.

Induction of Cre activity in mouse models

For gene ablation, a full Tamoxifen (Sigma) dose was administered as described (Verzi et al., 2010).

FACS sorting of Mex3a knock-in cells from small intestine

Proximal small intestines (duodenum and jejunum) were removed from age and sex-matched mice and cut open longitudinally. They were later incubated with HBSS EDTA (8 mM) for 5 min at room temperature. After this incubation, intestines were shaken vigorously to remove villi and the first supernatant was discarded. The intestines were then incubated with HBSS EDTA on ice for 20 min, after which time the shaking was repeated. This yielded the first crypt fraction. This process was repeated twice and after microscopic inspection of the samples the fractions enriched in crypts were kept (usually fractions 2 and 3). These fractions were then pooled together for each mouse, centrifuged at 1200 rpm for 5 min (4 ºC) and filtered through a 100 µm mesh (BD Biosciences) to further remove villi. The filtered fractions were then disaggregated by adding dispase (0.4 mg/mL) and incubating for 30 min at 37 ºC with orbital rotation. The media was then supplemented with 5% FBS (Gibco) to neutralize dispase and the samples were sequentially filtered through a 70 and 40 µm mesh. This procedure yielded single-cell preparations of small intestinal crypts that were then analyzed by FACS in a FACS Aria 2.0 (BD). To obtain the single cells expressing the Mex3a-driven tdTomato the following gating scheme was followed: Cells were selected in the FSC-A/SSC-A dotplot to remove debris. The cells were then gated to exclude cellular aggregates in the FSC-A/ FSC-W dot plot. Single cells were selected for viability by excluding positive staining with DAPI (1/400, Sigma Aldrich). Finally, the selected cells were viewed in a FSC-A/GreenE Dot plot. Gates of tdTomato cells were set comparing to a WT sample which has no detectable tdTomato expression. tdTomato cells were then sorted by their levels of expression and RNA of the sorted populations was performed as mentioned above.

Mouse models and genotyping

For inducible intestinal gene deletion in the adult mouse, Villin Cre-ERT2; Mex3a+/+ and Villin Cre-ERT2; Mex3a fl/fl mice were used (Villin Cre-ERT2 mice have been previously described and were obtained from Sylvie Robine).

For inducible intestinal tumorigenesis, Lgr5 Cre-ERT2; Apc fl/fl; Mex3a +/+ and Lgr5 Cre-ERT2; Apc fl/fl; Mex3a fl/fl mice were used (Lgr5 Cre-ERT2 mice have been previously described and were obtained from Hans Clevers).

For full KO mice, Sox2-Cre mice were crossed with Mex3a flox/flox mice to establish a Mex3a null (Δ) allele. The Mex3aΔ/+ mice were intercrossed and the Sox2-Cre was removed by selecting mice (Sox2-Cre mice have been previously described and were obtained from Ángel Nebreda).

For lineage tracing analysis Mex3aKI/+; ROSA26-LSL-LacZ were used. ROSA26-LSL-LacZ mice were obtained from the Jackson Laboratories.

All mice were genotyped with standard PCR protocols described in the references above.

Analysis of mouse bone marrow populations

Bone marrow from femur and tibia of mice was obtained by cutting the bone tips and flushing with PBS 1X. This cell suspension was then centrifuged for 5 min at 1600 rpm (4 ºC) and treated with ammonium chloride solution for 3 min at room temperature to lyse red blood cells. After this, cells were washed, centrifuged as before and resuspended in staining buffer (PBS-5%FBS). Cells were counted and around 2 x 10^6 cells were stained with individual primary antibodies or a combination of all of them. The primary staining was performed on ice for 25 min in the dark, followed by 2 washes with PBS 1X. This was repeated for the secondary staining when required. **Table 9** shows the antibodies used to stain for mouse lineage^{-ve}, Sca-1^{+ve} and cKit^{+ve} (LSK) cells.

Embryonic Stem Cell Culture

Mex3a targeted W4 ESCs were cultured on gelatin coated plates. Cell were grown in DMEM 10% FBS supplemented with Glutamine, non-essential aminoacids, sodium pyruvate, β-mercaptoethanol and leukemia inhibitory factor (LiF). Cells were passaged every two days and were analyzed by fluorescence microscopy and FACS sorting.

Protein	Antibody	Company (ref nº)
MEX3A	Rabbit polyclonal	Abcam (ab79046)
TOMM20	Mouse monoclonal	Santa Cruz (sc-11415)
VDAC1	Rabbit polyclonal	Abcam (ab15895)
EED	Mouse monoclonal	Millipore (05-1320)
CDX2	Mouse monoclonal	Biogenex (MU392A-UC)
HUR (ELAVL1)	Mouse monoclonal	Santa Cruz (sc-5261)
CDK1	Mouse monoclonal	Santa Cruz (sc-54)
ACTB	Rabbit polyclonal	Sigma Aldrich (A5316)
H3K27me3	Rabbit polyclonal	Active Motif (39155)
Flag	Mouse monoclonal	Sigma Aldrich (F3165)

Table 8: Antibodies used for Western Blot

Protein	Format	Clone	Cat. Number	Company
Ter119	Biotin	TER-119	13-5921-82	eBioscience
B220	Biotin	RA3-6B2	553085	BD Pharmingen
CD3e	Biotin	145-2C11	553059	BD Pharmingen
Gr1	Biotin	RB6-8C5	553124	BD Pharmingen
Streptavidin	PerCP-Cy5.5		45-4317-82	eBioscience
Sca-1	FITC	D7	557405	BD Pharmingen
C-Kit	APC-H7	2B8	560185	BD Pharmingen
CD48	PE	HM48-1	557485	BD Pharmingen
CD150	APC	9D1	17-1501-81	eBioscience

Table 9: Antibodies for HSC population analysis

Technique	Oligo name	Sequence
Southern Blot	Probe 2F	AAAAAGGCCAGGGAAACCTC
	Probe 2R	CAGGCCTGAGGATAGGAATG
	Probe 6F	GAAAGCTGAAGGCAGGACAC
	Probe 6R	TCCCATCTCTCCACTCATCC
Genotyping	U5F	AGTCCTGCCCTGGGCGTCAG
	U3R	CCCAGGCCCTCCTAGCATCCC
	D5F	TCCTGATTCGCTAGCCCTCTGGT
	D3R	TGAAGGGGGAAGAGAAGCCCCT
	D5F bGH	ATTGCATCGCATTGTCTGAG
	U3R WT	CAGCTCGGCCTCTTTGTAGA
	KI Seq F	CTCCCCCAGCTTTTGTTTCGCC
	Cre Seq F	GGATTTCCGTCTCTGGTGTAGCTG
	Ert2 Seq R	CAGATTCATCATGCGGAACCGAG
Mouse qPCR	Mm Mex3a F	ACACCACGGAGTGCGTTC
	Mm Mex3a R	GTTGGTTTTGGCCCTCAGA
	Mm Gapdh F	GGGAAATTCAACGGCACAGT
	Mm Gapdh F	AGATGGTGATGGGCTTCCC
	Mm Zbtb16 F	TGCGCAGCTATATTTGCAGT
	Mm Zbtb16 R	CACCGTTGTGTGTTCTCAGG
	Mm Tef F	GTTTGCAGAGGAGGACCTGA
	Mm Tef R	AGGTTACAAGGGCCCGTACT
	Mm Hist1H2ap F	AGCTCTTGCTCTTTGCAAGC
	Mm Hist1H2ap R	AGCTTGTTGAGCTCCTCGTC
	Mm Tial1 F	GAGCAACCCGATAGCAGAAG
	Mm Tial1 R	GGACTTTCCAGTTGCCATGT
	Mm Mrpl54 F	TAAAAAGCCAGTTGGCAAGG
	Mm Mrpl54 R	GTGGCGCCAGATATTCTGTT
Human qPCR	Hs Eed F	TGGTACATGAGGTTTTCTATGGATT
	Hs Eed R	GCATCATCACAAACAGCTATAAGAA
Cloning	Hs Mex3a ORF F	AATGTCGACCCACCATGCCTAGTCTAGTGGTATCTGG
	Hs Mex3a ORF R TAP Not I	aaaGCGGCCGCGGAGAATATTCGGATGGCTTGCGTGGC
	Hs Mex3a G240D F	GGTGGGGCTGGTGGTGGACCCCAAAGGGGCAACC
	Hs Mex3a G240D R	GGTTGCCCCTTTGGGGTCCACCACCAGCCCCACC
	Hs Mex3a C469G F	CGGCGGCGGGCGGGATGGCATGGTCTGCTTTGAGAGCGAAGTG
	Hs Mex3a C469G R	CACTTCGCTCTCAAAGCAGACCATGCCATCCCGCCCGCCGCCG
	Hs Mex3a ORF F	AATGTCGACCCACCATGCCTAGTCTAGTGGTATCTGG
	Hs Mex3a DN KH R NotI	AAAGCGGCCGCATTGTTGTACTCGAGGATCTTGCC

Table 10: Primers used for RT qPCR and cloning

References

Al-Hajj, M., Wicha, M.S., Benito-Hernandez, A., Morrison, S.J., and Clarke, M.F. (2003). Prospective identification of tumorigenic breast cancer cells. Proceedings of the National Academy of Sciences of the United States of America *100*, 3983-3988.

Balagopal, V., and Parker, R. (2009). Polysomes, P bodies and stress granules: states and fates of eukaryotic mRNAs. Current opinion in cell biology *21*, 403-408.

Barker, N., Bartfeld, S., and Clevers, H. (2010a). Tissue-resident adult stem cell populations of rapidly self-renewing organs. Cell stem cell *7*, 656-670.

Barker, N., Huch, M., Kujala, P., van de Wetering, M., Snippert, H.J., van Es, J.H., Sato, T., Stange, D.E., Begthel, H., van den Born, M.*, et al.* (2010b). Lgr5(+ve) stem cells drive self-renewal in the stomach and build long-lived gastric units in vitro. Cell stem cell *6*, 25-36.

Barker, N., Ridgway, R.A., van Es, J.H., van de Wetering, M., Begthel, H., van den Born, M., Danenberg, E., Clarke, A.R., Sansom, O.J., and Clevers, H. (2009). Crypt stem cells as the cells-of-origin of intestinal cancer. Nature *457*, 608-611.

Barker, N., Rookmaaker, M.B., Kujala, P., Ng, A., Leushacke, M., Snippert, H., van de Wetering, M., Tan, S., Van Es, J.H., Huch, M.*, et al.* (2012a). Lgr5(+ve) stem/progenitor cells contribute to nephron formation during kidney development. Cell Rep *2*, 540-552.

Barker, N., van de Wetering, M., and Clevers, H. (2008b). The intestinal stem cell. Genes & development *22*, 1856-1864.

Barker, N., van Es, J.H., Kuipers, J., Kujala, P., van den Born, M., Cozijnsen, M., Haegebarth, A., Korving, J., Begthel, H., Peters, P.J.*, et al.* (2007a). Identification of stem cells in small intestine and colon by marker gene Lgr5. Nature *449*, 1003-1007.

Barker, N., van Oudenaarden, A., and Clevers, H. (2012b). Identifying the stem cell of the intestinal crypt: strategies and pitfalls. Cell stem cell *11*, 452-460.

Batlle, E., Bacani, J., Begthel, H., Jonkheer, S., Gregorieff, A., van de Born, M., Malats, N., Sancho, E., Boon, E., Pawson, T.*, et al.* (2005). EphB receptor activity suppresses colorectal cancer progression. Nature *435*, 1126-1130.

Batlle, E., Henderson, J.T., Beghtel, H., Van den Born, M., Sancho, E., Huls, G., Meeldijk, J., Robertson, J., Van de Wetering, M., Pawson, T.*, et al.* (2002a). B-Catenin and TCF Mediate Cell Positioning in the Intestinal Epithelium by Controlling the Expression of EphB/EphrinB. Cell *111*, 251-263

Begus-Nahrmann, Y., Lechel, A., Obenauf, A.C., Nalapareddy, K., Peit, E., Hoffmann, E., Schlaudraff, F., Liss, B., Schirmacher, P., Kestler, H.*, et al.* (2009). p53 deletion impairs clearance of chromosomal-instable stem cells in aging telomere-dysfunctional mice. Nature genetics *41*, 1138-1143.

Berthier, A., Jimenez-Sainz, J., and Pulido, R. (2013). PINK1 regulates histone H3 trimethylation and gene expression by interaction with the polycomb protein EED/WAIT1. Proceedings of the National Academy of Sciences of the United States of America *2013*, 19.

Besson, V., Smeriglio, P., Wegener, A., Relaix, F., Nait Oumesmar, B., Sassoon, D.A., and Marazzi, G. (2011). PW1 gene/paternally expressed gene 3 (PW1/Peg3) identifies multiple adult stem and progenitor cell populations. Proceedings of the National Academy of Sciences of the United States of America *108*, 11470-11475.

Bjerknes, M., and Cheng, H. (1981). Methods for the isolation of intact epithelium from the mouse intestine. Anat Rec *199*, 565-574.

Boiko, A.D., Razorenova, O.V., van de Rijn, M., Swetter, S.M., Johnson, D.L., Ly, D.P., Butler, P.D., Yang, G.P., Joshua, B., Kaplan, M.J.*, et al.* (2010). Human melanoma-initiating cells express neural crest nerve growth factor receptor CD271. Nature *466*, 133-137.

Bonnet, D., and Dick, J.E. (1997). Human acute myeloid leukemia is organized as a hierarchy that originates from a primitive hematopoietic cell. Nat Med *3*, 730-737.

Boyd, M., Hansen, M., Jensen, T.G., Perearnau, A., Olsen, A.K., Bram, L.L., Bak, M., Tommerup, N., Olsen, J., and Troelsen, J.T. (2010). Genome-wide analysis of CDX2 binding in intestinal epithelial cells (Caco-2). The Journal of biological chemistry *285*, 25115-25125.

Buczacki, S.J., Zecchini, H.I., Nicholson, A.M., Russell, R., Vermeulen, L., Kemp, R., and Winton, D.J. (2013). Intestinal label-retaining cells are secretory precursors expressing Lgr5. Nature *495*, 65-69.

Buchet-Poyau, K., Courchet, J., Le Hir, H., Seraphin, B., Scoazec, J.Y., Duret, L., Domon-Dell, C., Freund, J.N., and Billaud, M. (2007). Identification and characterization of human Mex-3 proteins, a novel family of evolutionarily conserved RNA-binding proteins differentially localized to processing bodies. Nucleic acids research *35*, 1289-1300.

Burga, A., Casanueva, M.O., and Lehner, B. (2011). Predicting mutation outcome from early stochastic variation in genetic interaction partners. Nature *480*, 250-253.

Cadigan, K.M. (2008). Wnt-beta-catenin signaling. Current biology : CB *18*, R943-947.

Cairns, J. (1975). Mutation selection and the natural history of cancer. Nature *255*, 197-200.

Cano, F., Bye, H., Duncan, L.M., Buchet-Poyau, K., Billaud, M., Wills, M.R., and Lehner, P.J. (2012). The RNA-binding E3 ubiquitin ligase MEX-3C links ubiquitination with MHC-I mRNA degradation. The EMBO journal *31*, 3596-3606.

Casali, A., and Batlle, E. (2009). Intestinal stem cells in mammals and Drosophila. Cell stem cell *4*, 124-127.

Cifuentes, D., Martinez-Pons, C., Garcia-Rocha, M., Galina, A., Ribas de Pouplana, L., and Guinovart, J.J. (2008). Hepatic glycogen synthesis in the absence of glucokinase: the case of embryonic liver. J Biol Chem *283*, 5642-5649.

Ciosk, R., DePalma, M., and Priess, J.R. (2006). Translational regulators maintain totipotency in the Caenorhabditis elegans germline. Science *311*, 851-853.

Cizkova, A., Stranecky, V., Mayr, J.A., Tesarova, M., Havlickova, V., Paul, J., Ivanek, R., Kuss, A.W., Hansikova, H., Kaplanova, V.*, et al.* (2008). TMEM70 mutations cause isolated ATP synthase deficiency and neonatal mitochondrial encephalocardiomyopathy. Nat Genet *40*, 1288-1290.

Clevers, H. (2011). The cancer stem cell: premises, promises and challenges. Nature medicine *17*, 313-319.

Clevers, H., and Batlle, E. (2013). SnapShot: the intestinal crypt. Cell *152*, 1198-1198.

Cortina, C., Palomo-Ponce, S., Iglesias, M., Fernandez-Masip, J.L., Vivancos, A., Whissell, G., Huma, M., Peiro, N., Gallego, L., Jonkheer, S.*, et al.* (2007a). EphB-ephrin-B interactions suppress colorectal cancer progression by compartmentalizing tumor cells. Nature genetics *39*, 1376-1383.

Courchet, J., Buchet-Poyau, K., Potemski, A., Bres, A., Jariel-Encontre, I., and Billaud, M. (2008). Interaction with 14-3-3 adaptors regulates the sorting of hMex-3B RNA-binding protein to distinct classes of RNA granules. The Journal of biological chemistry *283*, 32131-32142.

Chaffer, C.L., Brueckmann, I., Scheel, C., Kaestli, A.J., Wiggins, P.A., Rodrigues, L.O., Brooks, M., Reinhardt, F., Su, Y., Polyak, K.*, et al.* (2011). Normal and neoplastic nonstem cells can spontaneously convert to a stem-like state. Proceedings of the National Academy of Sciences of the United States of America *108*, 7950-7955.

Chawengsaksophak, K., James, R., Hammond, V.E., Köntgen, F., and Beck, F. (1997). Homeosis and intestinal tumors in *Cdx2* mutant mice. Nature *386*, 84-87.

Chen, J., Li, Y., Yu, T.S., McKay, R.M., Burns, D.K., Kernie, S.G., and Parada, L.F. (2012). A restricted cell population propagates glioblastoma growth after chemotherapy. Nature *488*, 522-526.

Cheng, H., and Leblond, C.P. (1974). Origin, differentiation and renewal of the four main epithelial cell types in the mouse small intestine. I. Columnar cell. Am J Anat *141*, 461-479.

Dalerba, P., Cho, R.W., and Clarke, M.F. (2007a). Cancer stem cells: models and concepts. Annual review of medicine *58*, 267-284.

Dalerba, P., Dylla, S.J., Park, I.K., Liu, R., Wang, X., Cho, R.W., Hoey, T., Gurney, A., Huang, E.H., Simeone, D.M.*, et al.* (2007b). Phenotypic characterization of human colorectal cancer stem cells. Proceedings of the National Academy of Sciences of the United States of America *104*, 10158-10163.

Dalerba, P., Kalisky, T., Sahoo, D., Rajendran, P.S., Rothenberg, M.E., Leyrat, A.A., Sim, S., Okamoto, J., Johnston, D.M., Qian, D.*, et al.* (2011). Single-cell dissection of transcriptional heterogeneity in human colon tumors. Nature biotechnology *29*, 1120-1127.

de Lau, W., Barker, N., Low, T.Y., Koo, B.K., Li, V.S., Teunissen, H., Kujala, P., Haegebarth, A., Peters, P.J., van de Wetering, M.*, et al.* (2011). Lgr5 homologues associate with Wnt receptors and mediate R-spondin signalling. Nature *476*, 293-297.

de Sousa, E.M.F., Colak, S., Buikhuisen, J., Koster, J., Cameron, K., de Jong, J.H., Tuynman, J.B., Prasetyanti, P.R., Fessler, E., van den Bergh, S.P.*, et al.* (2011). Methylation of cancer-stem-cell-associated Wnt target genes predicts poor prognosis in colorectal cancer patients. Cell stem cell *9*, 476-485.

Deshaies, R.J., and Joazeiro, C.A. (2009). RING domain E3 ubiquitin ligases. Annual review of biochemistry *78*, 399-434.

Devaux, F., Lelandais, G., Garcia, M., Goussard, S., and Jacq, C. (2010). Posttranscriptional control of mitochondrial biogenesis: spatio-temporal regulation of the protein import process. FEBS Lett *584*, 4273-4279.

Dick, J.E. (2008). Stem cell concepts renew cancer research. Blood *112*, 4793-4807.

Diehn, M., and Clarke, M.F. (2006). Cancer stem cells and radiotherapy: new insights into tumor radioresistance. Journal of the National Cancer Institute *98*, 1755-1757.

Diehn, M., Cho, R.W., Lobo, N.A., Kalisky, T., Dorie, M.J., Kulp, A.N., Qian, D., Lam, J.S., Ailles, L.E., Wong, M.*, et al.* (2009). Association of reactive oxygen species levels and radioresistance in cancer stem cells. Nature *458*, 780-783.

Dieter, S.M., Ball, C.R., Hoffmann, C.M., Nowrouzi, A., Herbst, F., Zavidij, O., Abel, U., Arens, A., Weichert, W., Brand, K.*, et al.* (2011). Distinct types of tumor-initiating cells form human colon cancer tumors and metastases. Cell stem cell *9*, 357-365.

Donnini, M., Lapucci, A., Papucci, L., Witort, E., Jacquier, A., Brewer, G., Nicolin, A., Capaccioli, S., and Schiavone, N. (2004). Identification of TINO: a new evolutionarily conserved BCL-2 AU-rich element RNA-binding protein. The Journal of biological chemistry *279*, 20154-20166.

Draper, B.W., Mello, C.C., Bowerman, B., Hardin, J., and Priess, J.R. (1996). MEX-3 Is a KH Domain Protein That Regulates Blastomere Identity in Early C. Elegans Embryos. Cell *87*, 205-216.

Driessens, G., Beck, B., Caauwe, A., Simons, B.D., and Blanpain, C. (2012). Defining the mode of tumour growth by clonal analysis. Nature *488*, 527-530.

el Marjou, F., Janssen, K.P., Chang, B.H., Li, M., Hindie, V., Chan, L., Louvard, D., Chambon, P., Metzger, D., and Robine, S. (2004). Tissue-specific and inducible Cre-mediated recombination in the gut epithelium. Genesis *39*, 186-193.

Eppert, K., Takenaka, K., Lechman, E.R., Waldron, L., Nilsson, B., van Galen, P., Metzeler, K.H., Poeppl, A., Ling, V., Beyene, J.*, et al.* (2011). Stem cell gene expression programs influence clinical outcome in human leukemia. Nature medicine *17*, 1086-1093.

Eulalio, A., Behm-Ansmant, I., and Izaurralde, E. (2007). P bodies: at the crossroads of post-transcriptional pathways. Nature reviews Molecular cell biology *8*, 9-22.

Ezhkova, E., Pasolli, H.A., Parker, J.S., Stokes, N., Su, I.H., Hannon, G., Tarakhovsky, A., and Fuchs, E. (2009). Ezh2 orchestrates gene expression for the stepwise differentiation of tissue-specific stem cells. Cell *136*, 1122-1135.

Fearon, E.R. (2011). Molecular genetics of colorectal cancer. Annu Rev Pathol *6*, 479-507.

Feng, B., Jiang, J., Kraus, P., Ng, J.H., Heng, J.C., Chan, Y.S., Yaw, L.P., Zhang, W., Loh, Y.H., Han, J.*, et al.* (2009). Reprogramming of fibroblasts into induced pluripotent stem cells with orphan nuclear receptor Esrrb. Nat Cell Biol *11*, 197-203. doi: 110.1038/ncb1827. Epub 2009 Jan 1011.

Fernandez-Rozadilla, C., Palles, C., Carvajal-Carmona, L., Peterlongo, P., Nici, C., Veneroni, S., Pinheiro, M., Teixeira, M.R., Moreno, V., Lamas, M.J.*, et al.* (2013). BMP2/BMP4 colorectal cancer susceptibility loci in northern and southern European populations. Carcinogenesis *34*, 314-318.

Ficara, F., Murphy, M.J., Lin, M., and Cleary, M.L. (2008). Pbx1 regulates self-renewal of long-term hematopoietic stem cells by maintaining their quiescence. Cell Stem Cell *2*, 484-496. doi: 410.1016/j.stem.2008.1003.1004.

Fuchs, E. (2009). The tortoise and the hair: slow-cycling cells in the stem cell race. Cell *137*, 811-819.

Fuchs, E., and Chen, T. (2013). A matter of life and death: self-renewal in stem cells. EMBO reports *14*, 39-48.

Gao, N., White, P., and Kaestner, K.H. (2009). Establishment of intestinal identity and epithelial-mesenchymal signaling by Cdx2. Developmental cell *16*, 588-599.

Gerbe, F., Brulin, B., Makrini, L., Legraverend, C., and Jay, P. (2009). DCAMKL-1 expression identifies Tuft cells rather than stem cells in the adult mouse intestinal epithelium. Gastroenterology *137*, 2179-2180; author reply 2180-2171.

Ghosh, M., Aguila, H.L., Michaud, J., Ai, Y., Wu, M.T., Hemmes, A., Ristimaki, A., Guo, C., Furneaux, H., and Hla, T. (2009). Essential role of the RNA-binding protein HuR in progenitor cell survival in mice. J Clin Invest *119*, 3530-3543.

Gloeckner, C.J., Boldt, K., Schumacher, A., Roepman, R., and Ueffing, M. (2007). A novel tandem affinity purification strategy for the efficient isolation and characterisation of native protein complexes. Proteomics *7*, 4228-4234.

Gloeckner, C.J., Boldt, K., Schumacher, A., and Ueffing, M. (2009). Tandem affinity purification of protein complexes from mammalian cells by the Strep/FLAG (SF)-TAP tag. Methods Mol Biol *564*, 359-372.

Gregorieff, A., Pinto, D., Beghtel, H., Destrée, O., Kielman, M., and Clevers, H. (2005). Expression Pattern of Wnt Signaling Components in the Adult Intestine. Gastroenterology *129*, 626-638.

Grompe, M. (2012). Tissue stem cells: new tools and functional diversity. Cell stem cell *10*, 685-689.

Gross, I., Duluc, I., Benameur, T., Calon, A., Martin, E., Brabletz, T., Kedinger, M., Domon-Dell, C., and Freund, J.N. (2008). The intestine-specific homeobox gene Cdx2 decreases mobility and antagonizes dissemination of colon cancer cells. Oncogene *27*, 107-115.

Guo, D.L., Zhang, J., Yuen, S.T., Tsui, W.Y., Chan, A.S., Ho, C., Ji, J., Leung, S.Y., and Chen, X. (2006). Reduced expression of EphB2 that parallels invasion and metastasis in colorectal tumours. Carcinogenesis *27*, 454-464. Epub 2005 Nov 2004.

Gupta, P.B., Chaffer, C.L., and Weinberg, R.A. (2009). Cancer stem cells: mirage or reality? Nature medicine *15*, 1010-1012.

Habib, A.M., Richards, P., Cairns, L.S., Rogers, G.J., Bannon, C.A., Parker, H.E., Morley, T.C., Yeo, G.S., Reimann, F., and Gribble, F.M.

(2012). Overlap of endocrine hormone expression in the mouse intestine revealed by transcriptional profiling and flow cytometry. Endocrinology *153*, 3054-3065.

Hanahan, D., and Weinberg, R.A. (2000). The hallmarks of cancer. Cell *100*, 57-70.

Hansen, K.H., Bracken, A.P., Pasini, D., Dietrich, N., Gehani, S.S., Monrad, A., Rappsilber, J., Lerdrup, M., and Helin, K. (2008). A model for transmission of the H3K27me3 epigenetic mark. Nature cell biology *10*, 1291-1300.

Haramis, A.P., Begthel, H., van den Born, M., van Es, J., Jonkheer, S., Offerhaus, G.J., and Clevers, H. (2004). De novo crypt formation and juvenile polyposis on BMP inhibition in mouse intestine. Science *303*, 1684-1686.

Hardwick, J.C., Kodach, L.L., Offerhaus, G.J., and Van den Brink, G.R. (2008). Bone morphogenetic protein signalling in colorectal cancer. Nature reviews Cancer *8*, 806-812.

Hatzis, P., van der Flier, L.G., van Driel, M.A., Guryev, V., Nielsen, F., Denissov, S., Nijman, I.J., Koster, J., Santo, E.E., Welboren, W.*, et al.* (2008). Genome-wide pattern of TCF7L2/TCF4 chromatin occupancy in colorectal cancer cells. Molecular and cellular biology *28*, 2732-2744.

Hayashi, S., Lewis, P., Pevny, L., and McMahon, A.P. (2002). Efficient gene modulation in mouse epiblast using a Sox2Cre transgenic mouse strain. Mech Dev *119S*, S97-S101.

Hemberger, M., Dean, W., and Reik, W. (2009). Epigenetic dynamics of stem cells and cell lineage commitment: digging Waddington's canal. Nature reviews Molecular cell biology *10*, 526-537.

Hermann, P.C., Huber, S.L., Herrler, T., Aicher, A., Ellwart, J.W., Guba, M., Bruns, C.J., and Heeschen, C. (2007). Distinct populations of cancer stem cells determine tumor growth and metastatic activity in human pancreatic cancer. Cell stem cell *1*, 313-323.

Hu, T., Fu, Q., Chen, P., Zhang, K., and Guo, D. (2009). Generation of a stable mammalian cell line for simultaneous expression of multiple genes by using 2A peptide-based lentiviral vector. Biotechnology letters *31*, 353-359.

Huang, N.N., Mootz, D.E., Walhout, A.J.M., Vidal, M., and Hunter, C.P. (2002). MEX-3 interacting proteins link cell polarity to asymmetric gene expression in *Caenorhabditis elegans*. Development *129*, 747-759.

Huch, M., Dorrell, C., Boj, S.F., van Es, J.H., Li, V.S., van de Wetering, M., Sato, T., Hamer, K., Sasaki, N., Finegold, M.J.*, et al.* (2013). In vitro expansion of single Lgr5+ liver stem cells induced by Wnt-driven regeneration. Nature *494*, 247-250.

Hunter, C.P., and Kenyon, C. (1996). Spatial and Temporal Controls Target *pal-1* Blastomere-Specification Activity to a Single Blastomere Lineage in C. elegans Embryos. Cell *87*, 217-226.

Insinga, A., Cicalese, A., Faretta, M., Gallo, B., Albano, L., Ronzoni, S., Furia, L., Viale, A., and Pelicci, P.G. (2013). DNA damage in stem cells activates p21, inhibits p53, and induces symmetric self-renewing divisions. Proceedings of the National Academy of Sciences of the United States of America *110*, 3931-3936.

Jaenisch, R., and Young, R. (2008). Stem cells, the molecular circuitry of pluripotency and nuclear reprogramming. Cell *132*, 567-582.

Jaks, V., Barker, N., Kasper, M., van Es, J.H., Snippert, H.J., Clevers, H., and Toftgard, R. (2008). Lgr5 marks cycling, yet long-lived, hair follicle stem cells. Nature genetics *40*, 1291-1299.

Jiao, Y., Bishop, C.E., and Lu, B. (2012a). Mex3c regulates insulin-like growth factor 1 (IGF1) expression and promotes postnatal growth. Molecular biology of the cell *23*, 1404-1413.

Jiao, Y., George, S.K., Zhao, Q., Hulver, M.W., Hutson, S.M., Bishop, C.E., and Lu, B. (2012b). Mex3c mutation reduces adiposity and increases energy expenditure. Molecular and cellular biology *32*, 4350-4362.

Jones, D.L., and Wagers, A.J. (2008). No place like home: anatomy and function of the stem cell niche. Nature reviews Molecular cell biology *9*, 11-21.

Jordan, C.T. (2009). Cancer stem cells: controversial or just misunderstood? Cell stem cell *4*, 203-205.

Jordan, C.T., Guzman, M.L., and Noble, M. (2006). Cancer Stem Cells. N Engl J Med *335*, 1253-1261.

Jung, P., Sato, T., Merlos-Suarez, A., Barriga, F.M., Iglesias, M., Rossell, D., Auer, H., Gallardo, M., Blasco, M.A., Sancho, E.*, et al.* (2011). Isolation and in vitro expansion of human colonic stem cells. Nature medicine *17*, 1225-1227.

Kakizaki, F., Aoki, K., Miyoshi, H., Carrasco, N., Aoki, M., and Taketo, M.M. (2010). CDX transcription factors positively regulate expression of

solute carrier family 5, member 8 in the colonic epithelium. Gastroenterology *138*, 627-635.

Kedersha, N., and Anderson, P. (2007). Mammalian Stress Granules and Processing Bodies. *431*, 61-81.

Keene, J.D., Komisarow, J.M., and Friedersdorf, M.B. (2006). RIP-Chip: the isolation and identification of mRNAs, microRNAs and protein components of ribonucleoprotein complexes from cell extracts. Nature protocols *1*, 302-307.

Kelly, P.N., Dakic, A., Adams, J.M., Nutt, S.L., and Strasser, A. (2007). Tumor growth need not be driven by rare cancer stem cells. Science *317*, 337.

Kemper, K., Sprick, M.R., de Bree, M., Scopelliti, A., Vermeulen, L., Hoek, M., Zeilstra, J., Pals, S.T., Mehmet, H., Stassi, G.*, et al.* (2010). The AC133 epitope, but not the CD133 protein, is lost upon cancer stem cell differentiation. Cancer research *70*, 719-729.

Kim, J., Woo, A.J., Chu, J., Snow, J.W., Fujiwara, Y., Kim, C.G., Cantor, A.B., and Orkin, S.H. (2010). A Myc network accounts for similarities between embryonic stem and cancer cell transcription programs. Cell *143*, 313-324.

Kim, K.A., Kakitani, M., Zhao, J., Oshima, T., Tang, T., Binnerts, M., Liu, Y., Boyle, B., Park, E., Emtage, P.*, et al.* (2005). Mitogenic influence of human R-spondin1 on the intestinal epithelium. Science *309*, 1256-1259.

Kim, T.H., Escudero, S., and Shivdasani, R.A. (2012). Intact function of Lgr5 receptor-expressing intestinal stem cells in the absence of Paneth cells. Proceedings of the National Academy of Sciences of the United States of America *109*, 3932-3937.

Kinzler, K.W., and Vogelstein, B. (1996). Lessons from hereditary colorectal cancer. Cell *87*, 159-170.

Klaus, A., and Birchmeier, W. (2008). Wnt signalling and its impact on development and cancer. Nature reviews Cancer *8*, 387-398.

Klomp, L.W., de Koning, T.J., Malingre, H.E., van Beurden, E.A., Brink, M., Opdam, F.L., Duran, M., Jaeken, J., Pineda, M., Van Maldergem, L.*, et al.* (2000). Molecular characterization of 3-phosphoglycerate dehydrogenase deficiency--a neurometabolic disorder associated with reduced L-serine biosynthesis. Am J Hum Genet *67*, 1389-1399. Epub 2000 Oct 1327.

Konuma, T., Nakamura, S., Miyagi, S., Negishi, M., Chiba, T., Oguro, H., Yuan, J., Mochizuki-Kashio, M., Ichikawa, H., Miyoshi, H.*, et al.* (2011).

Forced expression of the histone demethylase Fbxl10 maintains self-renewing hematopoietic stem cells. Exp Hematol *39*, 697-709.

Koo, B.K., Spit, M., Jordens, I., Low, T.Y., Stange, D.E., van de Wetering, M., van Es, J.H., Mohammed, S., Heck, A.J., Maurice, M.M.*, et al.* (2012). Tumour suppressor RNF43 is a stem-cell E3 ligase that induces endocytosis of Wnt receptors. Nature *488*, 665-669.

Korinek, V., Barker, N., Moerer, P., van Donselaar, E., Huls, G., Peters, P.J., and Clevers, H. (1998). Depeltion of epithelial stem-cell compartments in the small intestine of mice lacking Tcf-4. Nature genetics *19*, 379-383.

Korinek, V., Barker, N., Morin, P.J., van Wichen, D., de Weger, R., Kinzler, K.W., Vogelstein, B., and Clevers, H. (1997). Constitutive transcriptional activation by a beta-catenin-Tcf complex in APC-/- colon carcinoma. Science *275*, 1784-1787.

Kuzmichev, A., Jenuwein, T., Tempst, P., and Reinberg, D. (2004). Different Ezh2-Containing Complexes Target Methylation of Histone H1 or Nucleosomal Histone H3. Molecular cell *14*, 183-193.

Kuzmichev, A., Margueron, R., Vaquero, A., Preissner, T.S., Scher, M., Kirmizis, A., Ouyang, X., Brockdorff, N., Abate-Shen, C., Farnham, P.*, et al.* (2005). Composition and histone substrates of polycomb repressive group complexes change during cellular differentiation. Proceedings of the National Academy of Sciences of the United States of America *102*, 1859-1864.

Kwon, S.C., Yi, H., Eichelbaum, K., Fohr, S., Fischer, B., You, K.T., Castello, A., Krijgsveld, J., Hentze, M.W., and Kim, V.N. (2013). The RNA-binding protein repertoire of embryonic stem cells. Nature structural & molecular biology *2013*, 2638.

Lafarga, V., Cuadrado, A., Lopez de Silanes, I., Bengoechea, R., Fernandez-Capetillo, O., and Nebreda, A.R. (2009). p38 Mitogen-activated protein kinase- and HuR-dependent stabilization of p21(Cip1) mRNA mediates the G(1)/S checkpoint. Mol Cell Biol *29*, 4341-4351. doi: 4310.1128/MCB.00210-00209. Epub 02009 Jun 00215.

Lapidot, T., Sirard, C., Vormoor, J., Murdoch, B., Hoang, T., Caceres-Cortes, J., Minden, M., Paterson, B., Caligiuri, M.A., and Dick, J.E. (1994). A cell initiating human acute myeloid leukaemia after transplantation into SCID mice. Nature *367*, 645-648.

Liang, C., Feng, P., Ku, B., Dotan, I., Canaani, D., Oh, B.H., and Jung, J.U. (2006). Autophagic and tumour suppressor activity of a novel Beclin1-binding protein UVRAG. Nat Cell Biol *8*, 688-699.

Liu, H., Patel, M.R., Prescher, J.A., Patsialou, A., Qian, D., Lin, J., Wen, S., Chang, Y.F., Bachmann, M.H., Shimono, Y.*, et al.* (2010). Cancer stem cells from human breast tumors are involved in spontaneous metastases in orthotopic mouse models. Proceedings of the National Academy of Sciences of the United States of America *107*, 18115-18120.

Liu, Z., Scannell, D.R., Eisen, M.B., and Tjian, R. (2011). Control of embryonic stem cell lineage commitment by core promoter factor, TAF3. Cell *146*, 720-731.

Lobo, N.A., Shimono, Y., Qian, D., and Clarke, M.F. (2007). The biology of cancer stem cells. Annual review of cell and developmental biology *23*, 675-699.

Mao, W., Luis, E., Ross, S., Silva, J., Tan, C., Crowley, C., Chui, C., Franz, G., Senter, P., Koeppen, H.*, et al.* (2004). EphB2 as a Therapeutic Antibody Drug Target for the Treatment of Colorectal Cancer. Cancer Res *64*, 781-788.

Margueron, R., Justin, N., Ohno, K., Sharpe, M.L., Son, J., Drury, W.J., 3rd, Voigt, P., Martin, S.R., Taylor, W.R., De Marco, V.*, et al.* (2009). Role of the polycomb protein EED in the propagation of repressive histone marks. Nature *461*, 762-767.

Margueron, R., and Reinberg, D. (2011). The Polycomb complex PRC2 and its mark in life. Nature *469*, 343-349.

Marks, H., Kalkan, T., Menafra, R., Denissov, S., Jones, K., Hofemeister, H., Nichols, J., Kranz, A., Stewart, A.F., Smith, A.*, et al.* (2012). The transcriptional and epigenomic foundations of ground state pluripotency. Cell *149*, 590-604.

Masuda, K., Abdelmohsen, K., Kim, M.M., Srikantan, S., Lee, E.K., Tominaga, K., Selimyan, R., Martindale, J.L., Yang, X., Lehrmann, E.*, et al.* (2011). Global dissociation of HuR-mRNA complexes promotes cell survival after ionizing radiation. The EMBO journal *30*, 1040-1053.

Merlos-Suarez, A., Barriga, F.M., Jung, P., Iglesias, M., Cespedes, M.V., Rossell, D., Sevillano, M., Hernando-Momblona, X., da Silva-Diz, V., Munoz, P.*, et al.* (2011). The intestinal stem cell signature identifies colorectal cancer stem cells and predicts disease relapse. Cell stem cell *8*, 511-524.

Miller, J.L., Koc, H., and Koc, E.C. (2008). Identification of phosphorylation sites in mammalian mitochondrial ribosomal protein DAP3. Protein Sci *17*, 251-260. doi: 210.1110/ps.073185608.

Modica, S., Morgano, A., Salvatore, L., Petruzzelli, M., Vanier, M.T., Valanzano, R., Esposito, D.L., Palasciano, G., Duluc, I., Freund, J.N.*, et*

al. (2009). Expression and localisation of insulin receptor substrate 2 in normal intestine and colorectal tumours. Regulation by intestine-specific transcription factor CDX2. Gut *58*, 1250-1259.

Montgomery, N.D., Yee, D., Chen, A., Kalantry, S., Chamberlain, S.J., Otte, A.P., and Magnuson, T. (2005). The murine polycomb group protein Eed is required for global histone H3 lysine-27 methylation. Current biology : CB *15*, 942-947.

Montgomery, N.D., Yee, D., Montgomery, S.A., and Magnuson, T. (2007). Molecular and functional mapping of EED motifs required for PRC2-dependent histone methylation. Journal of molecular biology *374*, 1145-1157.

Montgomery, R.K., Carlone, D.L., Richmond, C.A., Farilla, L., Kranendonk, M.E., Henderson, D.E., Baffour-Awuah, N.Y., Ambruzs, D.M., Fogli, L.K., Algra, S.*, et al.* (2011). Mouse telomerase reverse transcriptase (mTert) expression marks slowly cycling intestinal stem cells. Proceedings of the National Academy of Sciences of the United States of America *108*, 179-184.

Morin, P.J., Sparks, A.B., Korinek, V., Barker, N., Clevers, H., Vogelstein, B., and Kinzler, K.W. (1997). Activation of beta-catenin-Tcf signaling in colon cancer by mutations in beta-catenin or APC. Science *275*, 1787-1790.

Morrison, S.J., and Kimble, J. (2006). Asymmetric and symmetric stem-cell divisions in development and cancer. Nature *441*, 1068-1074.

Morrison, S.J., and Spradling, A.C. (2008). Stem cells and niches: mechanisms that promote stem cell maintenance throughout life. Cell *132*, 598-611.

Mukamel, Z., and Kimchi, A. (2004). Death-associated protein 3 localizes to the mitochondria and is involved in the process of mitochondrial fragmentation during cell death. J Biol Chem *279*, 36732-36738.

Mukherjee, N., Corcoran, D.L., Nusbaum, J.D., Reid, D.W., Georgiev, S., Hafner, M., Ascano, M., Jr., Tuschl, T., Ohler, U., and Keene, J.D. (2011). Integrative regulatory mapping indicates that the RNA-binding protein HuR couples pre-mRNA processing and mRNA stability. Molecular cell *43*, 327-339.

Munoz, J., Stange, D.E., Schepers, A.G., van de Wetering, M., Koo, B.K., Itzkovitz, S., Volckmann, R., Kung, K.S., Koster, J., Radulescu, S.*, et al.* (2012). The Lgr5 intestinal stem cell signature: robust expression of proposed quiescent '+4' cell markers. The EMBO journal *31*, 3079-3091.

Nakanishi, Y., Seno, H., Fukuoka, A., Ueo, T., Yamaga, Y., Maruno, T., Nakanishi, N., Kanda, K., Komekado, H., Kawada, M.*, et al.* (2013). Dclk1 distinguishes between tumor and normal stem cells in the intestine. Nature genetics *45*, 98-103.

Nguyen, L.V., Vanner, R., Dirks, P., and Eaves, C.J. (2012). Cancer stem cells: an evolving concept. Nature reviews Cancer *12*, 133-143.

Nicolas, N., Marazzi, G., Kelley, K., and Sassoon, D. (2005). Embryonic deregulation of muscle stress signaling pathways leads to altered postnatal stem cell behavior and a failure in postnatal muscle growth. Dev Biol *281*, 171-183.

Noubissi, F.K., Elcheva, I., Bhatia, N., Shakoori, A., Ougolkov, A., Liu, J., Minamoto, T., Ross, J., Fuchs, S.Y., and Spiegelman, V.S. (2006). CRD-BP mediates stabilization of betaTrCP1 and c-myc mRNA in response to beta-catenin signalling. Nature *441*, 898-901.

Novoa, I., Gallego, J., Ferreira, P.G., and Mendez, R. (2010). Mitotic cell-cycle progression is regulated by CPEB1 and CPEB4-dependent translational control. Nature cell biology *12*, 447-456.

O'Brien, C.A., Pollett, A., Gallinger, S., and Dick, J.E. (2007). A human colon cancer cell capable of initiating tumour growth in immunodeficient mice. Nature *445*, 106-110.

Park, I.K., Qian, D., Kiel, M., Becker, M.W., Pihalja, M., Weissman, I.L., Morrison, S.J., and Clarke, M.F. (2003). Bmi-1 is required for maintenance of adult self-renewing haematopoietic stem cells. Nature *423*, 302-305. Epub 2003 Apr 2020.

Pece, S., Tosoni, D., Confalonieri, S., Mazzarol, G., Vecchi, M., Ronzoni, S., Bernard, L., Viale, G., Pelicci, P.G., and Di Fiore, P.P. (2010). Biological and molecular heterogeneity of breast cancers correlates with their cancer stem cell content. Cell *140*, 62-73.

Pereira, B., Sousa, S., Barros, R., Carreto, L., Oliveira, P., Oliveira, C., Chartier, N.T., Plateroti, M., Rouault, J.P., Freund, J.N.*, et al.* (2013). CDX2 regulation by the RNA-binding protein MEX3A: impact on intestinal differentiation and stemness. Nucleic acids research *41*, 3986-3999. Epub 2013 Feb 3913.

Pfeiffer, V., and Lingner, J. (2013). Replication of telomeres and the regulation of telomerase. Cold Spring Harb Perspect Biol *5*.

Pierce, G.B. (1977). Relationship between differentiation and carcinogenesis. J Toxicol Environ Health *2*, 1335-1342.

Pinto, D., Gregorieff, A., Begthel, H., and Clevers, H. (2003). Canonical Wnt signals are essential for homeostasis of the intestinal epithelium. Genes Dev *17*, 1709-1713.

Potten, C.S. (1975). Kinetics and possible regulation of crypt cell populations under normal and stress conditions. Bull Cancer *62*, 419-430.

Potten, C.S. (1977). Extreme sensitivity of some intestinal crypt cells to X and gamma irradiation. Nature *269*, 518-521.

Powell, A.E., Wang, Y., Li, Y., Poulin, E.J., Means, A.L., Washington, M.K., Higginbotham, J.N., Juchheim, A., Prasad, N., Levy, S.E.*, et al.* (2012). The pan-ErbB negative regulator Lrig1 is an intestinal stem cell marker that functions as a tumor suppressor. Cell *149*, 146-158.

Quintana, E., Shackleton, M., Sabel, M.S., Fullen, D.R., Johnson, T.M., and Morrison, S.J. (2008). Efficient tumour formation by single human melanoma cells. Nature *456*, 593-598.

Ricci-Vitiani, L., Lombardi, D.G., Pilozzi, E., Biffoni, M., Todaro, M., Peschle, C., and De Maria, R. (2007). Identification and expansion of human colon-cancer-initiating cells. Nature *445*, 111-115.

Riccio, O., van Gijn, M.E., Bezdek, A.C., Pellegrinet, L., van Es, J.H., Zimber-Strobl, U., Strobl, L.J., Honjo, T., Clevers, H., and Radtke, F. (2008). Loss of intestinal crypt progenitor cells owing to inactivation of both Notch1 and Notch2 is accompanied by derepression of CDK inhibitors p27Kip1 and p57Kip2. EMBO Rep *9*, 377-383. doi: 310.1038/embor.2008.1037. Epub 2008 Feb 1015.

Richter, R., Rorbach, J., Pajak, A., Smith, P.M., Wessels, H.J., Huynen, M.A., Smeitink, J.A., Lightowlers, R.N., and Chrzanowska-Lightowlers, Z.M. (2010). A functional peptidyl-tRNA hydrolase, ICT1, has been recruited into the human mitochondrial ribosome. The EMBO journal *29*, 1116-1125.

Rosell, D. (In press). GaGa: a simple and fexible hierarchical model for diferential expression analysis. Annals of Applied Statistics.

Sancho, E., Batlle, E., and Clevers, H. (2004). Signaling pathways in intestinal development and cancer. Annual review of cell and developmental biology *20*, 695-723.

Sangiorgi, E., and Capecchi, M.R. (2008). Bmi1 is expressed in vivo in intestinal stem cells. Nature genetics *40*, 915-920.

Sansom, O.J., Meniel, V.S., Muncan, V., Phesse, T.J., Wilkins, J.A., Reed, K.R., Vass, J.K., Athineos, D., Clevers, H., and Clarke, A.R. (2007). Myc deletion rescues Apc deficiency in the small intestine. Nature *446*, 676-679.

Sato, T., van Es, J.H., Snippert, H.J., Stange, D.E., Vries, R.G., van den Born, M., Barker, N., Shroyer, N.F., van de Wetering, M., and Clevers, H. (2011). Paneth cells constitute the niche for Lgr5 stem cells in intestinal crypts. Nature *469*, 415-418.

Sato, T., Vries, R.G., Snippert, H.J., van de Wetering, M., Barker, N., Stange, D.E., van Es, J.H., Abo, A., Kujala, P., Peters, P.J.*, et al.* (2009). Single Lgr5 stem cells build crypt-villus structures in vitro without a mesenchymal niche. Nature *459*, 262-265.

Schatton, T., Murphy, G.F., Frank, N.Y., Yamaura, K., Waaga-Gasser, A.M., Gasser, M., Zhan, Q., Jordan, S., Duncan, L.M., Weishaupt, C.*, et al.* (2008). Identification of cells initiating human melanomas. Nature *451*, 345-349.

Schepers, A.G., Snippert, H.J., Stange, D.E., van den Born, M., van Es, J.H., van de Wetering, M., and Clevers, H. (2012). Lineage tracing reveals Lgr5+ stem cell activity in mouse intestinal adenomas. Science *337*, 730-735.

Schepers, A.G., Vries, R., van den Born, M., van de Wetering, M., and Clevers, H. (2011). Lgr5 intestinal stem cells have high telomerase activity and randomly segregate their chromosomes. The EMBO journal *30*, 1104-1109.

Schoppmeier, M., Fischer, S., Schmitt-Engel, C., Lohr, U., and Klingler, M. (2009). An ancient anterior patterning system promotes caudal repression and head formation in ecdysozoa. Curr Biol *19*, 1811-1815.

Shackleton, M., Quintana, E., Fearon, E.R., and Morrison, S.J. (2009). Heterogeneity in cancer: cancer stem cells versus clonal evolution. Cell *138*, 822-829.

Shimomura, Y., Agalliu, D., Vonica, A., Luria, V., Wajid, M., Baumer, A., Belli, S., Petukhova, L., Schinzel, A., Brivanlou, A.H.*, et al.* (2010). APCDD1 is a novel Wnt inhibitor mutated in hereditary hypotrichosis simplex. Nature *464*, 1043-1047.

Siegmund, K.D., Marjoram, P., Woo, Y.J., Tavare, S., and Shibata, D. (2009). Inferring clonal expansion and cancer stem cell dynamics from DNA methylation patterns in colorectal cancers. Proceedings of the National Academy of Sciences of the United States of America *106*, 4828-4833.

Silberg, D.G., Swain, G.P., Suh, E.R., and Traber, P.G. (2000). Cdx1 and Cdx2 expression during intestinal development. Gastroenterology *119*, 961-971.

Slattery, M.L., Herrick, J., Curtin, K., Samowitz, W., Wolff, R.K., Caan, B.J., Duggan, D., Potter, J.D., and Peters, U. (2010). Increased risk of colon cancer associated with a genetic polymorphism of SMAD7. Cancer research *70*, 1479-1485.

Slattery, M.L., Potter, J., Caan, B., Edwards, S., Coates, A., Ma, K.N., and Berry, T.D. (1997). Energy balance and colon cancer--beyond physical activity. Cancer Res *57*, 75-80.

Snippert, H.J., van Es, J.H., van den Born, M., Begthel, H., Stange, D.E., Barker, N., and Clevers, H. (2009). Prominin-1/CD133 marks stem cells and early progenitors in mouse small intestine. Gastroenterology *136*, 2187-2194 e2181.

Stringer, E.J., Duluc, I., Saandi, T., Davidson, I., Bialecka, M., Sato, T., Barker, N., Clevers, H., Pritchard, C.A., Winton, D.J.*, et al.* (2012). Cdx2 determines the fate of postnatal intestinal endoderm. Development *139*, 465-474.

Takashima, S., Gold, D., and Hartenstein, V. (2013). Stem cells and lineages of the intestine: a developmental and evolutionary perspective. Dev Genes Evol *223*, 85-102.

Takeda, N., Jain, R., LeBoeuf, M.R., Wang, Q., Lu, M.M., and Epstein, J.A. (2011). Interconversion between intestinal stem cell populations in distinct niches. Science *334*, 1420-1424.

Tenenbaum, S.A., Lager, P.J., Carson, C.C., and Keene, J.D. (2002). Ribonomics; identifying mRNA subsets in mRNP complexes using antibodies to RNA-binding proteins and genomic arrays. Methods *26*, 191-198.

Tian, H., Biehs, B., Warming, S., Leong, K.G., Rangell, L., Klein, O.D., and de Sauvage, F.J. (2011). A reserve stem cell population in small intestine renders Lgr5-positive cells dispensable. Nature *478*, 255-259.

Till, J.E., and McCulloch, E.A. (1961). A direct measurement of the radiation sensitivity of normal mouse bone marrow cells. Radiat Res *14*, 213-222.

Tomlinson, I.P., Carvajal-Carmona, L.G., Dobbins, S.E., Tenesa, A., Jones, A.M., Howarth, K., Palles, C., Broderick, P., Jaeger, E.E., Farrington, S.*, et al.* (2011). Multiple common susceptibility variants near BMP pathway loci GREM1, BMP4, and BMP2 explain part of the missing heritability of colorectal cancer. PLoS genetics *7*, 2.

Turgeon, B., and Meloche, S. (2009). Interpreting neonatal lethal phenotypes in mouse mutants: insights into gene function and human diseases. Physiol Rev *89*, 1-26. doi: 10.1152/physrev.00040.02007.

Ura, H., Usuda, M., Kinoshita, K., Sun, C., Mori, K., Akagi, T., Matsuda, T., Koide, H., and Yokota, T. (2008). STAT3 and Oct-3/4 control histone modification through induction of Eed in embryonic stem cells. J Biol Chem *283*, 9713-9723. doi: 9710.1074/jbc.M707275200. Epub 707272008 Jan 707275216.

Van de Wetering, M., Sancho, E., Verweij, C., de Lau, W., Oving, I., Hurlstone, A., van der Horn, K., Batlle, E., Coudreuse, D., Haramis, A.P.*, et al.* (2002). The B-Catenin/TCF-4 Complex Imposes a Crypt Progenitor Phenotype on Colorectal Cancer Cells. Cell *111*, 241-250.

van der Flier, L.G., and Clevers, H. (2009). Stem cells, self-renewal, and differentiation in the intestinal epithelium. Annual review of physiology *71*, 241-260.

van der Flier, L.G., Sabates-Bellver, J., Oving, I., Haegebarth, A., De Palo, M., Anti, M., Van Gijn, M.E., Suijkerbuijk, S., Van de Wetering, M., Marra, G.*, et al.* (2007a). The Intestinal Wnt/TCF Signature. Gastroenterology *132*, 628-632. Epub 2006 Aug 2018.

Van der Flier, L.G., Sabates-Bellver, J., Oving, I., Haegebarth, A., De Palo, M., Anti, M., Van Gijn, M.E., Suijkerbuijk, S., Van de Wetering, M., Marra, G.*, et al.* (2007b). The Intestinal Wnt/TCF Signature. Gastroenterology *132*, 628-632.

van der Flier, L.G., van Gijn, M.E., Hatzis, P., Kujala, P., Haegebarth, A., Stange, D.E., Begthel, H., van den Born, M., Guryev, V., Oving, I.*, et al.* (2009). Transcription factor achaete scute-like 2 controls intestinal stem cell fate. Cell *136*, 903-912.

van Es, J.H., Jay, P., Gregorieff, A., van Gijn, M.E., Jonkheer, S., Hatzis, P., Thiele, A., van den Born, M., Begthel, H., Brabletz, T.*, et al.* (2005). Wnt signalling induces maturation of Paneth cells in intestinal crypts. Nature cell biology *7*, 381-386.

van Es, J.H., Sato, T., van de Wetering, M., Lyubimova, A., Nee, A.N., Gregorieff, A., Sasaki, N., Zeinstra, L., van den Born, M., Korving, J.*, et al.* (2012). Dll1+ secretory progenitor cells revert to stem cells upon crypt damage. Nature cell biology *14*, 1099-1104.

Vermeulen, L., De Sousa, E.M.F., van der Heijden, M., Cameron, K., de Jong, J.H., Borovski, T., Tuynman, J.B., Todaro, M., Merz, C., Rodermond, H.*, et al.* (2010). Wnt activity defines colon cancer stem cells and is regulated by the microenvironment. Nature cell biology *12*, 468- 476.

Vermeulen, L., Todaro, M., de Sousa Mello, F., Sprick, M.R., Kemper, K., Perez Alea, M., Richel, D.J., Stassi, G., and Medema, J.P. (2008). Single-cell cloning of colon cancer stem cells reveals a multi-lineage differentiation capacity. Proceedings of the National Academy of Sciences of the United States of America *105*, 13427-13432.

Verzi, M.P., Shin, H., He, H.H., Sulahian, R., Meyer, C.A., Montgomery, R.K., Fleet, J.C., Brown, M., Liu, X.S., and Shivdasani, R.A. (2010). Differentiation-specific histone modifications reveal dynamic chromatin interactions and partners for the intestinal transcription factor CDX2. Developmental cell *19*, 713-726.

Volk, T., Israeli, D., Nir, R., and Toledano-Katchalski, H. (2008). Tissue development and RNA control: "HOW" is it coordinated? Trends in genetics : TIG *24*, 94-101.

Wang, D., and Dubois, R.N. (2006). Prostaglandins and cancer. Gut *55*, 115-122.

Wang, Y., Giel-Moloney, M., Rindi, G., and Leiter, A.B. (2007). Enteroendocrine precursors differentiate independently of Wnt and form serotonin expressing adenomas in response to active beta-catenin. Proceedings of the National Academy of Sciences of the United States of America *104*, 11328-11333.

Wehkamp, J., and Stange, E.F. (2006). Paneth cells and the innate immune response. Curr Opin Gastroenterol *22*, 644-650.

Willert, K., and Jones, K.A. (2006). Wnt signaling: is the party in the nucleus? Genes & development *20*, 1394-1404.

Wong, V.W., Stange, D.E., Page, M.E., Buczacki, S., Wabik, A., Itami, S., van de Wetering, M., Poulsom, R., Wright, N.A., Trotter, M.W.*, et al.* (2012). Lrig1 controls intestinal stem-cell homeostasis by negative regulation of ErbB signalling. Nature cell biology *14*, 401-408.

Yan, K.S., Chia, L.A., Li, X., Ootani, A., Su, J., Lee, J.Y., Su, N., Luo, Y., Heilshorn, S.C., Amieva, M.R.*, et al.* (2012). The intestinal stem cell markers Bmi1 and Lgr5 identify two functionally distinct populations. Proceedings of the National Academy of Sciences of the United States of America *109*, 467-471.

Yarden, Y., and Shilo, B.Z. (2007). SnapShot: EGFR signaling pathway. Cell *131*, 1018.

Yin, X., Cao, L., Kang, R., Yang, M., Wang, Z., Peng, Y., Tan, Y., Liu, L., Xie, M., Zhao, Y.*, et al.* (2011). UV irradiation resistance-associated gene suppresses apoptosis by interfering with BAX activation. EMBO reports *12*, 727-734.

Yui, S., Nakamura, T., Sato, T., Nemoto, Y., Mizutani, T., Zheng, X., Ichinose, S., Nagaishi, T., Okamoto, R., Tsuchiya, K.*, et al.* (2012). Functional engraftment of colon epithelium expanded in vitro from a single adult Lgr5(+) stem cell. Nature medicine *18*, 618-623.

Zamore, P.D., and Lehmann, R. (1996). Drosophila development: homeodomains and translational control. Curr Biol *6*, 773-775.

Zeilstra, J., Joosten, S.P., Dokter, M., Verwiel, E., Spaargaren, M., and Pals, S.T. (2008). Deletion of the WNT target and cancer stem cell marker CD44 in Apc(Min/+) mice attenuates intestinal tumorigenesis. Cancer Res *68*, 3655-3661.

Zernicka-Goetz, M., Morris, S.A., and Bruce, A.W. (2009). Making a firm decision: multifaceted regulation of cell fate in the early mouse embryo. Nature reviews Genetics *10*, 467-477.

Zhao, Z., Oh, S., Li, D., Ni, D., Pirooz, S.D., Lee, J.H., Yang, S., Lee, J.Y., Ghozalli, I., Costanzo, V.*, et al.* (2012). A dual role for UVRAG in maintaining chromosomal stability independent of autophagy. Developmental cell *22*, 1001-1016.

Zhou, H.L., Geng, C., Luo, G., and Lou, H. (2013). The p97-UBXD8 complex destabilizes mRNA by promoting release of ubiquitinated HuR from mRNP. Genes & development *27*, 1046-1058.